

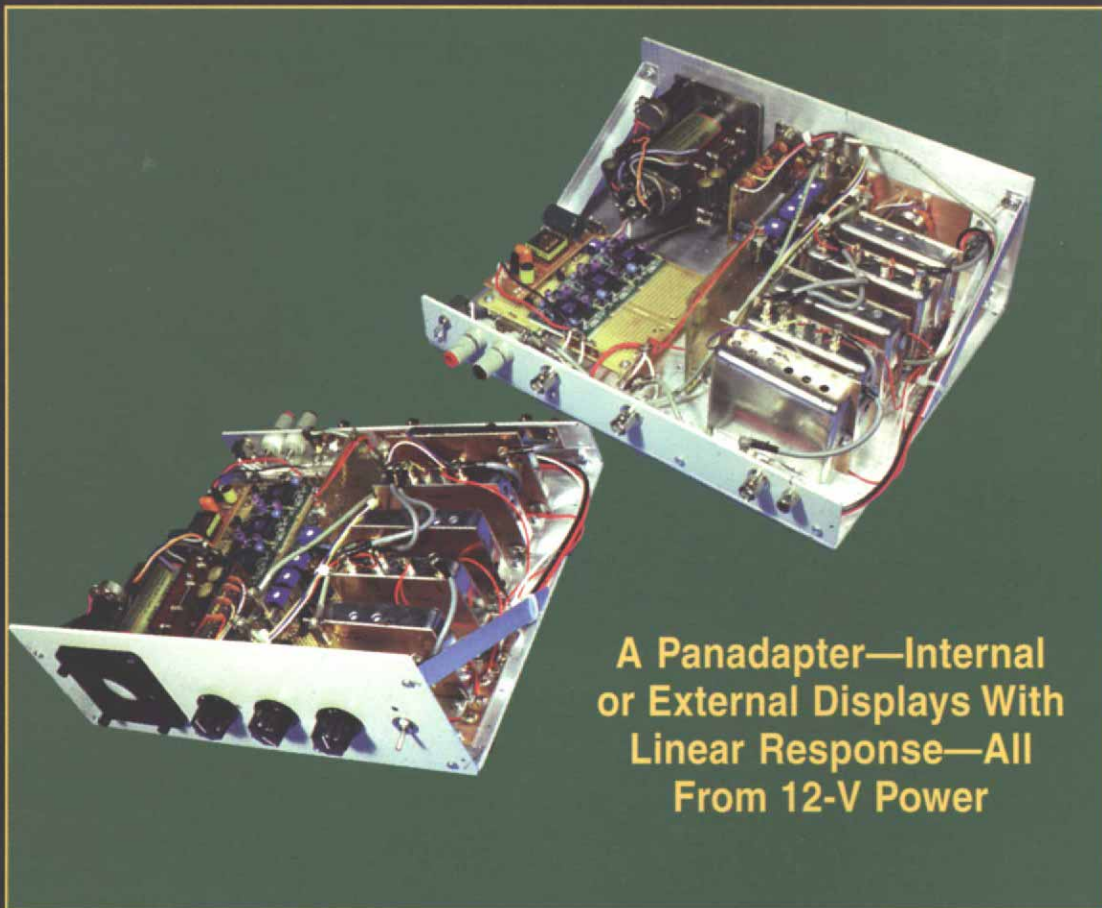
QEX

May/June 1999

\$5



Forum for Communications Experimenters



A Panadapter—Internal
or External Displays With
Linear Response—All
From 12-V Power

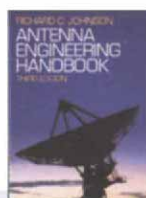
**QEX: Forum for
Communications Experimenters**
American Radio Relay League
225 Main Street
Newington, CT USA 06111-1494

TECHNICAL BOOKS

the antennas & propagation collection



Microstrip Antennas
David M. Pozar and Daniel H. Schaubert
 430 pages of antenna designs, theoretical and practical techniques for microstrip antennas. Covers element types, feed systems, polarization, bandwidth improvement and more.



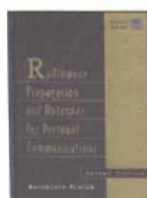
Antenna Engineering Handbook
Richard C. Johnson, editor
 The most widely-used reference for antenna engineering from VLF to microwaves, covering all standard antenna types and more. Each chapter written by an expert contributor.
MH-4 \$120.00



Introduction to Radio Propagation for Fixed and Mobile Communications
John Doble
 Basic insight into fixed-link and mobile radio propagation effects. Includes data on in-building systems and diversity techniques.
AH-48 \$69.00



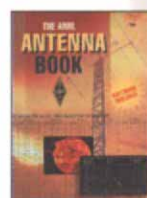
Antennas
John Kraus
 A classic text by an important researcher and teacher, required for any antenna design reference library. Has a good combination of strong theory and practical applications.
MH-14 \$89.00



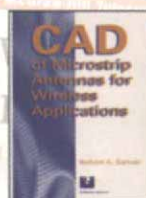
Radiowave Propagation and Antennas for Personal Communications
Kazimierz Siwiak
 A thorough review of propagation in mobile environments, antenna types and their performance. Includes a program disk.
AH-7 \$89.00



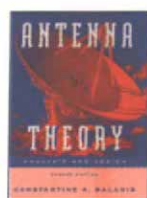
Phased Array Antennas
R.C. Hansen
 Detailed coverage of both practice and theory in the design and analysis of antenna arrays, from sidelobe considerations to superdirectivity and HTS antennas.



The ARRL Antenna Book
Gerald L. Hall, editor
 A practical guide to the design and construction of antennas for HF through microwave, valuable data for amateur and professional designers and experimenters.
AR-2 \$30.00



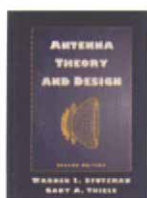
CAD of Microstrip Antennas for Wireless Applications
Robert A. Sainati
 Provides understanding of microstrip antennas and supplies the tools for design work. Written for engineers who are not antenna specialists.
AH-59 \$89.00



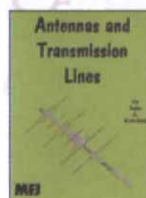
Antenna Theory: Analysis & Design, Second Edition
Constantine A. Balanis
 Emphasis on design, with a solid theoretical foundation. Excellent coverage of antenna terminology and performance parameters.
JW-11 \$103.00



Ionospheric Radio
Kenneth Davies
 An especially well-written and understandable text on radiowave propagation. A complete summary of all aspects of solar-terrestrial interaction and its effects.
IN-1 \$88.00



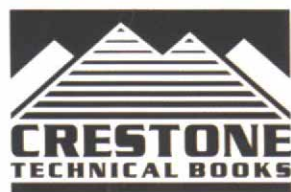
Antenna Theory and Design, Second Edition
Warren L. Stutzman and Gary A. Thiele
 New edition covers resonant, broadband and aperture antennas, lines and feeds, arrays, systems and electromagnetic modeling.
JW-29 \$100.00



Antennas and Transmission Lines
John A. Kuecken
 A handy collection of short, to-the-point chapters with the basic design equations for various antennas, matching, self-impedance, noise and radio range prediction.
MF-2 \$20.00

THE POWER OF INFORMATION

www.noblepub.com



Crestone Technical Books
 Division of Noble Publishing Corp.
 4772 Stone Drive
 Tucker, GA 30084
 Tel: 770-908-2320
 Fax: 770-939-0157

Order today by phone, fax or on the web, using your VISA, Mastercard or American Express!

QEX

QEX (ISSN: 0886-8093) is published bimonthly in **January '99**, **March '99**, **May '99**, **July '99**, **September '99**, and **November '99** by the American Radio Relay League, 225 Main Street, Newington CT 06111-1494. Subscription rate for 6 issues to ARRL members is \$22; nonmembers \$34. Other rates are listed below. Periodicals postage paid at Hartford, CT and at additional mailing offices.

POSTMASTER: Form 3579 requested. Send address changes to: QEX, 225 Main St, Newington, CT 06111-1494
Issue No 194

David Sumner, K1ZZ
Publisher

Doug Smith, KF6DX
Editor

Robert Schetgen, KU7G
Managing Editor

Lori Weinberg
Assistant Editor

Zack Lau, W1VT
Contributing Editor

Production Department

Mark J. Wilson, K1RO
Publications Manager

Michelle Bloom, WB1ENT
Production Supervisor

Sue Fagan
Graphic Design Supervisor

David Pingree, N1NAS
Technical Illustrator

Joe Shea
Production Assistant

Advertising Information Contact:

Robin Micket, N1WAL, *Advertising*
American Radio Relay League
860-594-0207 direct
860-594-0200 ARRL
860-594-0259 fax

Circulation Department

Debra Jahnke, *Manager*
Kathy Capodicasa, N1GZO, *Deputy Manager*
Cathy Stepina, *QEX Circulation*

Offices

225 Main St, Newington, CT 06111-1494 USA
Telephone: 860-594-0200
Telex: 650215-5052 MCI
Fax: 860-594-0259 (24 hour direct line)
e-mail: qex@arrl.org

Subscription rate for 6 issues:

In the US: ARRL Member \$22,
nonmember \$34;

US, Canada and Mexico by First Class Mail:
ARRL member \$35, nonmember \$47;

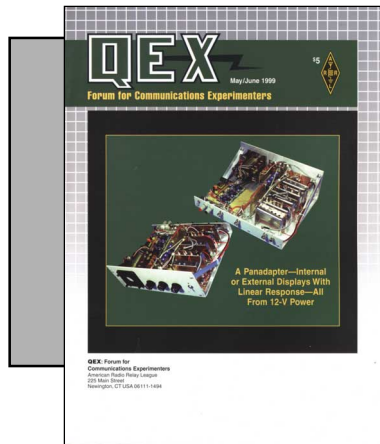
Elsewhere by Surface Mail (4-8 week delivery):
ARRL member \$27,
nonmember \$39;

Elsewhere by Airmail: ARRL member \$55,
nonmember \$67.

Members are asked to include their membership control number or a label from their QST wrapper when applying.

In order to ensure prompt delivery, we ask that you periodically check the address information on your mailing label. If you find any inaccuracies, please contact the Circulation Department immediately. Thank you for your assistance.

Copyright ©1999 by the American Radio Relay League Inc. For permission to quote or reprint material from QEX or any ARRL publication, send a written request including the issue date (or book title), article, page numbers and a description of where you intend to use the reprinted material. Send the request to the office of the Publications Manager (permission@arrl.org)



About the Cover

Details of Bob Dildine's improved Panadapter appear on [page 9](#).



Features

3 A Digital Commutating Filter

By Mike Kossor, WA2EBY

9 A Calibrated Panoramic Adapter

By Bob Dildine, 7J1AFR, W6FSH

23 A New Look at the Gamma Match

By Ron Barker, G4JNH, VK2INH

32 HF Whips on Cars, Campers and RVs

By Peter Madle, KE6RBV

43 Performance Specifications for Amateur Receivers of the Future

By Ulrich Graf, DK4SX

50 A 300-W MOSFET Linear Amplifier for 50 MHz

By Richard Frey, K4XU

55 Measuring Distortion in Linear Amplifiers

By Walter Schreuer, K1YZW/G3DCU

Columns

58 RF By Zack Lau, W1VT

61 Letters to the Editor

60 Upcoming Technical Conferences

62 Next Issue in QEX

May/June 1999 QEX Advertising Index

American Radio Relay League: 62, 64, Cov III

CCT, Inc: 31

Communications Specialists, Inc: 59

Crestone Technical Books: Cov II

DCI Digital Communications, Inc: 22, 57

Kachina Communications, Inc: Cov IV

SHF Microwave Parts Company: 63

Tucson Amateur Packet Radio Corp: 63

Z Domain Technologies, Inc: 49



The American Radio Relay League, Inc. is a noncommercial association of radio amateurs, organized for the promotion of interests in Amateur Radio communication and experimentation, for the establishment of networks to provide communications in the event of disasters or other emergencies, for the advancement of radio art and of the public welfare, for the representation of the radio amateur in legislative matters, and for the maintenance of fraternalism and a high standard of conduct.

ARRL is an incorporated association without capital stock chartered under the laws of the state of Connecticut, and is an exempt organization under Section 501(c)(3) of the Internal Revenue Code of 1986. Its affairs are governed by a Board of Directors, whose voting members are elected every two years by the general membership. The officers are elected or appointed by the Directors. The League is noncommercial, and no one who could gain financially from the shaping of its affairs is eligible for membership on its Board.

"Of, by, and for the radio amateur," ARRL numbers within its ranks the vast majority of active amateurs in the nation and has a proud history of achievement as the standard-bearer in amateur affairs.

A bona fide interest in Amateur Radio is the only essential qualification of membership; an Amateur Radio license is not a prerequisite, although full voting membership is granted only to licensed amateurs in the US.

Membership inquiries and general correspondence should be addressed to the administrative headquarters at 225 Main Street, Newington, CT 06111 USA.

Telephone: 860-594-0200

Telex: 650215-5052 MCI

MCIMAIL (electronic mail system) ID: 215-5052

FAX: 860-594-0259 (24-hour direct line)

Officers

President: RODNEY STAFFORD, W6ROD
5155 Shadow Estates, San Jose, CA 95135

Executive Vice President: DAVID SUMNER, K1ZZ

The purpose of *QEX* is to:

- 1) provide a medium for the exchange of ideas and information among Amateur Radio experimenters,
- 2) document advanced technical work in the Amateur Radio field, and
- 3) support efforts to advance the state of the Amateur Radio art.

All correspondence concerning *QEX* should be addressed to the American Radio Relay League, 225 Main Street, Newington, CT 06111 USA.

Envelopes containing manuscripts and letters for publication in *QEX* should be marked Editor, *QEX*.

Both theoretical and practical technical articles are welcomed. Manuscripts should be submitted on IBM or Mac format 3.5-inch diskette in word-processor format, if possible. We can redraw any figures as long as their content is clear. Photos should be glossy, color or black-and-white prints of at least the size they are to appear in *QEX*. Further information for authors can be found on the Web at www.arrl.org/qex/ or by e-mail to qex@arrl.org.

Any opinions expressed in *QEX* are those of the authors, not necessarily those of the Editor or the League. While we strive to ensure all material is technically correct, authors are expected to defend their own assertions. Products mentioned are included for your information only; no endorsement is implied. Readers are cautioned to verify the availability of products before sending money to vendors.

Empirically Speaking

At its annual meeting in January, the ARRL Board of Directors voted to form the Amateur Radio Technology Task Force. This initiative, proposed by League President Rodney Stafford, W6ROD, deserves praise and support from us in the technical community. The Task Force is charged with developing a strategy for exploring new technologies and assessing their potential use in Amateur Radio. League First Vice President Stephen Mendelsohn, W2ML, a technologist, has been selected to organize and lead this effort.

Rod and Stephen's first order of business is to define the direction of the Task Force. It seems there are as many models for improving our hobby through technology as there are modelers. This is a big chance for *QEX* readers and contributors to make a positive difference in the shaping of policy. We can help set goals that ensure a lasting legacy for ourselves and promote our basic charter of voluntary public service by providing emergency communications, contributing to the advancement of the state of our art, developing engineering and operational skills and enhancing international goodwill.

Almost all of you are involved in the evolution of new technical applications. I hope you'll think about this matter and send me your ideas on how modern technology can improve our lot, not only now, but into the next century. I'll make sure they get read by the Task Force—and by your fellow *QEX* readers—as appropriate.

Many thanks to you folks who've already taken the time to write us letters. You are sustaining our forum as a place for spirited, yet civil, discussion. A special thank you to all authors who've contributed articles. Your support has reestablished *QEX* as a preeminent voice in applied communications science. You've also helped readers through correspondence we don't always see.

Our republication of Peter Martinez, G3PLX's "PSK31: A New Radio-Teletype Mode" has been delayed an issue. I note with interest, though, that some of you are already on the air with it! Any reports of performance? What receiver bandwidth

and modem hardware are you using?

Please note on [page 1](#) that our reprint policy has changed to conform with *QST*'s. Reprint permission is ordinarily granted.

This Issue in *QEX*

In a companion piece to his two-part article "A Doppler Radio-Direction Finder" beginning in the [May '99 *QST*](#), Michael Kossor, WA2EBY, describes a [digital commutating filter](#). While this concept has been around for a while, not much has appeared in the literature. It's a neat way to get a narrow BPF with precision and repeatability.

[Dick Frey, K4XU](#), completes our selection of 6-meter power amplifiers with a solid-state, MOSFET design. It represents the culmination of a lot of work Dick has done with these devices. [Walter Schreuer, K1YZW](#), gives us some good information on testing amplifier linearity. His setup should come in handy after those MOSFETs are soldered in.

We're fortunate to have quite an international flavor in this issue. [Ron Barker, G4JNH](#), has cast a critical eye on the design and performance of the celebrated gamma match for Yagis and donates some new results. This technique, renowned for its difficulty in adjustment, benefits from his studies. [Ulrich Graf, DK4SX](#), has some counsel about the performance goals of the next generation of Amateur Radio receivers. In many ways, he is expressing the needs of hams who endure lots of QRM from the international broadcast service, but also of contesters operating "multi-multi."

[Bob Dildine, 7J1AFR](#), returns with an update on his popular panoramic adapter. This really is a heck of a good tool, especially on HF. In the middle of a QSO, it's slick to tell someone exactly what activity you're seeing on the band! [Peter Madle, KE6RBV](#), also has continued working on his topic, modeling antennas on vehicles. This time, he extends his examples to HF, and comes up with some interesting—and, in some cases, surprising—results. [Zack](#) describes transmission-line models for *Amateur Radio Designer*. See you at Dayton!—[Doug Smith, KF6DX, kf6dx@arrl.org](#) □□

A Digital Commutating Filter

This kind of filter has been around a long time, but there has been little mention of it in the ham literature.

By Mike Kossor, WA2EBY

[Mike created this filter as part of a Doppler RDF project, the balance of which is covered in the [May 1999 QST](#). Commutating filters have been known for some time, but for reasons beyond my ken, have seen little employment. The technique is put to good use here. The RDF system uses a multiple-antenna spatial-diversity system to produce Doppler-induced FM (at about 500 Hz) on the signal being examined. The exact nature of the induced modulation is then taken to indicate the bearing of the distant source. The circuit described here comprises a very narrow band-pass filter that isolates the near-500-Hz tone. See also Nichols

in the [Mar/Apr 1999 QEX](#) for additional discussion of spatial diversity. The Mar/Apr 1998 QEX has some material on sampling theory. —Ed.]

Digital filters have long been an integral part of radio-navigation and direction-finding systems. One of the earliest references I found dated back to the late forties.¹ The paper credits G. R. Clark as the inventor of the type of digital filter used in our Doppler RDF project. Digital switching technology did not exist—as we know it today—in 1947, so an electromechanical switching method was devised to implement Clark's original filter. The design was known as a filter using synchronously commutated capacitors, or a digital commutating filter as

is illustrated in [Fig 1](#). The input signal to be filtered is applied to one side of the resistor, while the filtered output signal is taken from the other side that is common to all capacitors. A motor was used to continuously turn the switch shaft at a fixed rate. Each capacitor is momentarily switched to ground as the switch contact spins around. The center frequency of the filter is determined by the rate at which the switch spins around, not by the values of R and C, as is the case with a conventional RC filter.

How it Works

At dc, the voltage applied to the input results in all capacitors charging to the same value. The filter output follows the dc voltage applied to the input ($V_o = V_i$) assuming that it's feed-

244 N. 17th St
Kenilworth, NJ 07033
mkossor@lucent.com

¹Notes appear on [page 8](#).

ing a high-impedance monitoring device that does not load the output.

Now we apply a periodic input signal, such as a sine wave, with amplitude of 1 V. The output of the filter decays rapidly to near zero volts as the frequency of the input signal is increased from dc. The output becomes zero as the input-signal frequency is increased to exactly one half the frequency of switch rotation. Under this condition, the switch makes two complete revolutions for each single cycle of the input sine wave. Each capacitor is charged to a specific value during the positive half-cycle of the input sine wave as the switch completes its first revolution. It is then completely discharged by the same values of opposite polarity on the next revolution of the switch during the negative half-cycle of the input sine wave. The net result is zero output signal.

The filter output remains near zero as the frequency of the input signal is increased further. Capacitors charge and discharge to various levels, yielding near-zero output until the input signal frequency is increased to the frequency of rotation of the switch. Under this condition, each capacitor charges to exactly the same value of the input signal amplitude each time it is switched to ground. For example, capacitors 1 through 8 will charge to the value of input signal amplitude at 0° , 45° , 90° , 135° , 180° , 225° , 270° and 315° , respectively, during the first rotation of the switch. The same cycle repeats on the second rotation as capacitor 1 is selected and the input signal, being periodic, has the same amplitude at 360° as it did at 0° . The output amplitude of the filter follows the input signal amplitude of filter ($V_o = V_i$) under this unique condition.

The output amplitude of the filter again decays rapidly as the frequency of the input signal is increased beyond the frequency of rotation of the switch. The output hits another null when the signal frequency equals 1.5 times the switch-rotation frequency. The output again follows the input when the input signal frequency is exactly twice the switch rotation frequency. The amplitude response of the filter continues to repeat this pattern as the frequency of the input signal is increased further. This response is illustrated in Fig 2.

The filter output tracks the amplitude of a periodic input signal that is the same frequency as the switch rotation frequency or an integral multiple (harmonic) of it. The periodic peaks

in the filter's frequency response resemble a comb, hence the name "comb" filter is given to this type of response. The comb response poses a problem in our RDF application, since we are only interested in extracting the 500-Hz Doppler tone from the audio. The comb-filter response would allow dc and all harmonics of 500 Hz to appear at the filter output if we did not prefilter the input signal. This explains the 500-Hz low-pass and high-pass filters that precede the digital filter in our Doppler RDF project. Band-pass filtering the input signal before it reaches the digital filter changes the comb response into a single-frequency, high-Q band-pass response with a center frequency determined by the frequency of rotation of the switch.

Bandwidth limiting the input signal also constrains the maximum input-signal frequency. The Nyquist sampling theorem states that a bandwidth-limited signal can be uniquely determined by sampling if the sampling rate is at least twice the highest-frequency component. The sampling

rate in our filter is defined as the number of times a capacitor samples and stores the input signal each second. Let's assume there are eight samples taken of the 500-Hz ($t = 2$ ms) Doppler tone. So a new sample is taken every $2 / 8$ ms = 0.25 ms, making the sampling rate ($1 / t$) 4 kHz. That means the highest input signal frequency that can be processed by our filter is $4 / 2$ kHz = 2 kHz. This frequency limitation is known as the *Nyquist frequency* or *Nyquist rate*. Applying input-signal frequencies above the Nyquist limit to our digital filter will result in erroneous responses. These errors due to under-sampling of the input signal are known as *aliasing*. We avoid aliasing errors by choosing a sampling rate that is greater than the Nyquist rate. Accurately filtering the 500-Hz Doppler tone requires a minimum sampling rate of $500 \times 2 = 1$ kHz. The 4-kHz sampling rate used here is four times the Nyquist rate. A high sampling rate makes it easier to convert the digitized filter output back into an analog form. More information

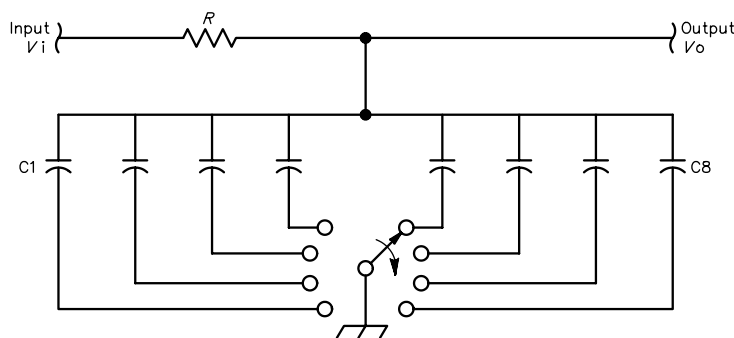


Fig 1—A digital commutating filter using a mechanical switch.

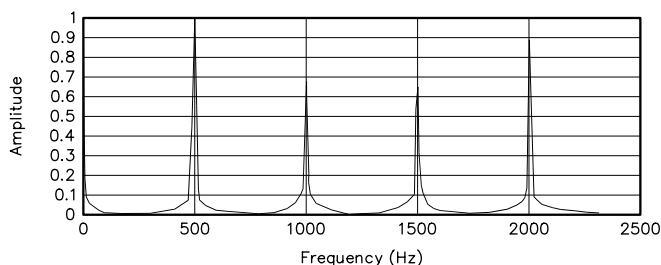


Fig 2—Amplitude versus frequency of a commutating filter.

on digital signal processing fundamentals can be found in *The ARRL Handbook*.³

Modern Implementation

Refer to Fig 3. The electromechanical switch / motor combination of Clark's filter is replaced with octal analog switch, U5, resulting in the modern, digital, commutating filter. The BCD address applied to pins 9, 10 and 11 of U5 determines which capacitor is connected to analog ground on pin 3. Digital counter U7 sequences the BCD addresses to switch capacitors 1 through 8 to ground—in order—emulating the physical rotating switch in Fig 1.

The response time of the digital filter can be changed by changing the value of R. This is accomplished by damping control R19. Changing the value of R19 does not change the center frequency of the filter, just how fast the filter responds to input signals. This is extremely useful in RDF applications, where reflected (multipath) signals cause false direction indications. These false signals cause rapid phase changes in the Doppler tone and can be filtered out by slowing the response time of the digital filter.

Analysis of Operation

Conventional ac analysis has been used to characterize the switched-capacitor comb filter response.² The approach to this complex problem assumes that the sinusoidal input signal is quantized, as illustrated in Fig 4.

The voltage of the input signal, V_i , is considered to be constant (quantized) during the time a capacitor is switched to ground and charged (sampling interval). This is illustrated by the square-wave representation in Fig 4. The circuit of Fig 5 is used to analyze the charge on each capacitor during the time it is switched to ground.

The switch closes when capacitor C_n is switched to ground and remains closed until the switch rotates to the next capacitor, C_{n+1} . The quantized (constant) value of V_i is connected to the series RC combination when the switch closes. The voltage on capacitor C_n may charge or discharge as it is switched to ground, depending upon the polarity of V_i and the charge already on the capacitor, V_c . The output voltage V_o represents the voltage across the capacitor V_c just as the switch opens. It is proportional to the charge on the capacitor from the present value of V_i plus the previous value of V_c from the last iteration. The

value of V_o can be calculated as follows:

$$V_o(t) = V_i \left(1 - e^{-\frac{t}{nRC}} \right) + V_c e^{-\frac{t}{nRC}} \quad (\text{Eq 1})$$

where:

$V_o(t)$ = voltage on the capacitor as the switch opens

V_i = quantized input-signal voltage (assumed constant until the switch opens)

V_c = initial charge on the capacitor (from the last time it was switched to ground)

R = series resistor value

C_n = the capacitor switched to ground

n = number of capacitor

t = dwell time the switch remains closed

Eq 1 represents the continuous time response of charging a capacitor (C_n) for a single switch closure to ground. Note that the present calculated value of $V_o(t)$ becomes the value of V_c the next time the switch completes its rotation back to capacitor C_n and the new value of $V_o(t)$ is to be calculated.

So V_c is really $V_o(t)$ calculated n switch positions ago, or $V_c = V_o(t - n)$. Determination of the steady-state filter response requires that Eq 1 be used to calculate $V_o(t)$ continually as the switch completes many rotations. All of the successive values of $V_o(t)$ calculated must then be summed to produce the steady-state filter response. Indeed, it was done that way before modern digital-analysis techniques were in common use. Consistent with the theme of modernizing the design, the use of Z-transform techniques is introduced to develop the response of the filter. This technique is far simpler to analyze and understand.

We start the analysis by assuming that the input signal to be filtered is "sampled" at periodic intervals as illustrated by the dots in Fig 4. (Rules regarding the Nyquist sampling theorem discussed earlier must be observed.) The periodic samples of the input-signal amplitude can be delayed in time, multiplied (scaled) by fixed numbers and added together with present and past scaled values of the input-signal samples to produce the resulting sampled output. The sampled output is a digital simulation of the analog filter output. The term *digital simulation* means the filter-output amplitude is also described by discrete samples, rather than continuously, as in the case

of an analog system. This is a fundamental concept of DSP: A computer does the sampling, delaying, multiplying and summing of past and present scaled values of the sampled input signal to produce the digitally filtered output. The Z transform is a mathematical tool that describes exactly how the input signal samples are delayed in time, scaled and added together with past and present scaled samples to produce the desired output.

The signal-flow diagram of Fig 6 should help to understand the process better. The filtered output $V_o(Z)$ is equal to the sampled input signal $V_i(Z)$ multiplied by constant $(1 - h)$ plus the previous value of $V_o(Z)$ —taken n samples ago—multiplied by constant (h) . In our case, $n = 8$ because there are eight capacitors and the switch takes eight units of delay (samples) to make one complete rotation. How does this relate to our hardware example with the rotating switch? The present output $V_o(t)$ across a capacitor C_n as it is switched to ground is equal to the charge from the present input $[(1 - h) V_i]$ plus the voltage already on the capacitor $(h V_c)$ that was put there eight units of delay (switch positions) ago, $V_c = V_o(t - 8)$. Note that by substituting $h = e^{-t/(RCn)}$ you have Eq 1. Also note that $V_c = V_o(t - n)$ is analogous to $V_o(Z) Z^{-n}$ used to indicate the value of V_o taken n units of delay ago.

The equation describing the digital filter output in terms of the sampled input signal of our RDF filter is as follows:

$$V_o(Z) = (1 - h)V_i(Z) + hV_o(Z)Z^{-n} \quad (\text{Eq 2})$$

where

$V_o(Z)$ = the present output sample of the of the filter

$V_i(Z)$ = the present sample of the input signal

$V_o(Z) Z^{-n}$ was the value of the filter output $V_o(Z)$ n units of delay ago

h = scaling constant; $h = e^{-t/(RCn)}$

Eq 2 can be rearranged as follows:

$$H(Z) = \frac{V_o(Z)}{V_i(Z)} = \frac{1 - h}{1 - hZ^{-n}} \quad (\text{Eq 3})$$

Eq 3 is commonly referred to as the *system response*, $H(Z)$. Note that only simple algebra is needed to obtain the system response from Eq 2. Obtaining the system response from Eq 1 with conventional ac analysis is considerably more complicated, as it requires an infinite sum. The frequency response of the digital filter, $H(j\omega)$ is found by substituting $e^{-jn\omega t}$ for Z^{-n} in Eq 3. The frequency response of the

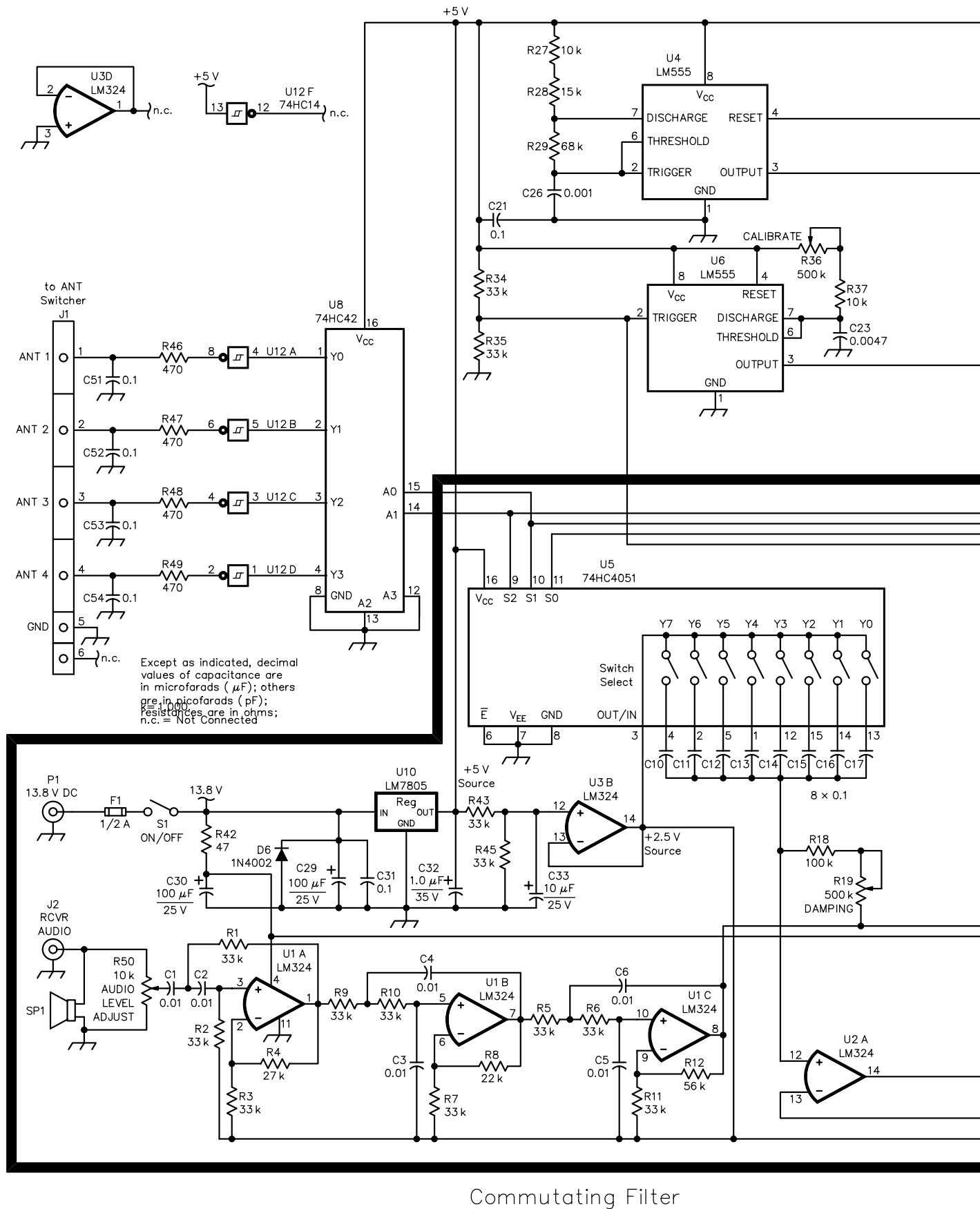
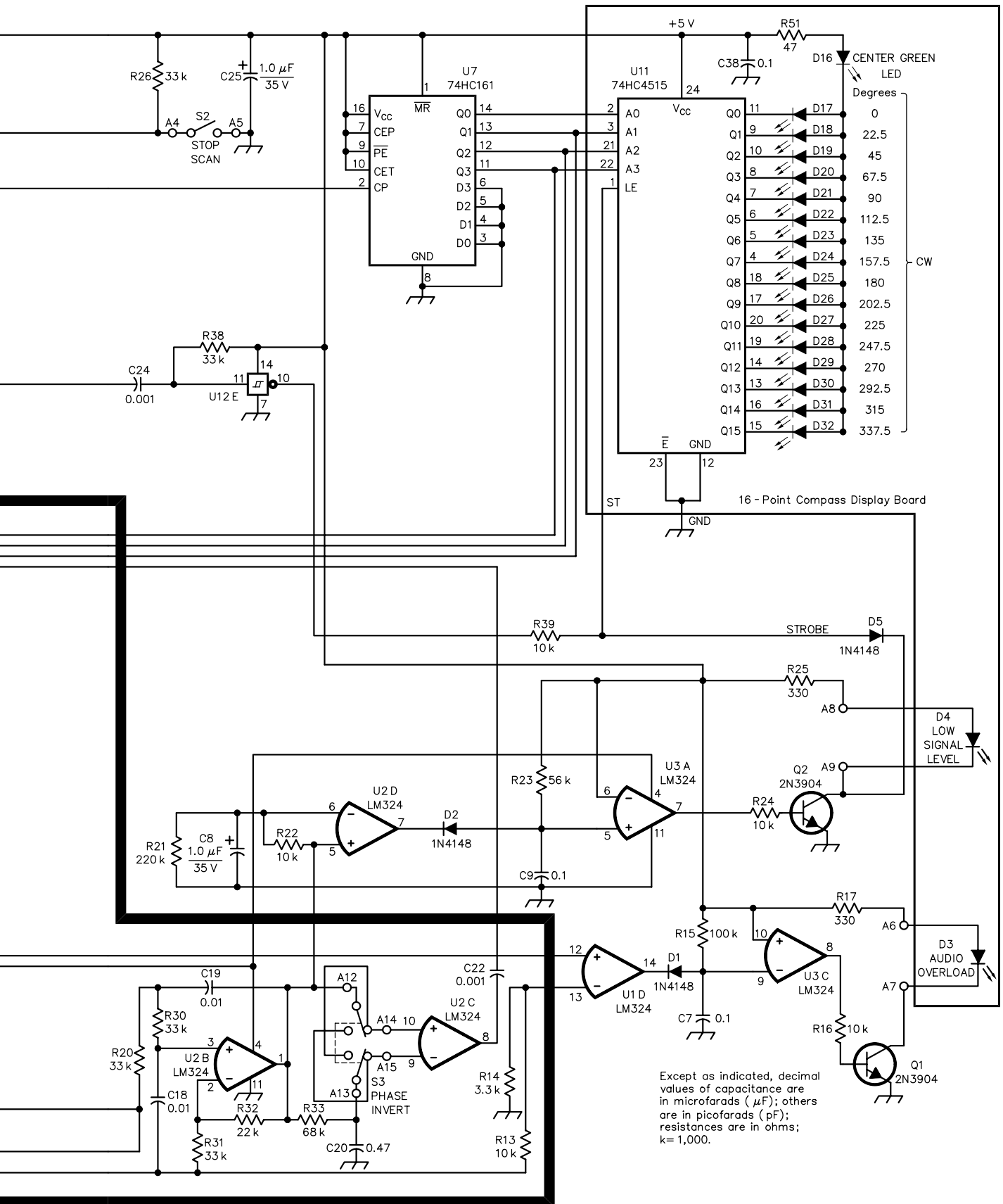


Fig 3—A modern implementation.



digital filter is:

$$H(j\omega) = \frac{1-h}{1-he^{-j\omega t}} \quad (\text{Eq 4})$$

This is the same result that would be obtained using conventional ac analysis but is much simpler. We need to call on a well-known identity to simplify this equation further. Recalling:

$$e^{-j\omega t} = \cos(\omega t) + j\sin(\omega t) \quad (\text{Eq 5})$$

Substituting Eq 5 into Eq 4 yields:

$$H(j\omega) = \frac{1-h}{1-h[\cos(\omega t) + j\sin(\omega t)]} \quad (\text{Eq 6})$$

Eq 6 describes the amplitude and phase response of our RDF digital filter as a function of frequency. We can separate the real and imaginary parts of the denominator as follows:

$$H(j\omega) = \frac{1-h}{[1-h\cos(\omega t)] + j[h\sin(\omega t)]} \quad (\text{Eq 7})$$

Eq 7 is of the form:

$$Y(j\omega) = \frac{1}{a + jb} \quad (\text{Eq 8})$$

We can determine the amplitude response of an equation in this form by taking the absolute value of both sides:

$$|Y(j\omega)| = \frac{1}{\sqrt{(a^2 + b^2)}} \quad (\text{Eq 9})$$

Applying this same process to Eq 7 yields:

$$|H(j\omega)| = \frac{1-h}{\sqrt{[1-h\cos(\omega t)]^2 + [h\sin(\omega t)]^2}} \quad (\text{Eq 10})$$

Multiplying out the denominator and recognizing the identity:

$$\sin^2(\omega t) + \cos^2(\omega t) = 1 \quad (\text{Eq 11})$$

Eq 10 becomes:

$$|H(j\omega)| = \frac{1}{\sqrt{\frac{h^2 - 2h\cos(\omega t) + 1}{(1-h)^2}}} \quad (\text{Eq 12})$$

The constant h we have been referring to is really just $e^{-t/(RCn)}$, where t is the sampling period, R is the value of resistor and C_n is the value of capacitor. Substituting the value of h into Eq 12 results in the amplitude-versus-frequency response illustrated in Fig 7 with values as follows: Clock period $t = 0.25$ ms, $R = 100$ k Ω and $C = 0.1$ μ F.

We can determine the bandwidth of our digital filter from Eq 12. Recall that 3-dB bandwidth is defined as the

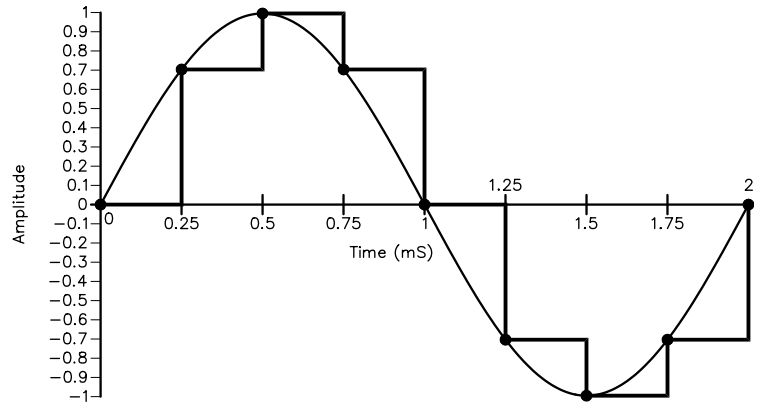


Fig 4—Sampling of an input sinusoid and the Sampled signal.

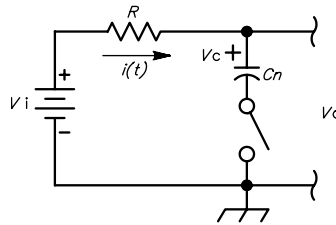


Fig 5—Charge analysis circuit.

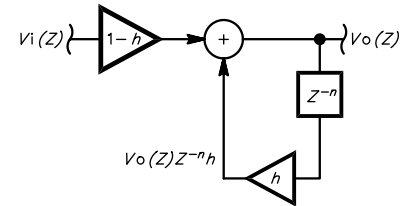


Fig 6—Signals in a commutating filter.

points where the amplitude response falls to 0.707 of the mid-band response. All we have to do is find the values of ω that make the value of $H(j\omega)$ equal to 0.707. This calculation is complicated by the fact that two such values reside on either side of each amplitude peak. Sorting through the math leads to the following relationship for bandwidth:

$$BW_{\text{Hz}} = \frac{1}{\pi n RC} \quad (\text{Eq 13})$$

where:

- BW_{Hz} = bandwidth in hertz
- R = resistance in ohms
- C = capacitance in farads
- $\pi = 3.1415926$
- n = the order of the filter (number of capacitors)

Note that the bandwidth of the filter only depends upon R , C and the order of the filter. It does not depend upon the sampling rate of the input signal. The bandwidth of our filter with $R = 100$ k Ω $C = 0.1$ μ F and filter order of 8 is 3.97 Hz. The Q of the filter

is determined by the relationship: $Q = f_o/BW$. The Q of our filter is $500 / 3.97 = 126$.

Mike Kossor, WA2EBY, was first licensed in 1975. He earned his MSEE degree in 1987 from Stevens Institute of Technology in Hoboken, New Jersey. Mike has been employed by Lucent Technologies for 15 years, where he designs high-linearity RF amplifiers for PCS and cellular base stations.

Notes

- ¹H. Busignies, M. Dishal, "Some Relations Between Speed of Indication, Bandwidth and Signal-To-Random-Noise Ratio in Radio Navigation and Direction Finding", *Proceedings of the Institute of Radio Engineers (IRE)*, May 1949, Volume 37, pp 478-488.
- ²W. R. LePage, C. R. Cahn, J. S. Brown, "Analysis of a Comb Filter Using Synchronously Commutated Capacitors," *AIEE*, March 1953, pp 63-68.
- ³C. Hutchinson, K8CH, and J. Kleinman, N1BKE, Editors, *The ARRL Handbook*, 1992 edition (Newington, CT: ARRL, 1991), p 8-20. □□

A Calibrated Panoramic Adapter

Build this panadapter for your station. It features a linearly calibrated sweep, a calibrated logarithmic detector with 80 dB on-screen dynamic range on a one-inch built-in display. It needs only a +12 V supply, ideal for battery-powered operation.

By Bob Dildine, 7J1AFR, W6FSH

This panadapter results from improvements made to my earlier version described in the July 1998 *QEX*.¹ The original design was for the 39-MHz IF of an ICOM 720A transceiver. This design is for the 70.455-MHz IF of a JST-245 transceiver. In addition to changing the input frequency, several improvements were made to the original design to improve frequency sweep linearity and increase dynamic range. An internal display was also added, and circuitry was redesigned to eliminate the need for several dc-dc converters

that were used to supply tuning voltage in the original design.

Objectives

The design goals remain the same as those for the panadapter previously described:

- Indicated signal level calibrated in decibels
- Linear, calibrated horizontal sweep
- Easily adaptable for different input frequencies
- Built-in display
- Powered from +12 V
- Simple, straightforward, reliable design
- No exotic parts

Block Diagram

The block diagram is shown in [Fig 1](#). The 70.455-MHz input signal is band limited and amplified before being

down-converted to 6.59 MHz by a crystal-controlled 77.045 MHz first LO. The 6.59 MHz first-IF signal is passed through a band-pass filter and amplified. It is then down-converted to 455 kHz by mixing it with the second LO signal. The second LO is a VCO that can be tuned from approximately 5.93 MHz to 6.34 MHz. The 455-kHz IF signal is amplified by a three-stage tuned amplifier, then passed to a log detector. The output of the log detector is a 0 to 10 V signal that is proportional to the logarithm of the input power to the panadapter at the rate of 10-dB per V. It is amplified and applied to the vertical deflection plates of the CRT. The overall gain of the panadapter is adjustable over a 50-dB range, in 10-dB steps, by changing the gain of individual stages with diode switches. This gain change is ar-

¹Notes appear on [page 22](#).

ranged such that gain is added at the stages closest to the detector first, so the sensitive front stages are not overloaded.

A scan generator produces a sawtooth wave that sweeps the second LO and provides 0 to 10 V of horizontal sweep for the display. This horizontal sweep signal is amplified and applied to the horizontal deflection plates of the CRT. A blanking pulse generated by the saw-tooth oscillator is used to blank the CRT during retrace.

The vertical output from the log detector, along with the horizontal and blanking outputs from the scan generator, are brought to connectors on the rear panel to drive an external display, if desired.

A small switching power supply—operating from +12 V—provides high voltage to the CRT and its deflection amplifiers. All other circuits are powered directly from +12 V.

Circuit Details: First Converter

The first converter is shown in Fig 2. The input signal to the panadapter is band limited by a six-pole band-pass filter centered at 70.455 MHz to reduce spurious responses. This filter is best

adjusted using a network analyzer or a spectrum analyzer and tracking generator, but a signal generator and detector can also be used.

A feedback amplifier provides about 6 dB of gain before the signal is applied to the first mixer. A pair of diodes switch additional resistors in parallel with one of the feedback resistors to increase the amplifier gain by 10 dB. An identical amplifier can be used to increase the gain of the first converter and provide another 10 dB of gain adjustment. When this was tried, the additional gain resulted in instability, probably because of unwanted coupling between the two stages, since they were built so close together. With just one amplifier stage, the panadapter is stable and its noise floor is still below atmospheric noise on the HF bands. The additional gain stage may be desirable if the panadapter is used with VHF equipment where atmospheric noise is lower.

The first LO is a 77.045-MHz crystal-controlled oscillator patterned after one from the *ARRL Handbook*.² This frequency was chosen because a crystal was readily available. A Minicircuits SRA-1 mixer converts the 70.455-MHz

input signal to the 6.59 MHz first IF.

Second Converter

The second converter is shown in Fig 3. A six-pole band-pass filter removes unwanted mixing products from the first converter. Again, this filter is best adjusted using a network analyzer or a spectrum analyzer and tracking generator, but a signal generator and a detector or oscilloscope can be used.

A feedback amplifier similar to the one used in the first converter provides about 6 dB of gain to overcome the loss of the second mixer. Resistors are switched in parallel with one of the feedback resistors to increase the gain by 10 dB.

The 6.59-MHz IF signal is mixed with the second LO signal in a Minicircuits SRA-1 mixer to produce the 455-kHz IF.

Second LO

The second LO, shown in Fig 4, is a varactor-tuned Hartley oscillator patterned after one of the VFOs shown in the *ARRL Handbook*.³ The varactor is a 400-pF unit designed for tuning AM radios. It is placed in series with a smaller capacitor. The value was

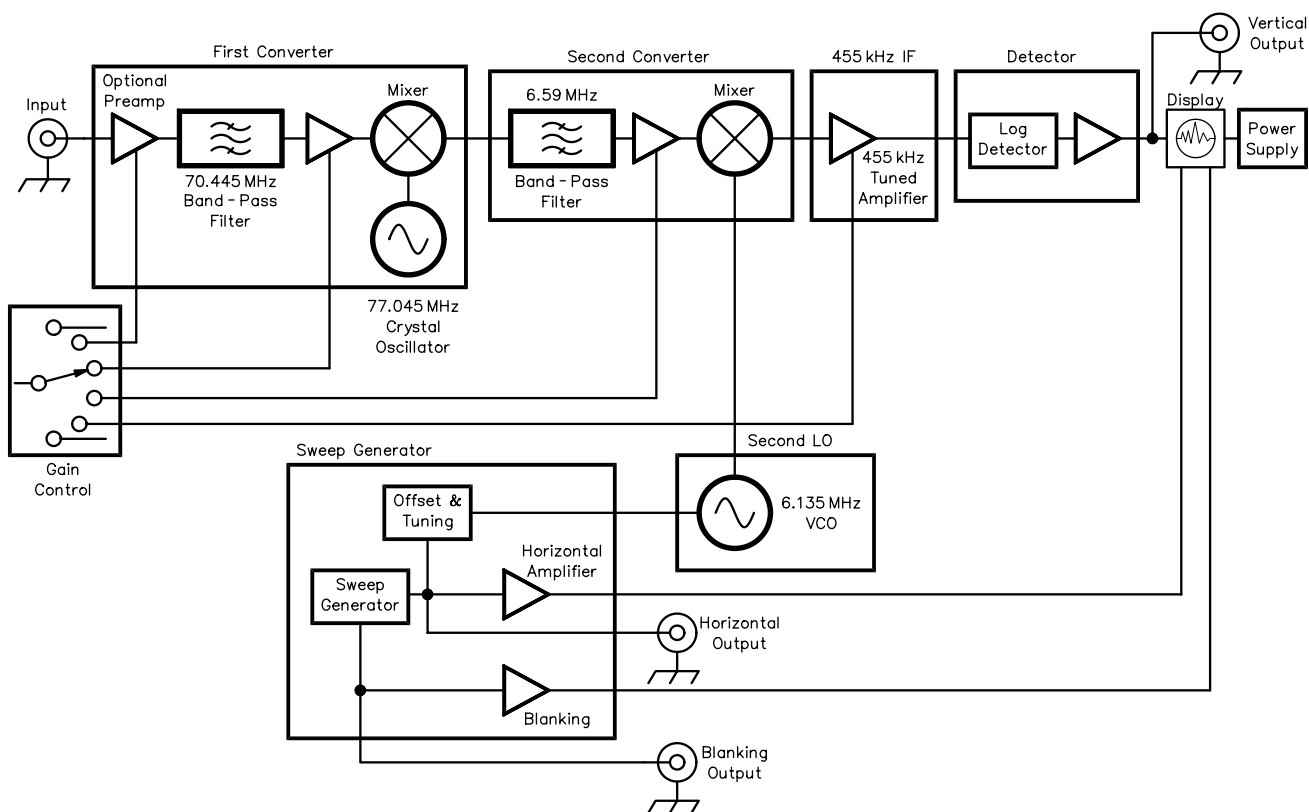


Fig 1—Block diagram.

Diodes are used to switch additional resistors across the emitters of the first and second stages to increase their gains by 10 dB.

Log Detector

The log detector is based on an

NE604 IF/Detector IC and is shown in Fig 6. This IC has a dc current output proportional to the logarithm of the input signal level over a range of approximately 80 dB. The detector circuit is patterned after the applications circuits shown in the Signetics data

book.⁴ The input to the IC is terminated with a 510-Ω resistor and is further loaded by ac coupling it to a 51 Ω resistor. This provides a 50-Ω input impedance for the detector circuit overall. This and the 510-Ω resistor across the input of the third amplifier stage con-

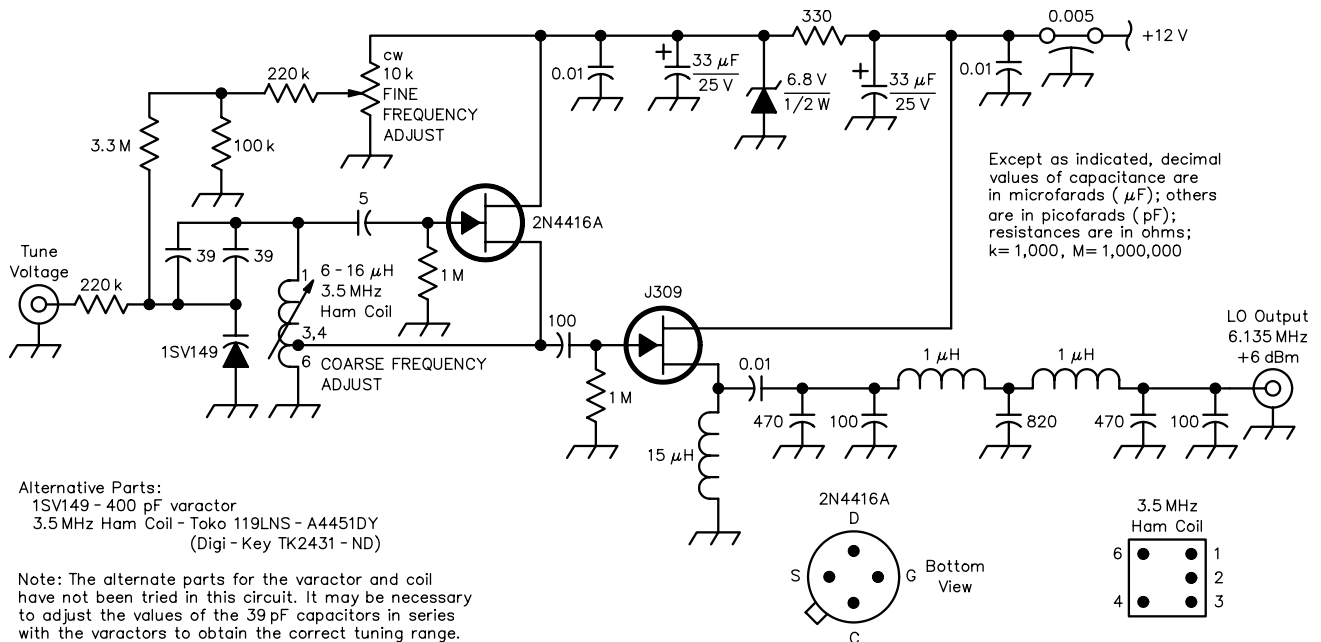


Fig 4—Schematic of second LO.

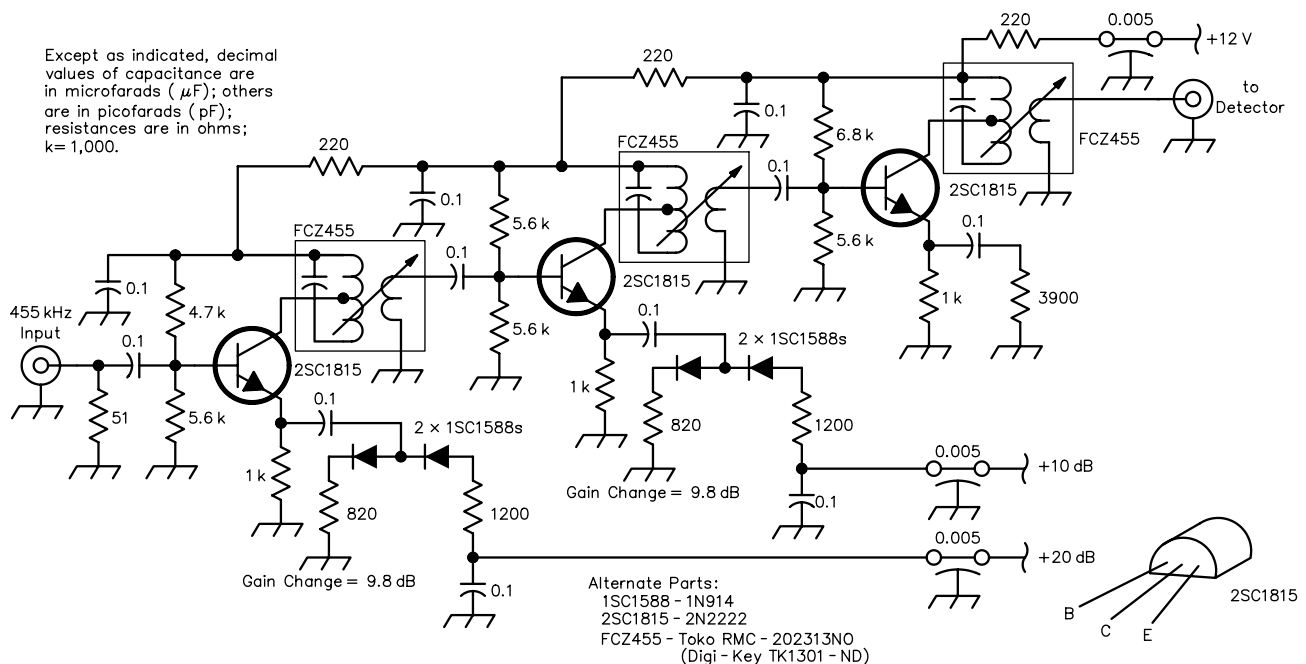


Fig 5—Schematic of 455 kHz IF amplifier.

the third stage, and that stage's 1500- Ω input impedance results in close to 12 dB of inter-stage loss. With this arrangement, over 80 dB of dynamic range was observed, and no effect of broadband noise from the first two stages was noticed.

The detector output is taken from the "RSSI" output (pin 5) of the NE604. This current source is about 50 μ A at full scale. It is terminated with a 100-k Ω resistor in series with a 50-k Ω trim-pot. The resulting voltage is am-

plified by an LM10 op amp configured to give a noninverting gain of two. The 50-k Ω trim-pot is adjusted to yield an output of 1 V for each 10 dB change in input signal. The LM10 was chosen because its input common-mode range includes its negative power supply, and its output can swing within a few millivolts of the negative power supply. This makes it easy to power the LM10 from a single 12-V power supply. The NE604 is powered from a 6.2-V Zener diode.

Note that with no input signal, the

detector output voltage should be close to zero. According to Signetics, a voltage greater than about 250 mV at pin 5 (500 mV at the output of the LM10) with no input signal indicates possible oscillation or regeneration.

Gain Control

A rotary switch and a simple diode matrix control the total gain of the panadapter by progressively increasing the gains of each gain-controlled stage. At the 0 dB setting, all stages

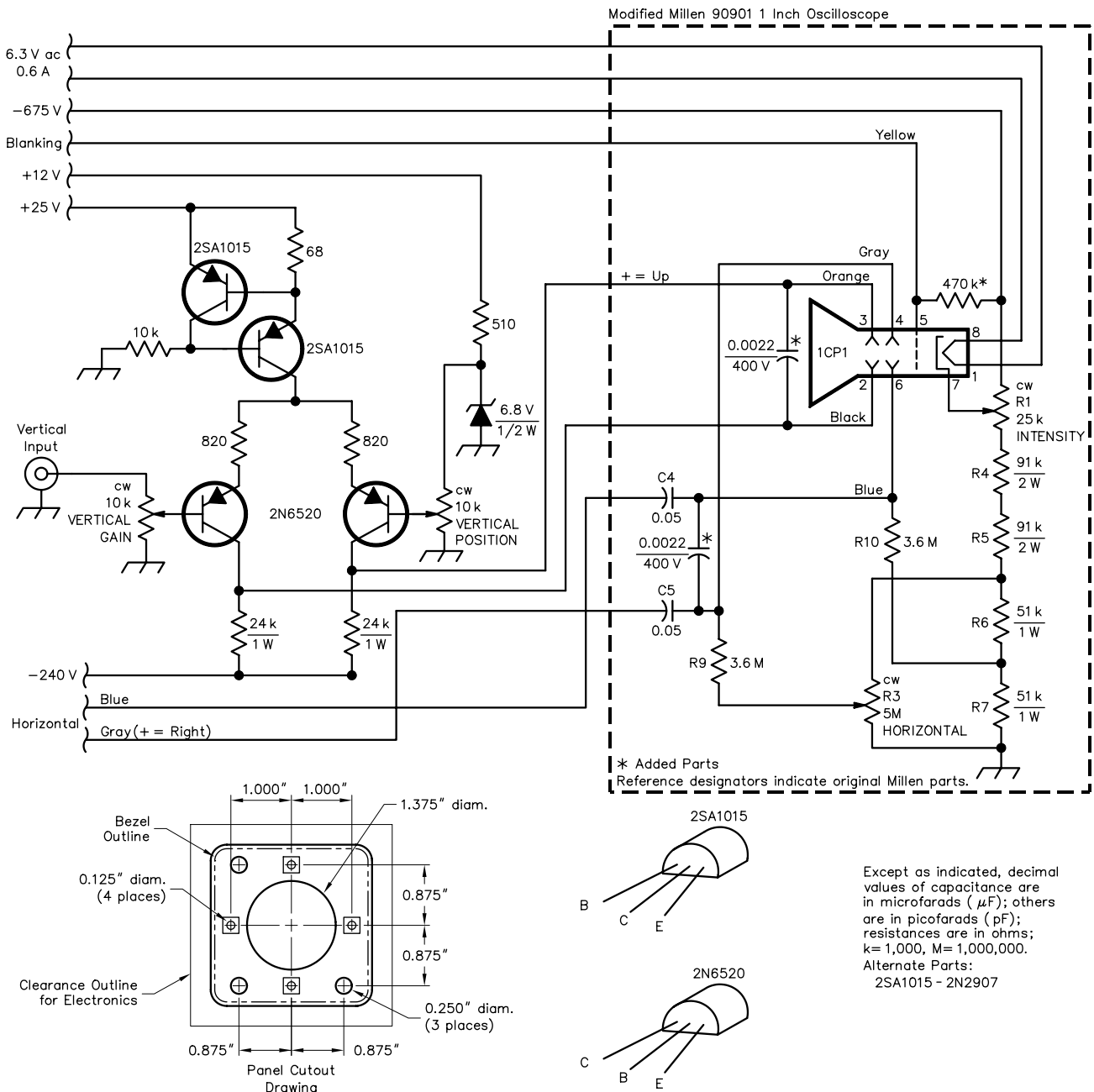


Fig 9—Schematic of CRT assembly.

are set to minimum gain. For each 10 dB increase in total gain, the gain of one stage at a time is increased, starting with the last 455-kHz IF amplifier, and ending with the 70.455-MHz input amplifier. Switching the gains in this order ensures that each stage is less likely to be overloaded by strong signals. Fig 7 shows the gain switch and diode matrix.

Scan Generator: The Ramp

The scan generator, shown in Fig 8, provides sweep voltage for the display and tune voltage for the VCO in the second converter. The sweep generator is based on a 555 timer and a current source consisting of a pair of PNP transistors. This same circuit was used in my original panadapter.⁵ The 555 timer is connected in the usual manner for an astable multivibrator,⁶ except that the timing capacitor is charged from the current source instead of a resistor. The 3.3- μ F timing capacitor is charged until its voltage trips the threshold comparator in the 555 at $\frac{2}{3} V_{CC}$. When that happens, the timer trips and discharges the timing capacitor through the 330- Ω resistor until its voltage falls below the trigger level of $\frac{1}{3} V_{CC}$. Thus, the voltage across the timing capacitor oscillates between $\frac{1}{3} V_{CC}$ and $\frac{2}{3} V_{CC}$. Because the capacitor is charged from a constant-current source, the rising part of this waveform is a linear saw-tooth. Its period is determined by the current source and the capacitor value. Sweep rate is adjusted by a trim-pot that adjusts the value of the current source. V_{CC} for the 555 and current source is provided by a 9-V regulated supply to make the sweep period and magnitude of the sweep voltage independent of variations in the panadapter's supply voltage. A small trim-pot is used to set this supply voltage to exactly 9 V. This assures that the horizontal sweep output is exactly 10 V peak-to-peak. The EXTERNAL DISPLAY trim-pot is used to set the start of the horizontal sweep at exactly 0 V. However, this may not be possible if the LM324 cannot pull its output all the way down to its negative power supply.

Tune Voltage

One half of an LM10 op amp buffers the 3 to 6-V saw-tooth signal to prevent loading the timing capacitor. One quarter of an LM324 op amp amplifies and offsets this voltage to provide a 0 to 10-V sweep signal for the display. The other three sections of the LM324 are used to generate the tune voltage for the VCO. One section provides a dc

voltage of 4.5 V that is referenced to the 9 V supplying the ramp generator. A portion of this dc voltage (determined by the setting of the CENTER FREQUENCY control) is summed with a portion of the ramp voltage (determined by the setting of the SPAN control) to provide the VCO tune voltage. The SPAN SET trim-pot is used to adjust the maximum span as described later.

Display Blanking

When the 555 timer trips, its output goes from about +9 V to about 0 V. This signal is inverted by a single transistor and made available at the rear panel as a positive-going 12 V pulse to blank an external display. The 555 output is also amplified by a two-transistor pulse amplifier to provide a negative-going pulse of about 65 V to blank the internal CRT display. A transistor of adequate voltage rating must be used for this amplifier.

Display: The CRT

The CRT assembly is a modified Millen model 90901 that was picked up at a swap meet. This is a one-inch CRT assembly—about the size of a panel meter—that was manufactured by Millen in the early 1950s. Its original use was as a general-purpose indicator for applications such as RTTY tuning or modulation monitoring. Because of the vintage nature of this unit, modifications were kept to a minimum. Nothing was done that would prevent the unit from being restored to its original condition. If another CRT is used, the following points should still be useful.

The schematic for the modified CRT assembly is shown in Fig 9. The original circuit used ac coupling for both horizontal and vertical inputs. The average value of the saw-tooth wave used for the horizontal sweep is constant, so ac coupling is acceptable for the horizontal input. However, the average value of the vertical signal changes according to what signals are displayed, so it is necessary to use dc coupling to the vertical input.

Deflection Amplifiers

The Millen CRT assembly was designed for use with a negative high-voltage power supply. This places the CRT deflection plates at about -120 V. Therefore, a single-stage PNP differential amplifier, shown in Fig 9, operating from a -240 V power supply was used to drive the vertical deflection plates of the CRT. The gain of this

amplifier is about 15, which is sufficient to provide more than full deflection with the 0 to 10 V signal from the log detector. A small trim-pot is used as a vertical gain control to set the height of the trace. The original 5-M Ω potentiometer used as vertical position control on the front panel of the CRT assembly was replaced with a 10 k Ω pot, connected to the differential amplifier to provide vertical position control. The emitters of the differential pair are supplied from a constant-current source (referenced to +25 V) to accommodate the 0 to 10 V swing of the input signal. Because of the high voltages used on the CRT deflection plates, it is necessary to use high-voltage transistors for the deflection amplifier. The 2N6520 transistors shown here have a collector-breakdown voltage of 350 V, and they are designed for small-signal applications. At first, a small amount of interference (probably from the switching power supply located close to the CRT) caused unwanted deflection of the CRT beam. Small capacitors placed across the vertical and horizontal deflection plates eliminated this problem. The deflection amplifiers cannot drive a large capacitance so use the minimum value necessary or distortion in the display may result.

The horizontal-deflection amplifier, shown with the scan generator in Fig 8, was built on the scan-generator board. It is identical to the vertical-deflection amplifier.

Power Supply

A small switching power supply, shown in Fig 10, was built to provide operating voltages for the CRT and the deflection amplifiers. A 555 timer provides a drive signal at approximately 100 kHz. This drives a 74HC74 flip-flop connected as a divide-by-two circuit to provide two symmetrical signals 180° out of phase, which in turn drive the switching FETs. This approach was used instead of the simpler self-oscillating or flyback circuits because it is easier to design.

The power transformer is wound on a ferrite pot core. Take care to insulate the high-voltage windings from each other, the primary winding and the pot core. A separate winding provides 6 V for the CRT filament. Because of the high-voltage applied to the CRT cathode, this filament winding should be well insulated.

Simple half-wave rectifiers are used for the +25 V and -240 V supplies, and a voltage doubler is used for the CRT

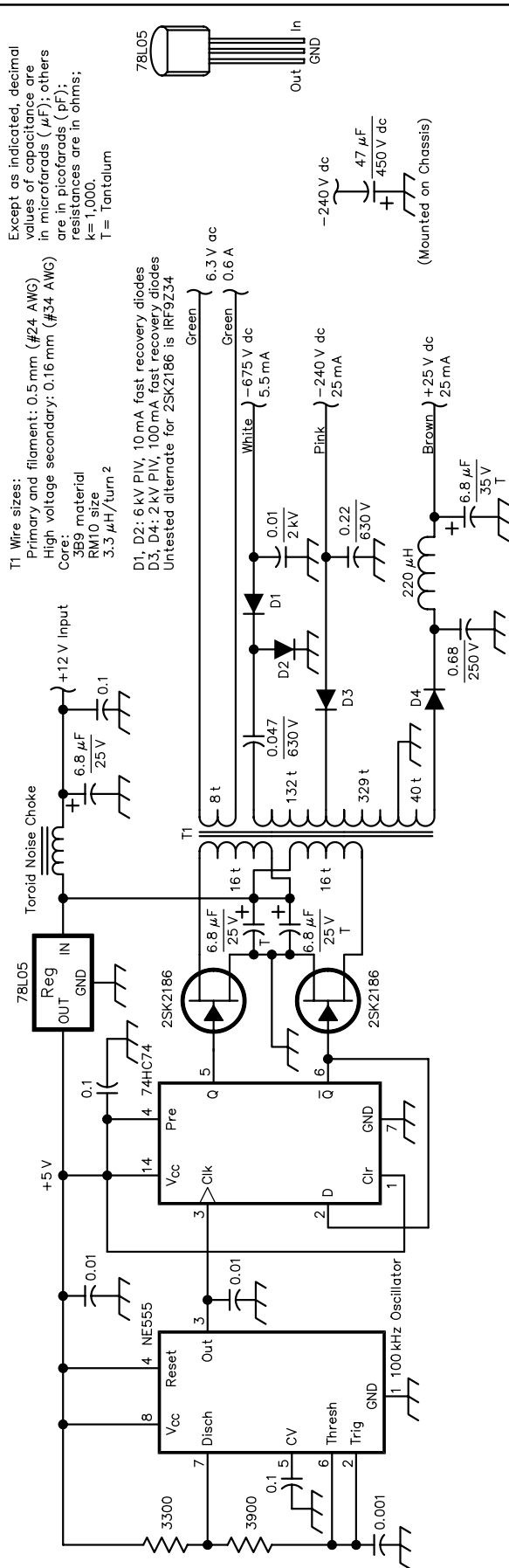


Fig 10—Schematic of high-voltage power supply.

high-voltage supply. Be sure to use fast-recovery high-voltage diodes here. Use adequately sized filter capacitors, since any ripple on the power supplies distorts the spot on the CRT and causes the trace to be fat. With the inputs to both the vertical and horizontal deflection amplifiers disconnected, you should see a pinpoint spot on the CRT at normal viewing brightness. *Be careful of the high voltages, and be sure to discharge all filter capacitors before working on the circuits.* The 47- μF capacitor on the -240 V supply will hold its charge for several days.

Both the high-voltage outputs and the primary circuits of the power supply were properly filtered with great care to prevent interference to the RF circuits of the panadapter or the station receiver. The power supply was built on a small piece of copper-clad board on which the circuit pattern was etched with a small hand grinder. Small heat sinks were used for the switching FETs. There has been no evidence of RFI from the power supply.

A small toggle switch on the rear panel turns off the 12 V feeding the CRT's power supply to disable it when using an external display.

Transceiver Interface

Some transceivers and receivers have built-in IF-output ports for use with a panadapter. Check the output-signal level of this port to make sure there is not excessive loss between the antenna input and the IF-output port. If it is necessary to add an output port to the receiver or transceiver, take the signal from the output of the first mixer, before any filters. (Most modern high-performance receivers have a crystal filter or other narrow-band filter right after the first mixer.) Use a buffer amplifier with high input impedance between the mixer output and the panadapter input to avoid loading the circuits in the receiver. Otherwise, the performance of the receiver could be seriously degraded.

The buffer amplifier should be placed inside the receiver with its input connected through the shortest possible coax lead. Even a few inches of 50- Ω coax have significant capacitance. The *output* lead of the buffer amplifier can be coax of any convenient length. It can usually be run through a vent hole in the receiver's cabinet rather than drilling extra holes for a connector. A suitable buffer amplifier using a dual-gate FET is shown in Fig 11.

Construction

The RF circuits were built dead-bug or ugly-style on copper-clad board. This makes modification and experimentation easy and avoids the mess and trouble of making PC boards. After testing, a small steel can was soldered over each circuit for shielding. Individual circuits are connected together with small pieces of miniature coax. The scan-generator assembly, including the horizontal-deflection amplifier, was built on a piece of perf board.

All circuits were mounted on a 26-by-21-cm aluminum base plate 3 mm thick, as shown in Fig 12. A 26-by-9-cm piece of 3-mm aluminum was used as the front panel. Front-panel labeling was done by plotting the artwork on a sheet of label stock (Avery or similar). The label stock was stuck to the front panel, covered with clear plastic laminating stock and the excess trimmed away with a sharp knife. The result is shown in Fig 13. The rear panel is a 26-cm strip of 3-mm aluminum wide enough to mount the connectors. Aluminum angle stock was used to mount and brace the front and rear panels.

The CRT assembly is mounted directly to the front panel. The Millen unit is small enough that additional bracing was not necessary, but if a larger CRT assembly were used, extra bracing would be required. A thin marking pen and machinist's square were used to draw a horizontal baseline about 1/4 way up from the bottom of the screen, and a vertical line in the center of the screen to indicate center frequency.

Final Adjustment: The Display

The CRT's INTENSITY control should be set to normal viewing intensity. A small cardboard tube (such as a toilet paper tube) can be used as a light shield if necessary. The VERTICAL POSITION control on the CRT assembly should be set to place the trace on the horizontal baseline with no signal on the panadapter input.

The horizontal position and horizontal gain controls on the scan generator should be set to give a full-width trace centered on the screen.

VCO Center Frequency

Set the front-panel CENTER FREQUENCY control to zero (the midway point on the potentiometer), and set the SPAN control to zero (fully counterclockwise). Use a frequency counter or receiver to set the VCO frequency to exactly 6.135 MHz, as indicated in the

VCO section above. Then connect the panadapter to the receiver or transceiver. Set the CENTER FREQUENCY control to zero and the SPAN control to a convenient value—such as 100 kHz—and tune the receiver to a strong, steady signal such as a broadcast station or signal generator. The signal should appear on the CRT near the centerline.

Adjust the fine-frequency control on the VCO assembly to center the signal.

Span Set

Set the SPAN control to a convenient setting such as 100 kHz. Then, using either a comb generator or signal generator connected to the panadapter's input, or using off-the-air sig-

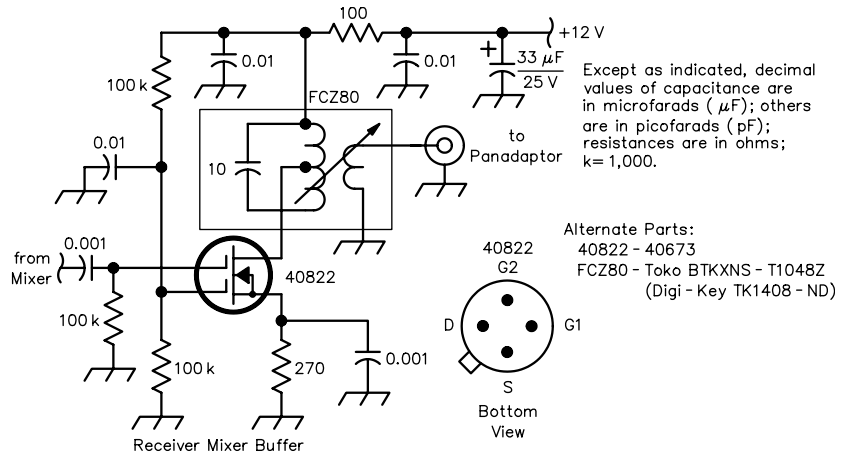


Fig 11—Schematic of IF buffer amplifier for use between receiver/transceiver first mixer and the panadapter.

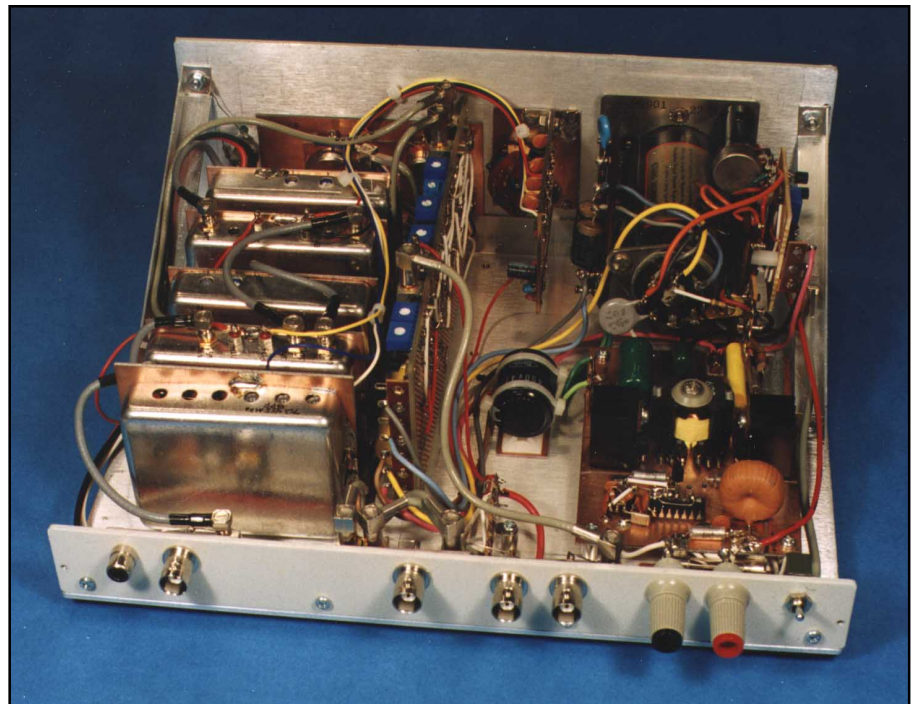


Fig 12—A rear view of the panadapter. RF circuits are on the left, the scan-generator board is in the middle and the Millen CRT assembly and high-voltage power supply are on the right. The RCA and BNC connectors on the left of the rear panel are the input, the three BNC connectors in the middle are outputs to an optional external display, and the binding posts are for the 12 V power. The CRT power switch is on the extreme right.

nals, adjust the SPAN SET trim-pot on the scan-generator assembly to set the panadapter sweep width equal to the SPAN control's setting.

Sweep Speed

Set the SPAN control to maximum, and adjust the SWEEP RATE trim-pot on the scan generator for a comfortable sweep rate. Be careful not to use too fast a sweep rate, or distortion will occur on displayed signals. This is because the signals sweep through the IF filters before they have time to respond.

Operation

Operation of the panadapter is straightforward. As the receiver is tuned upward in frequency, signals appear to move from right to left. Different types of modulation can be identified with practice, and it is interesting to watch occasional signals sweep across the band. The logarithmic response calibrated in decibels is a more-accurate way of measuring signal strength than the usual S-meter reading. Setting the span control to 100 kHz gives a good look at the band 50 kHz either side of the receive frequency. With a calibrated horizontal scale, you can tell exactly how far up, or down, the band a signal is, or where a clear spot is just by glancing at the panadapter display. Fig 14 shows 100 kHz of the 20-meter band on the internal display during a quiet evening. Figs 15 and 16 show 100-kHz segments of the 31-meter shortwave broadcast band and the 80-meter amateur band, re-

spectively, on an external display.

Finding Center Frequency

During normal operation, the VCO might drift slightly, but this can be compensated by slight adjustment of the CENTER FREQUENCY control. The actual center frequency can be found by tuning in a known station or by momentarily keying the transmitter. On most modern transceivers, the transmitter signal is generated by the same mixers used for the receiver, so it appears at the panadapter port during transmit at the exact IF of the transceiver. Thus it can be used to quickly set the CENTER FREQUENCY control so that the transmit signal (and thus the

received signal) is at the center of the screen.

The panadapter can also be used to check the bandwidth of the transmit signal, but bear in mind that this is the signal before any power amplification, and the panadapter will not show splatter caused by over driving the amplifiers.

Gain-Control Settings

The panadapter gain control should be kept to the minimum gain consistent with displaying the signals in the band of interest. For operation on the ham bands, use just enough gain to show the background noise on the screen; 30 or 40 dB is usually sufficient. On the do-



Fig 13—Front panel showing controls and display.



Fig 14—A close up of the CRT shows signals on 20 meters. Center frequency is 14.2 MHz, span is 100 kHz.

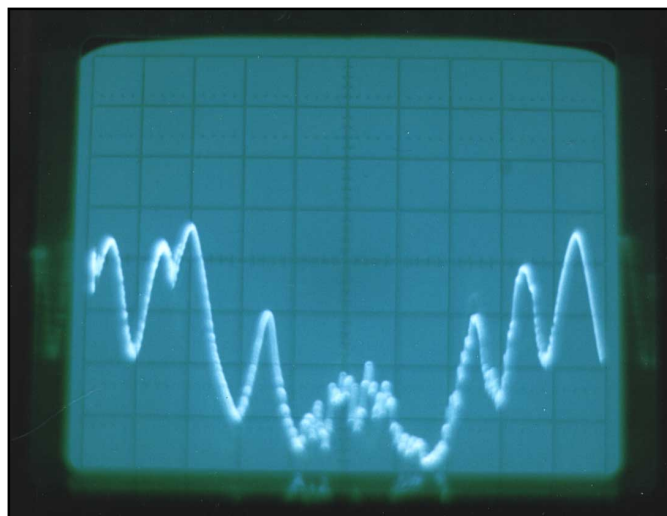


Fig 15—An external display shows the 31-meter shortwave broadcast band. The center frequency is the BBC signal at 9740 kHz. There was severe QSB and the camera caught the signal at the bottom of a fade.

mestic or international broadcast bands where many large signals are present, much less gain is required; 0 to 20 dB is usually sufficient.

Frequency Response: Dip at Receiver's IF Filter

With some receivers and transceivers, a dip of as much as 15 to 20 dB in the displayed signal level will be noticed as the receiver is tuned across a station. This is normal and is caused by the varying impedance match of the receiver's mixer and first IF filter. The impedance match is correct at the receiver's IF, so most of the signal is being absorbed by the receiver's IF filter, leaving less for the panadapter. Fig 17 shows the measured response as the JST-245 is tuned through a signal.

This dip at center frequency could be avoided by using a power divider between the receiver's mixer and IF filter to obtain the panadapter signal. This would mean significant modification of the receiver.

Spurious Responses

The panadapter is subjected to many signals from the receiver besides the ones being displayed. The receiver's first LO will be at a frequency equal to the receiver IF plus the received frequency, and the mixer's image signal will be at a frequency equal to the receiver IF plus twice the received frequency. Both these signals can be strong, and when the received frequency is low, such as in the AM broad-

cast band or the 160-meter band, it is likely they will fall within the passband of the panadapter's input filter. This can cause overload of the panadapter's first amplifier and result in spurious responses. For this reason, it is best to keep the panadapter's gain low, using only enough gain to provide an adequate display. If interference from other signals in the receiver is suspected, check the receiver's IF with a wideband spectrum analyzer, or place an attenuator (10 dB or so) between the receiver and the panadapter to see if this influences the level of any spurs.

With some receivers, occasional spurious signals will show up on the panadapter that are not heard in the receiver. These are usually mixing products from within the panadapter caused by the receiver's LO or image signals. For example, the panadapter has an image response at the frequency equal to the first LO plus the first IF. (77.045 MHz + 6.59 MHz = 83.635 MHz for the design shown here.) Although the input band-pass filter attenuates signals at this frequency, the receiver LO will probably be strong enough to show up as a weak signal on the panadapter when it is at this frequency. In this design, this happens when the receiver is tuned to 13.18 MHz. This signal can be readily identified because it moves in the opposite direction from the other displayed signals as the receiver is tuned.

Also, the receiver's mixer and LO produce IF signals at frequencies

equal to the sum and difference of the receiver's input frequency and its LO frequency. The IF signal corresponding to the difference is the desired IF and is displayed by the panadapter. The IF corresponding to the sum is filtered out by the receiver's IF filter, but when it falls at the panadapter's image-response frequency (83.635 MHz), strong signals can show up as spurious responses on the display. This happens when the receiver is tuned to 6.59 MHz, but as the receiver is tuned, the spurious responses move in a direction opposite to that of real signals being displayed.

Other Uses

The panadapter can be put to other uses. Combined with a general-coverage receiver and a signal generator with calibrated amplitude, it can be used as a calibrated selective-level meter with a total dynamic range of about 130 dB. This might be useful for measuring small signals or adjusting circuits.

The panadapter and general-coverage receiver combination can also be used as a narrow-sweep spectrum analyzer. The sweep range of the second LO could be expanded, or a wider-range VCO could be used for the first LO.

Use with Other Receiver IFs

The panadapter can be modified for other receiver IFs by changing the frequencies of the input band-pass filter and first LO. For receiver IFs lower

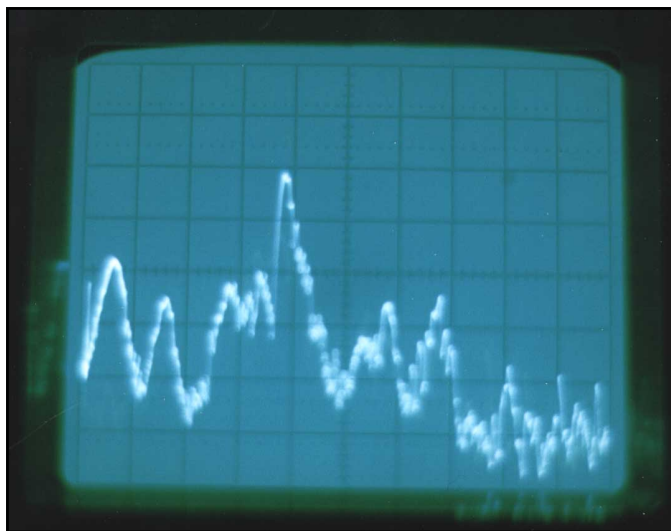


Fig 16—An external display shows the 80-meter band in Japan. Center frequency is 3550 kHz and span is 100 kHz. The Japanese 80-meter band is 3500 to 3600 kHz with the phone band from 3525 to 3600 kHz. Note the modulation sidebands on the phone signals.

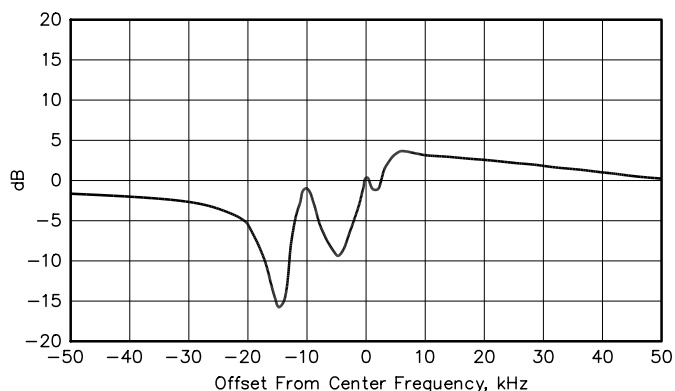


Fig 17—A chart of the JST-245 receiver IF response. See the text under "Frequency Response: Dip at Receiver's IF Filter" for a discussion of the phenomenon shown here.

than about 10 MHz, such as those around 8 MHz found in some Kenwood equipment, the first converter can be replaced by a suitable amplifier, or eliminated altogether.

The panadapter IF and LO frequencies were chosen based on crystals that were readily available, and the desire to use readily available IF transformers in the 455-kHz IF amplifier. Other IF and LO frequencies can be chosen to make use of readily available crystals and filters. They should work equally well if a few basic principles are followed.

Use a crystal-controlled oscillator for the first LO, especially if working with a receiver IF that is above about 10 MHz. Otherwise, it may be difficult to maintain adequate frequency stability. Choose the frequency of the panadapter's first IF such that it is not much less than about one tenth of the input frequency in order to minimize problems with mixer images in the first converter.⁷ The first LO can be either higher or lower than the input frequency, depending on what crystals are available. In this design, the first IF of 6.59 MHz was dictated by the 70.455-MHz input frequency and the availability of a 77.045-MHz crystal for the first LO. The frequency of the panadapter's second IF should be chosen such that good selectivity can be obtained with easily available tuned circuits. 455 kHz is convenient, but if good-quality tuned circuits such as crystal or ceramic filters are available at other frequencies, they should be considered. Be careful of using unknown filters without thoroughly evaluating them first. The second LO frequency is determined by the frequencies of the panadapter's first and second IFs. Again, the second LO can be either higher or lower than the second IF.

A good analysis of the mixing relationships of the first and second LO signals and the second IF should be done to make sure there are no spurious signals or responses generated by unwanted mixing products or harmonics. For example, don't choose a second LO frequency that has a harmonic that falls within 100 kHz or so of the panadapter's input frequency. Also, an analysis of the mixing relationships, including the receiver's input frequency and first LO, will determine the direction that the VCO needs to sweep so that signals appear to move from right to left as the receiver is tuned upward in frequency. If the signals appear to move from left to

right as the receiver is tuned upward, then the VCO sweep direction will need to be reversed.

Follow-on Work

There is always room for improvement in any project, and this one is no exception. I've mentioned that the frequency response of the 455-kHz IF filters is somewhat broad below about -60 dB. More work could improve the shape factor of the 455-kHz amplifier. Part of the problem may be coupling around the tuned circuits because of the compact nature of the construction used. It might be useful to spread this circuit out and incorporate more shielding between stages.

The one-inch CRT used for the internal display is somewhat small, but seems to be adequate after using it for a while. It should be possible to use a larger CRT without increasing the size of the panadapter too much. A larger high-voltage power supply would probably be required, and different deflection amplifiers may be needed. It should also be possible to incorporate a digital display of some sort. Of course, a small PC running an oscilloscope program could be used for an external display.

The VCO is somewhat sensitive to temperature. More effort could improve its frequency stability either with better parts or some sort of temperature compensation. It may also be possible to use a DDS chip to build a completely synthesized sweeping oscillator.

The log fidelity of the NE604 is adequate for this application, but it does have a slight nonlinearity that shows up as a wiggle on the side of the signal response about 40 dB down from the top. It may be possible to eliminate this wiggle with careful attention to the gain distribution in the log detector. On the other hand, it is only noticeable with very strong signals.

Summary

The panadapter has been in use for several months with no problems. It is easy to spot signals as they come on the air, especially when tuning across a band that has little activity. After using a panadapter for only a few hours, you quickly become accustomed to it. Without it, you feel like you are operating with tunnel vision.

Notes

¹R. Dildine, 7J1AFR, W6SFH, "An Updated Electronic Eyeball," *QEX*, July/August 1998, pp 38-44.

²B. Hale, KB1MW, *The 1989 ARRL Handbook* (Newington: ARRL, 1988), p 31-18.

³Ibid, p 10-8.

⁴*RF Communications Data Handbook*, Signetics Co, 1990.

⁵R. Dildine, 7J1AFR, W6SFH, "An Updated Electronic Eyeball," *QEX*, July/August 1998, pp 38-44.

⁶R. Marshall, WB6FOC, "Operational Characteristics of the 555 Timer," *Ham Radio*, March 1979, p 32.

⁷For receiver IFs higher than about 70 or 80 MHz, it may be necessary to add another stage of frequency conversion to the panadapter. □□

2 Meter and 440 Low Pass Filters

Reduce multi-multi harmonics and noise!

DCI now has high power, very low loss low-pass filters for 440 and 2 meters. These filters reduce your second harmonic by about 38 dB, and third and higher order harmonics by over 50 dB. They should go a long way toward reducing interference to 440 and 1296 from 2 meter and 440 transmitters in VHF/UHF multi-multi contest stations. They go between the linear and the antenna and reduce the broad band noise and harmonics generated in the linear. The estimated power handling capability is 2 KW, and the passband loss is about 0.15 dB.

If you are interested in these filters, they are priced at \$159 for the 440 model and \$259 for the 2 meter model. You are protected by DCI's unconditional return policy during the first year.

DCI DIGITAL COMMUNICATIONS INC.

Box 293, 29 Hummingbird Bay,
White City, SK, Canada S0G 5B0

Direct (306) 781-4451 • Fax (306) 781-2008

Toll-Free 1-800-563-5351

<http://www.dci.ca> email: dci@dci.ca

A New Look at the Gamma Match

For years the gamma match has been modeled as a folded dipole. What if its operation more closely resembles a hairpin match? Here is a model based on the hairpin that appears to predict reality better than the traditional models.

By Ron Barker, G4JNH, VK2INH

The gamma match provides antenna builders with a number of advantages over other methods of connecting coaxial feed to a beam antenna. It provides fully adjustable impedance matching, a balun function, and it eliminates the need for the driven element to be split at the center, thus enabling the use of “plumber’s delight” construction. The gamma match was described in *QST* in 1949 by Washburn¹ and has been widely used for nearly half a century. However, despite its many advantages, most commercially made HF Yagi’s use alternate matching methods that require the driven element to be split. The likely reason for this is that the gamma match has a reputation for adjustment difficulty. Whereas with other methods of feeder connection, only driven-element length

need be adjusted to optimize SWR, the gamma match adds two further variables—the gamma-section length and the gamma-capacitor tuning. All variables interact, and setup can be tiresome and frustrating.

Washburn’s groundbreaking article did not attempt to explain the operation of the gamma match other than the following: “It was reasoned that if the outside of the coax was to be cold, it should be connected to the center of the driven element, and so it was duly connected to the aluminum boom. It was also reasoned that if we started from the center (minimum impedance) and started looking toward one end (very high impedance) we should find a 52-Ω point at which we could connect the center conductor of the coax for the best possible match.”

Twenty years later, the problem of gamma-match adjustment was addressed by Healey in *QST*.² Healey proposed a model of the gamma match in which the impedance transformation is based on the principle of the folded dipole, wherein the transformation ratio is a function of the relative diameters of the two conductors. For the gamma match, these are the driven element and the gamma rod.

¹Notes appear on [page 31](#).

171 Leicester Rd
Ashby de la Zouch
Leicestershire LE 65 1TR
England

Healey went on to present a method of calculating the required gamma-section length and capacitor value that subsequently appeared in *The ARRL Antenna Book*.³

Several years later in 1973, Tolles detailed a method of designing gamma matching networks in which the mathematical technique differed significantly from Healey's, but which was based on the same folded-dipole approach.⁴ Since that time, the Healey/Tolles model of the gamma match has evidently become universally accepted.

Experience at G4JNH

Several years ago, an aged three-element tribander at G4JNH was replaced with a three-element, 20-meter monobander with a gamma match. Although the supporting tower has a tilt-over facility, it was not possible to use

the accepted method of making initial gamma match adjustments with the reflector at ground level and the antenna firing upwards. Because of space limitations at ground level, the antenna has to be partially dismantled to fully tilt the tower. It was therefore decided to take the trial and error out of the adjustment procedure by using Healey's model to work out the gamma-section length and capacitor setting. Unfortunately, it didn't work. At about that time, a copy of *The ARRL Antenna Book* (17th edition) was purchased. Included was a computer diskette containing a gamma-match program based—evidently—on Tolles' article (see Note 4). That didn't prove successful either.

It was therefore necessary to optimize the adjustments by a process of systematic trial and error. The tower was tilted and the antenna partially dismantled for each ad-

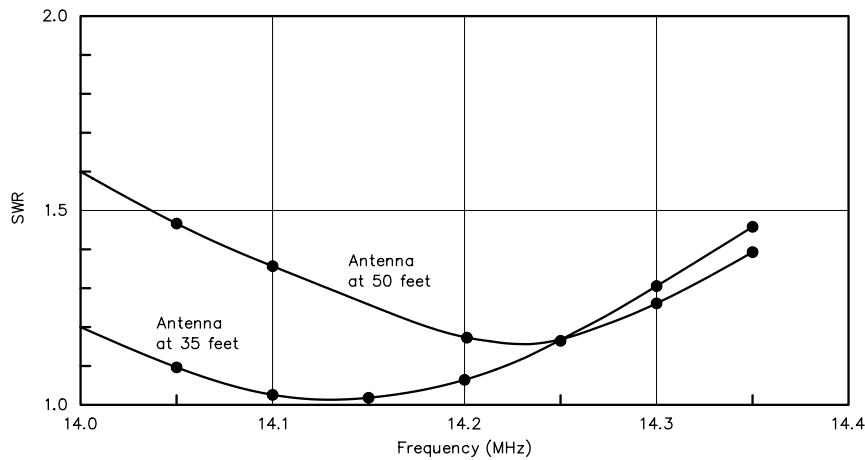


Fig 1—SWR versus frequency of G4JNH antenna.

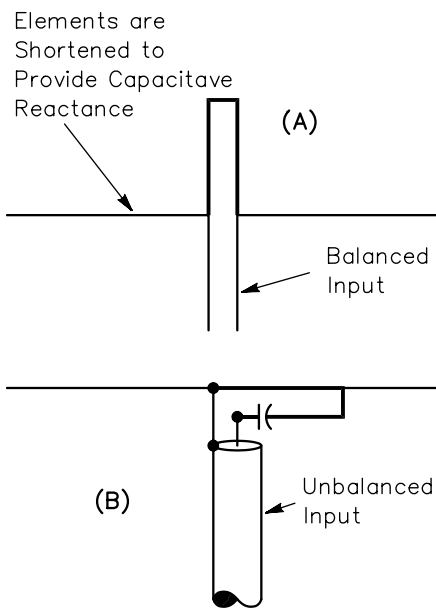


Fig 2—(A) Hairpin match. (B) Gamma match.

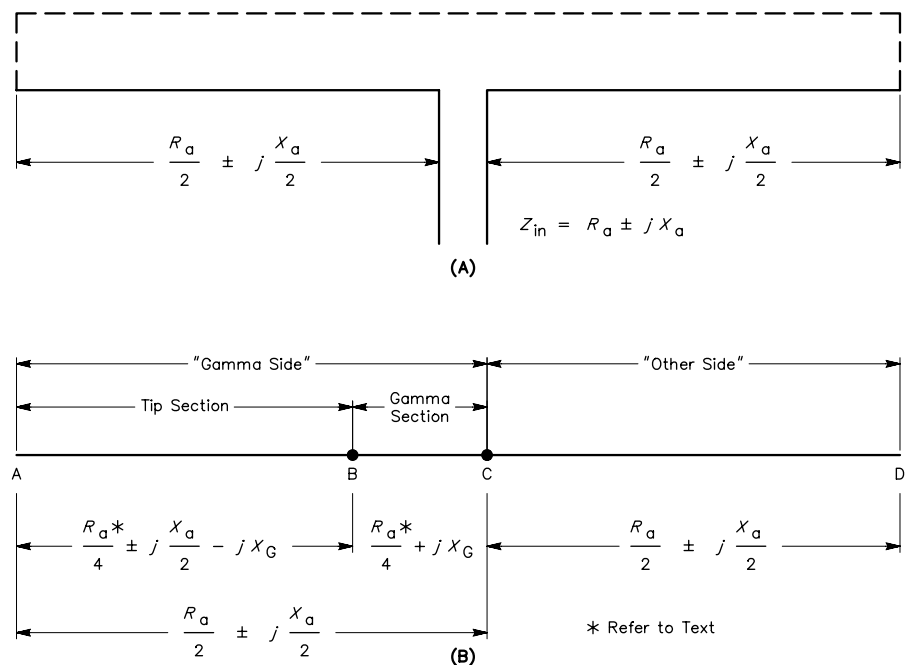


Fig 3—(A) $\lambda/2$ dipole. (B) Dipole configured for gamma match.

justment. An R-X bridge was available, which reduced the number of trials considerably over what would have otherwise been required measuring only SWR. The SWR curves obtained in this way are presented in Fig 1.

Because of this experience, a study was undertaken to explore an alternate approach as to how the gamma match might work. The outcome is the subject of this article. It approaches the problem from a different perspective and produces different results that are in very close agreement with my own observations.

The New Approach

For many years, I had been intrigued by the apparent similarity between the hairpin match and the gamma match (see Fig 2) and the very different explanations of how they work. The hairpin match was described by Gooch, et al, in a classic 1962 *QST* article.⁵ Briefly, the element is shortened slightly to introduce some capacitive series reactance, and the parallel inductor (the hairpin) provides the other arm of an L-match to bring the resistance up to that of the feed line, and thus to resonance. This depiction is very different from that of the accepted gamma match model, already outlined. During our discussion, it may be helpful to refer to the “List of Symbols” sidebar.

This study sought to explain the operation of the gamma match using a similar approach to that of the hairpin match. Fig 3A shows a $\lambda/2$ dipole with a feedpoint impedance of $R_a \pm jX_a$. At resonance, of course, jX_a would be zero. The feedpoint impedance can be considered to be divided equally between the two halves of the dipole, which behaves as though the two halves were connected in series, as shown by the dotted line in the figure.

Fig 3B shows the same element as it would be configured for use with a gamma match. On the left-hand side, point B represents the position of the gamma tap where the shorting bar connects the gamma rod to the element. In a typical case, the length of the gamma section BC is about 0.05λ . This makes it about 20% of the half-element λ length. The tip section AB can therefore be considered as one half of a dipole that has been shortened by 20% from its resonant length. Many sources were consulted to try to establish the impedance of such a dipole. *The ARRL Antenna Book*, 17th edition shows the effect of shortening a dipole by up to about 5%, and by extrapolation, shortening by 20% would reduce the radiation resistance by about 50%. The amount of capacitive reactance introduced is dependent on

the length-to-diameter ratio of the element.⁶ The same source shows that reducing the length of a vertical antenna from 88° at resonance to 70° (20%) also reduces the radiation resistance by about 50%.⁷ Two other sources gave similar figures.^{8,9} So if this situation holds good for a driven element with a gamma match, the radiation resistance on the gamma side of the element would be divided equally between the tip section and the gamma section. This point will be re-examined later in the article. Since the tip section has capacitive reactance, the gamma section must have a corresponding inductive reactance. At resonance, when $jX_a = 0$, the inductive reactance of the gamma section would have the same numerical value as the capacitive reactance of the tip section.

A value of X_G can be assigned to represent the reactance of the gamma section. If it is accepted that the radiation resistance of the half element is divided equally between the tip section and the gamma section, then the impedance of the gamma section will be $(R_a / 4) + jX_G$. But the gamma side of the element has an impedance of $(R_a / 4) \pm (jX_a / 2)$. The impedance of the tip section must therefore be the difference between the two:

$$Z_{\text{tip}} = \frac{R_a \pm jX_a}{2} - \left(\frac{R_a}{4} + jX_G \right) \\ = \frac{R_a}{4} \pm \frac{jX_a}{2} - jX_G \quad (\text{Eq 1})$$

If an RF voltage is applied between points B and C in Fig 3B, there are two current paths. One is through the gamma section, and the other—in parallel with the first—is through the tip section and the “other side,” which appear in series. The equivalent circuit is shown in Fig 4. The relationship among the various parameters is defined by the following equations:

$$\frac{1}{Z_{\text{in}}} = \frac{1}{Z_{\text{gamma section}}} + \frac{1}{Z_{\text{tip section}} + Z_{\text{other side}}} \quad (\text{Eq 2})$$

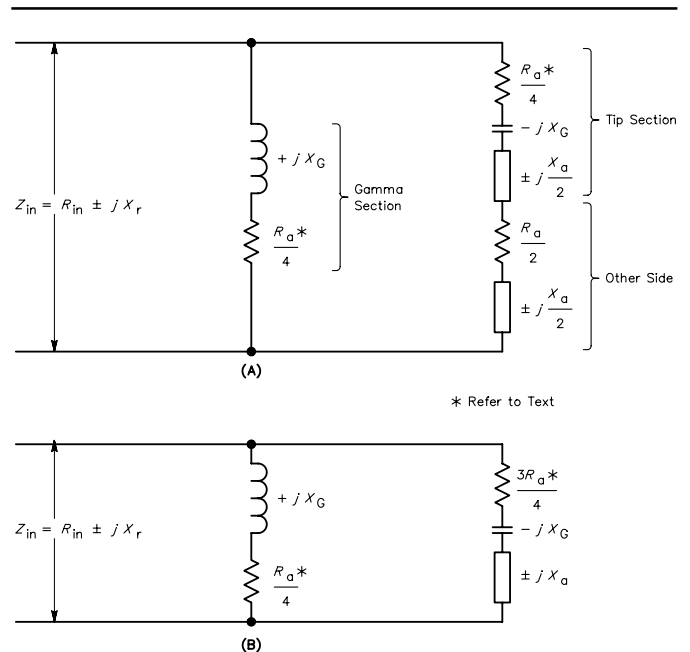


Fig 4—(A) Equivalent circuit of Fig 3B. (B) Simplified version of Fig 4A.

List of Symbols

- R_a : Feedpoint resistance of antenna
- X_a : Feedpoint reactance of antenna
- R_d : Free-space feedpoint resistance of the driven element
- X_G : Inductive reactance of gamma-section of driven element
- X_r : Residual reactance seen at the gamma tap point on driven element
- X_g : Inductive reactance of gamma rod
- X_s : Inductive reactance of shorting bar and connecting leads
- X_t : Total inductive reactance of gamma system, excluding gamma capacitor
- X_c : Gamma-capacitor reactance
- C_g : Gamma-capacitor capacitance
- L_G : Inductance of gamma section of driven element
- L_g : Inductance of gamma rod
- K : Correction factor (see text)
- R_{in} : Resistance seen at antenna feed terminal

$$\begin{aligned} \frac{1}{R_{in} + jX_r} &= \frac{1}{\frac{R_a}{4} + jX_G} + \frac{1}{\frac{R_a}{4} + \frac{jX_a}{2} - jX_G + \frac{R_a}{4} \pm \frac{jX_a}{2}} \\ &= \frac{1}{\frac{R_a}{4} + jX_G} + \frac{1}{\frac{3R_a}{4} \pm jX_a - jX_G} \end{aligned} \quad (\text{Eq 3})$$

where R_{in} is the resistance seen between points B and C, and X_r is the residual reactance between points B and C. Typical values can be assigned to R_a and X_a , and if the requirement is to match to 50 Ω , then R_{in} needs to be 50 Ω , because in this proposed model of the gamma match, the resistance seen at the gamma tap is the same as the resistance seen at the feed-line end of the gamma rod. Assuming that the driven element is resonant and has a resistance of 20 Ω , the jX_a term is zero, and the equation becomes:

$$\frac{1}{50 + jX_r} = \frac{1}{5 + jX_G} + \frac{1}{15 - jX_G} \quad (\text{Eq 4})$$

Readers interested in following the algebra are referred to [Appendix 1](#). For those readers who are not so inclined, the solution is $X_G = 30.4 \Omega$ and $X_r = 15.2 \Omega$.

This shows that an undivided driven element, which had it been divided at the center, would have presented a resistance of 20 Ω , presents an impedance between the tap point and the center of 50 + j15.2 when tapped at a position giving an inductive reactance of 30.4 Ω between the tap point and the center. So based on this proposed model, the element naturally provides impedance transformation without any involvement of the gamma rod, other than to deliver the power to the gamma tap point.

Before developing the proposal further, the question of division of radiation resistance between the gamma and the tip sections must be reconsidered. Based on information from several references, it was assumed that the typical split of radiation resistance would be 50/50. Using [Eq 3](#), the values of X_G required to transform 20 Ω to 50 Ω were calculated for the whole range of splits. That is, from all the resistance being in the tip section and none in the gamma

Table 1

The effect of radiation-resistance distribution between the tip and gamma sections of the gamma side of the driven element on X_G required to give 50 Ω input and on the accompanying residual reactance, X_r , when $R_a = 20$ and $jX_a = 0 \Omega$.

Radiation Resistance (Ω)

Tip Section	Gamma Section	X_G (Ω)	X_r (Ω)
0	10	30.0	0
1	9	30.0	3
2	8	30.1	6
3	7	30.1	9
4	6	30.3	12.1
5	5	30.4	15.2
6	4	30.6	18.4
7	3	30.8	21.6
8	2	31.0	24.8
9	1	31.3	28.2
10	0	31.6	31.6

section, to all of it in the gamma section and none in the tip section. The results are presented in [Table 1](#), together with values of associated residual reactance X_r . The data show that the variation in X_G is minimal. While the variation in X_r might appear significant, the effect on the gamma-capacitor setting for any likely difference in the 50/50 split would not amount to more than few picofarads, as will be shown later. Again using [Eq 3](#), the effects on R_{in} and X_r were calculated for the whole range of splits (as before), when the value of X_G was constant at 30.4 Ω , and the value of R_a was 20 Ω . The results are shown in [Table 2](#), and again it will be seen that over any likely range of splits, the differences aren't sufficient to invalidate the 50/50 assumption. All that follows is based on the 50/50 split.

The next point to be examined, again using [Eq 3](#), was the effect of varying X_G on the values of R_{in} and X_r for a fixed 20- Ω value of R_a . The results in [Table 3](#) show a progressive relationship between X_G and R_{in} and that the impedance transformation can be either up or down, depending on the value X_G .

Yet again using [Eq 3](#), the values of X_G to give $R_{in} = 50 \Omega$ together with the associated value of X_r were calculated for 42 combinations of $R_a + jX_a$ from 10 - j20 to 40 + j10. The results are presented in Tables 4A and 4B. An example of

Table 2

The effect of radiation-resistance distribution between the tip and gamma sections of the gamma side of the driven element on the input resistance and on the accompanying residual reactance, X_r , when the gamma-section reactance, X_G , is 30.4 Ω to give 50 Ω input and when the radiation resistance is equally divided and when $R_a = 20$ and $jX_a = 0 \Omega$.

Radiation Resistance (Ω)

Tip Section	Gamma Section	R_{in} (Ω)	X_r (Ω)
0	10	51.2	0
1	9	51.2	3
2	8	51.0	6.1
3	7	50.8	9.1
4	6	50.4	12.2
5	5	50.0	15.5
6	4	49.4	18.2
7	3	48.8	21.3
8	2	48.0	24.3
9	1	47.2	27.4
10	0	46.2	30.4

Table 3

Showing the effect of gamma-section reactance, X_G , on the input resistance and on the accompanying residual reactance, X_r , when $R_a = 20$ and $jX_a = 0 \Omega$.

X_G (Ω)	R_{in} (Ω)	X_r (Ω)
10	8.8	5
20	23.8	10
30	48.8	15
45	83.8	20
50	128.8	25

solving Eq 3 for a nonresonant situation is given in Appendix 2. Two very interesting points emerge from this: First, the value of X_G required to transform R_a to 50Ω reduces as R_a does. That is, larger transformation ratios require lower the values of X_G . An effect similar to this was found by Gooch (and others) in their studies of the hairpin match (see Note 5). However, this does not mean that low values of R_a require a shorter gamma section; as will be seen later, there is an additional overriding effect. The second interesting point is that for any given value of R_a , the lowest values of X_G are close to resonance on the capacitive side.

Determination of Gamma-Section Length

Having established a means of determining the required value of gamma-section reactance, the next step is to find

Table 4

Showing the values of gamma-section reactance, X_G , required to give a 50-Ω input (A) and on the accompanying residual reactance, X_r , (B) for input impedances of 10 -j20 to 40 +j10 Ω.

A. Gamma-Section Reactance

X_a (Ω)	X_G (Ω)					
	-20	-10	-5	0	5	10
10	44.1	28.5	23.3	21.9	25.8	33.5
15	38.0	29.5	26.8	26.6	29.3	34.5
20	38.0	31.5	30.1	30.4	32.6	36.5
25	38.1	33.8	33.1	33.7	35.6	39.3
30	38.9	36.0	35.7	36.5	38.2	41.0
35	39.9	38.1	38.5	39.0	40.6	43.1
40	43.2	40.0	40.3	41.2	42.8	45.0

B. Residual Reactance at the Gamma Tap

X_a (Ω)	X_r (Ω)					
	-20	-10	-5	0	5	10
10	117.0	61.8	38.7	11.0	-11.0	-31.0
15	80.7	45.5	28.8	13.3	-0.8	-14.0
20	64.0	38.3	26.3	15.2	5.0	-4.2
25	54.1	34.4	25.3	16.8	9.1	-2.8
30	47.8	32.1	24.9	18.2	12.0	6.30
35	43.6	30.8	25.1	19.5	14.4	9.70
40	41.6	30.0	25.2	20.6	16.4	12.5

Table 5

Inductance of the gamma-match section of the driven element required to provide the reactance values listed in Table 4A at 14.150 MHz when $R_d = 70$ Ω.

X_a (Ω)	R_a (Ω)	K	L_G (μH)				
			-20	-10	-5	0	5
10	7.0	3.47	2.24	1.83	1.72	2.03	2.64
15	4.67	2.00	1.55	1.41	1.40	1.54	1.81
20	3.50	1.50	1.24	1.19	1.20	1.28	1.44
25	2.80	1.20	1.06	1.04	1.06	1.12	1.24
30	2.33	1.02	0.94	0.94	0.96	1.00	1.07
35	2.00	0.90	0.86	0.87	0.88	0.91	0.97
40	1.75	0.85	0.79	0.79	0.81	0.84	0.89

the length of the gamma section to provide that reactance. This isn't as simple as it might appear. The problem is the effect of the parasitic elements on the driven element. Just as the feedpoint resistance of the driven element is reduced from that in free space, so is the reactance. So, when the inductance is calculated, it is necessary to include a correction factor, K . It is evident that an accurate value of K is essential to obtain an accurate value of inductance. We assume that the parasitic effect on the reactance is the same as the effect on the resistance. EZNEC¹⁰ is used to determine feed-point resistance, R_a , and the free-space feedpoint resistance of the driven element alone, R_d , at the same target frequency. Then it follows that:

$$K = \frac{R_d}{R_a} \quad (\text{Eq 5})$$

For the antenna at G4JNH, $R_d = 70.6$ Ω, $R_a = 29.7$ Ω and $K = 2.38$ at 14.150 MHz. The inductance to provide the required value of X_G can now be derived:

$$L = \frac{K X_G}{2\pi f} \quad (\text{Eq 6})$$

where L is the inductance in micro-henries and f is the frequency in megahertz. The values of inductance corresponding to values of X_G in Table 4A for 14.150 megahertz when $R_d = 70$ are presented in Table 5.

The 1995 ARRL Handbook gives the following equation relating the inductance of a straight conductor to its dimensions:¹¹

Table 6

The inductance of straight conductors in microhenries.

Length, Inches	Diameter in Inches						
	³ / ₈	¹ / ₂	⁵ / ₈	1	1 ¹ / ₈	1 ¹ / ₄	1 ¹ / ₂
20	0.47	0.44	0.42	0.37	0.36	0.35	0.33
22	0.53	0.50	0.47	0.42	0.40	0.39	0.37
24	0.59	0.55	0.52	0.47	0.45	0.44	0.42
26	0.64	0.61	0.58	0.51	0.50	0.49	0.46
28	0.70	0.66	0.63	0.56	0.55	0.53	0.51
30	0.77	0.72	0.69	0.62	0.60	0.58	0.55
32	0.83	0.78	0.74	0.67	0.65	0.63	0.60
34	0.89	0.84	0.80	0.72	0.70	0.68	0.65
36	0.95	0.90	0.86	0.77	0.75	0.73	0.70
38	1.01	0.96	0.92	0.83	0.80	0.78	0.75
40	1.08	1.02	0.97	0.88	0.86	0.83	0.80
42	1.14	1.08	1.03	0.93	0.91	0.89	0.85
44	1.21	1.14	1.09	0.99	0.96	0.94	0.90
46	1.27	1.21	1.15	1.04	1.02	0.99	0.95
48	1.34	1.27	1.21	1.10	1.07	1.05	1.00
50	1.40	1.33	1.28	1.16	1.13	1.10	1.05
52	1.47	1.40	1.34	1.21	1.18	1.15	1.11
54	1.54	1.46	1.40	1.27	1.24	1.21	1.16
56	1.61	1.52	1.46	1.33	1.29	1.26	1.21
58	1.67	1.59	1.52	1.38	1.35	1.32	1.26
60	1.74	1.65	1.59	1.44	1.41	1.37	1.32
62	1.81	1.72	1.65	1.50	1.46	1.43	1.37
64	1.88	1.78	1.71	1.56	1.53	1.49	1.43
66	1.95	1.85	1.78	1.62	1.58	1.54	1.48
68	2.02	1.92	1.84	1.68	1.64	1.60	1.54
70	2.09	1.98	1.90	1.74	1.70	1.66	1.59

$$L = 0.00508b \left[\ln\left(\frac{2b}{a}\right) - 0.75 \right] \quad (\text{Eq 7})$$

where L is the inductance in μH , a is the conductor radius in inches and b is the conductor length in inches. Unfortunately, this equation does not lend itself to rearrangement to give a value of length for known values of conductor diameter and inductance so a tabulation of conductor diameter and length versus inductance. Simple iteration, however, yields the values in Table 6 for appropriate sizes of gamma rod and driven elements for Yagis.

Using this information, the gamma-section lengths appropriate to the inductance values listed in Table 5 were determined for a driven-element diameter of 1.25 inches, and these results are presented in Table 7.

Table 7

Gamma-section lengths required to provide the inductance values listed in Table 5 when the driven-element diameter is 1.25 inches.

		Gamma-Section Length (Inches)					
X_a	R_a	-20	-10	-5	0	5	10
10	130	89.9	76.1	72.3	82.8	103	
15	81.4	66.2	61.2	60.8	65.9	75.3	
20	65.4	55.2	53.2	53.6	52.7	62.3	
25	53.7	48.7	47.9	48.6	50.9	55.1	
30	47.1	44.2	43.9	43.8	46.4	49.1	
35	42.5	40.9	41.2	41.7	43.1	45.2	
40	40.6	38.2	38.4	39.1	40.2	42.0	

Table 8

A. Gamma-Rod Reactance

X_g , for the gamma-section lengths listed in Table 7 when the gamma-rod diameter is 0.5 inches at 14.150 MHz.

		Gamma-Rod Reactance (Ω)					
X_a (Ω)	R_a	-20	-10	-5	0	5	10
10	363	236	195	183	215	277	
15	211	167	152	149	164	192	
20	163	133	127	129	137	154	
25	129	115	113	114	121	133	
30	110	102	101	101	108	116	
35	98	93	94	95	99	105	
40	92	86	86	88	91	96	

B. Total Gamma-Network Reactance (Less Capacitor)

Made of X_g from Table 8A, X_r from Table 4B and assuming $X_s = 20$.

		Total reactance (less capacitor), (Ω)					
X_a (Ω)	R_a (Ω)	-20	-10	-5	0	5	10
10	500	318	253	214	224	266	
15	311	232	201	183	183	199	
20	247	191	174	164	162	170	
25	203	169	158	151	150	150	
30	178	154	146	139	140	142	
35	151	144	139	135	134	135	
40	154	136	132	129	128	129	

Determination of Gamma-Capacitor Value

The gamma capacitor tunes out all the inductive reactance appearing at the antenna feedpoint, which comprises the following components in series:

1. The inductive reactance of the gamma rod, X_g .
2. The residual reactance X_r appearing at the gamma tap on the driven element.
3. The inductive reactance of the shorting bar connecting the rod to the tap point, plus the inductive reactance of the leads connecting the coax to the gamma rod and those to the center tap of the driven element, X_s .

Taking the above in order, the inductance of the gamma rod is readily established using either Eq 7 or Table 6. Knowing the inductance, the reactance is given by:

$$X = 2\pi f L \quad (\text{Eq 8})$$

where f is the frequency in megahertz, and L is in μH . Reactance values corresponding to the gamma-section lengths given in Table 7 for a gamma-rod diameter of 0.5 inches and a frequency of 14.150 megahertz are presented in Table 8A. Examples of residual reactance are found in Table 4B.

The reactance of the shorting bar and connecting leads should not be ignored, although they are low. Their inductances can be estimated using Eq 7 and the resulting reactance values using Eq 8. A typical total would be about 20 Ω for a 20-meter antenna. Guidance on estimating the inductance of conductors with noncircular cross sections is provided in the literature.¹² Total gamma-system reactance values for the gamma-section lengths in Table 7 are given in Table 8B.

The gamma capacitor must have the same value of capacitive reactance, X_c , as the total inductive reactance of the gamma system. C is computed as follows:

$$C = \frac{10^6}{2\pi f X_c} \quad (\text{Eq 9})$$

where C is the capacitance in picofarads, f the frequency in megahertz and X_c the reactance in ohms. The values of capacitance corresponding to the inductive reactances in Table 8B are found in Table 9. Comparing these two tables affirms the validity of the assumption regarding the 50/50 split. A reactance error of up to 10 Ω is not serious.

Calculating Gamma-Section Length and Capacitor Value

1. Model the antenna using EZNEC or equivalent to determine R_a and X_a at the target frequency.

Table 9

Showing capacitor values required to tune out the reactances listed in Table 8B at 14.150 MHz.

		Capacitance, picofarads					
X_a (Ω)	R_a (Ω)	-20	-10	-5	0	5	10
10	500	22.5	35.4	44.4	52.5	50.4	42.2
15	311	36.1	48.4	56.0	61.6	61.3	56.6
20	247	45.6	58.8	64.8	68.7	69.3	66.4
25	203	55.4	66.5	71.3	74.4	75.0	75.0
30	178	63.2	72.9	76.9	80.7	80.2	79.2
35	151	69.8	78.2	80.9	83.4	84.3	83.6
40	154	73.1	82.8	85.5	87.3	88.2	87.5

2. Using either Eq 3 or Table 4A, find the values of X_G and X_r .

3. Using EZNEC, determine the free-space resistance of the driven element, R_d .

4. Calculate the correction factor K .

5. Calculate the required gamma-section inductance, L_G , using Eq 6.

6. Estimate the gamma-section length using Table 6 and check with Eq 7.

7. Using Eq 7 or Table 6, determine the inductance of the gamma rod, L_g . The gamma rod's length is the distance to the shorting bar. The part extending beyond the shorting bar is ignored.

8. Determine the reactance of the gamma rod, X_G , using Eq 8.

9. Estimate the reactances of the shorting bar and connecting leads, X_s , using Eqs 7 and 8.

10. Determine the total gamma-system reactance, X_t and the gamma capacitor's reactance, X_c , as follows:

$$X_t = X_c = -(X_G + X_r + X_s) \quad (\text{Eq 10})$$

11. Compute the capacitance value using Eq 9.

Correlation to the Antenna at G4JNH

Details of the antenna at G4JNH are listed in Table 10. The value of the gamma capacitor was derived by calculation using the equation for capacitance of coaxial transmission lines in *The ARRL Antenna Book*¹³ which is:

$$C = \frac{7.26\epsilon}{\log_{10} \frac{D}{d}} \frac{\text{pF}}{\text{ft}} \quad (\text{Eq 11})$$

where ϵ is the dielectric constant of the inner insulator (air = 1.0 ϵ), D is the ID of the outer conductor (18.0 mm), and d is the OD of the inner conductor (16.0 mm). Therefore:

$$C = \frac{7.26}{\log_{10} \frac{18}{16}} = \frac{7.26}{0.0512} = 141.9 \frac{\text{pF}}{\text{ft}} \quad (\text{Eq 12})$$

When fully engaged, the overlap of the two tubes is 12 inches, so the maximum capacitance is 141.9 pF. As set up, there is only seven inches of overlap, giving a capacitance of:

$$\frac{(7)(141.9)}{12} = 82.8 \text{ pF} \quad (\text{Eq 13})$$

As was explained in the introduction, the gamma match was set up by trial and error before this study was undertaken. The procedure above can be applied to the G4JNH antenna to see how the proposed model stacks up to actual practice:

1. EZNEC gave an impedance at 14.150 MHz of 29.7 - j7.0 Ω .

2. Eq 3 gave the following: $X_G = 35.6 \Omega$ and $X_r = 27.8 \Omega$.

3. EZNEC gave a free-space resistance for the driven element of 70.6 Ω .

4. $K = R_d / R_a = 2.377$

5. Using Eq 6 to obtain the gamma-section inductance yields $L_G = 0.952 \mu\text{H}$.

6. Using Table 6, the required length of the gamma sec-

Table 10

Details of the three-element, 20-meter monobander at G4JNH.

Manufacturer:	COM-AN-TENNA, Melbourne, VK
Height (variable):	28 to 55 feet
Boom diameter:	2 inches
Reflector length:	421 inches
Driven-element length:	401 inches
Director length:	386 inches
Driven-to-reflector:	117 inches
Driven-to-director:	117 inches
All elements	(dimension from center / OD)
- Center section	0 to 54 inches / 1.125 inches
- 1st reduction:	54 to 102 inches / 1.00 inches
- 2nd reduction:	103 to 152 inches / 0.75 inches
- tip sections:	152 inches to tip / 0.63 inches
Gamma-section length:	44 inches
Gamma-rod diameter:	0.63 inches (16 mm)
Gamma-rod spacing (center-center):	6 inches
Gamma capacitor (see text):	83 pF

Feedpoint impedance, at 50 feet, EZNEC

14.00 MHz:	32.8 -j 14.9 Ω
14.05:	32.0 -j 12.3 Ω
14.10:	31.0 -j 9.8 Ω
14.15:	29.7 -j 7.0 Ω
14.20:	28.3 -j 3.9 Ω
14.25:	26.8 -j 0.6 Ω
14.30:	25.2 +j 3.0 Ω
14.35:	23.5 +j 7.0 Ω

(Assumed ground conductivity 5 mS/m and $\epsilon = 13.0$

SWR: See Fig 1



Fig 5—The G4JNH beam installed.

tion was estimated at 43.6 inches and confirmed using Eq 7.

7. Eq 7 gave 1.079 μH for the inductance of the gamma rod.

8. Eq 8 produces $X_g = 95.9 \Omega$.

9. Using Eqs 7 and 8, with help from Note 12, the following reactance values were estimated:

Shorting bar: 6.2 Ω

Coax-socket mounting plate: 3.2

Coax inner to gamma C lead: 11.3

$$X_s = 20.7 \Omega$$

10. Total gamma system reactance (excluding capacitor):

$$X_g: 95.9 \Omega$$

$$X_r: 27.8$$

$$X_s: 20.7$$

$$X_t: 144.4 \Omega.$$

11. Using Eq 9, $C_g = 77.9 \text{ pF}$.

Appendix 1

Fig 4 shows the equivalent circuit of the driven element, shown in Fig 3B. The following Eq A1 relates the various parameters when $R_a = 20$, $jX_a = 0$, the resistance required between points B and C of Fig 3B is 50 Ω , and X_r is any residual reactance in series with the 50 Ω :

$$\begin{aligned} \frac{1}{50 + jX_r} &= \frac{1}{5 + jX_G} + \frac{1}{15 - jX_G} \\ &:= \frac{(5 + jX_G) + (15 - jX_G)}{(5 + jX_G)(15 - jX_G)} \\ &:= \frac{20}{75 - 5jX_G + 15jX_G - j^2X_G^2} \end{aligned}$$

$$j^2 = -1$$

$$\therefore \frac{1}{50 + jX_r} = \frac{20}{75 + 10jX_G - X_G^2}$$

$$75 + 10jX_G + X_G^2 = 20(50 + jX_G^2)$$

$$\therefore 75 + 10jX_G + X_G^2 = 1000 + 20jX_r$$

$$\therefore 75 - 1000 + X_G^2 = 20jX_r$$

$$\therefore 75 - 1000 + X_G^2 = 20jX_r - 10jX_G$$

(Eq A1)

When real and imaginary components are equal both must be 0. Solving for the real part:

$$\therefore X_G^2 - 925 = 0$$

$$\therefore X_G = \sqrt{925} = 30.4 \Omega$$

$$20jX_r - 10jX_G = 0$$

$$\therefore 2X_r = X_G$$

$$\therefore X_r = \frac{X_G}{2} = 15.2 \Omega$$

To compare:

	Proposed Model	Actual Practice
Gamma-section length:	43.6"	44.0"
Gamma capacitor:	78 pF	83 pF

Appendix 2

This is the solution of Eq 3 as applied to the G4JNH beam at 14.150 MHz when $R_a = 29.7 \Omega$, $X_a = 7.0 \Omega$ and $R_{in} = 50 \Omega$:

$$\frac{1}{50 + jX_r} = \frac{1}{\frac{29.7}{4} + jX_G} + \frac{1}{\frac{(3)(29.7)}{4} - jX_G - j7.0}$$

For clarity, let $X_G = X$ and $X_r = Y$. Then:

$$\frac{1}{50 + jY} = \frac{1}{7.4 + jX} + \frac{1}{22.3 - jX - j7.0}$$

$$\therefore \frac{(7.4 + jX) + (22.3 - jX - j7.0)}{(7.4 + jX)(22.3 - jX - j7.0)}$$

$$\therefore \frac{29.7 - j7.0}{165 - 7.4jX - j51.8 + 22.3jX - j^2X^2 - j^27.0X}$$

$$\therefore \frac{29.7 - j7.0}{165 + 14.9jX - j51.8 + X^2 + 7.0X}$$

$$\therefore 165 + 14.9jX - j51.8 + X^2 + 7X = (29.7 - j7.0)(50 + jY)$$

$$\therefore 165 + 14.9jX - j51.8 + X^2 + 7X = 1485 - j350 + 29.7jY - j^27Y$$

$$\therefore 165 + X^2 + 7X - 1485 - 7Y = 29.7jY - j350 - 14.9jX + j51.8$$

Both sides must be equal to zero, so:

$$29.7jY - j350 - 14.9jX + j51.8 = 0$$

$$\therefore 2Y - 23.5 - X + 3.5 = 0$$

$$\therefore 2Y - 20 = X$$

$$\therefore Y = 0.5X + 10$$

$$\text{but } 165 + X^2 + 7X - 1485 - 7Y = 0$$

$$\therefore X^2 + 7X - 7Y - 1320 = 0$$

Substituting for Y yields:

$$X^2 + 7X - 7(0.5X + 10) - 1320 = 0$$

$$\therefore X^2 + 7X - 3.5X - 70 - 1320 = 0$$

$$\therefore X^2 + 3.5X - 1390 = 0$$

Only the positive root is valid, so:

$$X = \frac{-3.5 + \sqrt{3.5^2 + (4)(1390)}}{2}$$

$$\therefore X = X_G = 35.6 \Omega$$

$$Y = 0.5X + 10$$

$$Y = X_r = 27.8 \Omega$$

Conclusion

A model of the gamma match is proposed based on quite a different concept to that generally accepted. The model is based on familiar impedance-matching principles and agrees with practical experience.

The settings of any gamma match are obviously dependent on the impedance of the antenna. Any model of the match, therefore, relies heavily on accurate impedance measurements. In this study, that information was provided by *EZNEC*. The values of radiation resistance are enlightening (Table 10). They are generally higher than expected, and they fall with increasing frequency, which is totally unexpected.

In the course of using my model, a correction factor K was introduced to account for parasitic effects. Its value is critical. Its derivation was based on the simple presumption that the parasitic effects on the reactance of the driven element are the same as those on the feedpoint radiation resistance. This may well be an over-simplification, but the results on my beam are in remarkable agreement with practice, with regard to both gamma-section length and capacitor value.

My resources are not conducive to major research programs, but surely many readers are using gamma-matched antennas. Perhaps some of you have sufficient data to draw further comparisons with my work, favorable or otherwise. Such comparisons would be gratefully received.

My model is also applicable to the T and Omega matches, and the results it produces are in accordance with the rather limited information in the literature on these techniques. The model also provides a basis for vector analysis of the voltages and currents in the matching network, with quite interesting results. These matters, however, are beyond the scope of this article.

Orr and Cowan in the *Beam Antenna Handbook*¹⁴ write the following about the gamma match: "It is by far the best device to use when matching a parasitic array to a coaxial line." My experience supports that absolutely.

Acknowledgements

My excellently engineered antenna is offered with a hairpin match as an alternative to the gamma match. I have no doubt that I made the correct choice, and would make the same choice again.

I would like to thank Ian, VK3MO, for his enthusiastic assistance in conducting the antenna modeling, and Howarth, GW3TMP, for his patience in conducting countless runs of the ARRL gamma-match software.

Mr. Barker is a retired metallurgist and materials engineer. He never worked professionally in radio or electronics, but worked in the steel industry for 45 years. He has been interested in radio since his middle teens, but did not get a license until 1980.

Notes

- ¹H. H. Washburn, W3MTE, "The Gamma Match," *QST*, Sep 1949, pp 20, 21, 102.
- ²D. J. Healey, W3PG, "An Examination of the Gamma Match," *QST*, Apr 1969, pp 11-15, 57.
- ³J. Hall, K1TD, Ed., *The ARRL Antenna Book* (Newington, Connecticut: ARRL, 1974), 13th edition, pp 119-120.
- ⁴H. F. Tolles, W7ITB, "How to Design Gamma Matching Networks," *Ham Radio*, May 1973, pp 46-55.
- ⁵J. D. Gooch, W9YRV; O. E. Gardner, W9RWZ; G. L. Roberts, "The Hairpin Match," *QST*, Apr 1962, pp 11-14, 146, 156.
- ⁶R. D. Straw, N6BV, Ed., *The ARRL Antenna Book* (Newington: ARRL, 1994) 17th edition, p 2-6, Fig 6.
- ⁷*Ibid*, p 2-34, Fig 33.
- ⁸R. W. P King and C. W. Harrison, *Antennas and Waves—A Modern Approach* (Cambridge, Massachusetts: MIT Press, 1969), App 4, p 753.
- ⁹J. Devoldere, ON4UN, *Low Band DXing* (Newington: ARRL, 1987), p 11-8, Table 8.
- ¹⁰*EZNEC* antenna software by Roy Lewellen, W7EL, PO Box 6658, Beaverton, OR 97007.
- ¹¹R. Schetgen, KU7G, Ed., *The 1995 ARRL Handbook*, p 6-23.
- ¹²J. L. Lawson, W2PV, *Yagi Antenna Design* (Newington: ARRL, 1986), p 7-12.
- ¹³R. D. Straw, N6BV, Ed., *The ARRL Antenna Book*, 17th edition, p 24-18, Table 2, Eq 1.
- ¹⁴W. I. Orr, W6SAI and S. D. Cowan, W2LX, *Beam Antenna Handbook* (Wilton, Connecticut: Radio Publications, Inc, 1976) fifth edition, p 55.

CCT [®] **Radio**



Since
1976

- **Unique High Efficiency Antenna Designs / Kits**
- **Computer Systems / Sub-Systems / Upgrades**
- **Amateur Accessories / Parts / Services / Support**

CCT Radio / POB 193 / Stroudsburg, PA 18360-0193

<http://www.cctnetwork.com> • sales@cctnetwork.com

Call for info: 1-800-CCT-MENU / 717-421-7262 / 717-421-7151(Fax)

CCT Radio is a division of CCT, Inc. CCT[®] is a Registered Trademark.

HF Whips on Cars, Campers and RVs

The performance of whip antennas depends on the size of the vehicle on which they are mounted as well as where they are mounted.

By Peter Madle, KE6RBV

HF whip antennas mounted on vehicles are often inexplicably difficult to match to antenna feed lines. This article first explores a selected set of vehicles and mounting locations, and then investigates some of the factors that cause problems. The lengths and heights of the vehicles, measured in wavelengths, are found to play a major part.

Center or base-loaded HF whip antennas have low gain. It is well known that their foreshortened lengths limit their gain. Many hams have had difficulty matching them to feed cables—particularly if they are mounted near the front or rear of larger vehicles. Successful hams are rightly proud when they get good results but may not always understand why.

How many amateurs realize that the size of the vehicle can be as important as where the antenna is mounted? As a Technician, I have little direct HF experience; but I have

been involved in military electromagnetic analyses for a long time. I decided to investigate ham-band HF whip antennas mounted on cars, pickup trucks with camper shells, and large recreation vehicles.

Modeling

Mathematical modeling has come a long way in the past few decades. Major advances were driven by the need to design stealth aircraft, to protect satellites from nuclear electromagnetic pulse effects, and similar high-priority military problems. Many hams are now aware that PCs can be used to design Yagi and other antennas, but few are aware that they can also model complex objects such as cars.

I would be the first to admit that one must be cautious in interpreting the results of these mathematical extravaganzas. Simple models that can run on PCs typically ignore the joints, seams and other discontinuities in the conductive surfaces of vehicles. Even if the exact electrical details of these imperfections are known—entering the data is not an easy task.

My previous *QEX* article¹ explored how the antenna

2493 Malvern St
Cambria, CA 93428
pmadle@thegrid.net

¹Notes appear on [page 42](#).

pattern of a 2-meter whip was affected by its location on a car. This article extends the quest to the HF bands and investigates a few related variations.

As stated in my previous article: All transmitting antennas induce currents in all nearby conductors. The magnitude of these currents depends on the dimensions, separation distances, shapes, conductivities and other parameters. The resulting radiation pattern depends on the fields radiated by all of these currents in combination, not just the current flowing on the antenna itself.

Similarly, an incident electromagnetic field from afar excites currents on all conductive surfaces, and the interaction of these currents determines the resulting signal transferred to the feed cable.

Center-Loaded Whip Antennas

For this investigation, I modeled an 8-foot HF center-loaded mobile whip for the 20, 40, 80 and 160-meter bands using loading resistance and inductance values taken from *The ARRL Handbook*.² For the 10-meter band, I used the same antenna, but set the loading elements to 0 Ω and 0 H, essentially resulting in a simple vertical whip.

I included a base section three inches high and one inch in diameter to model a mounting spring and insulator. The drive point in the model is at the midpoint of this section. Above this is a fixed section 42 inches high and 0.25 inches

in diameter, and above this is a fixed section five inches high and one inch in diameter. At the center of the latter is a load resistance and inductance appropriate for each frequency. Finally, a top section 0.25 inches in diameter and of variable height was included to allow the antenna to be tuned for minimum input reactance. The general modeling technique first sets the frequency, location and loading of the antenna. It then makes repeated computer runs, while adjusting the height of the antenna top section until the input reactance is sufficiently low. In most cases, the reactance could be reduced to less than $\pm j1.0 \Omega$. Sometimes this required length changes of less than 0.1 inches, in which case I just stopped and accepted whatever low value of reactance had resulted.

In a few cases, which turned out to be the unexpected crux of this article, the antenna could not be resonated with any chosen length.

Antennas Located on the Ground

To “calibrate” the antenna model without its being influenced by the presence of a vehicle, I first located the antenna by itself on a “real” ground (conductivity of 0.005 siemens and relative dielectric constant of 13). Then I ran models for the 10, 20, 40, 80 and 160-meter bands—with the appropriate loading elements for each band—and adjusted the height for minimum input reactance.

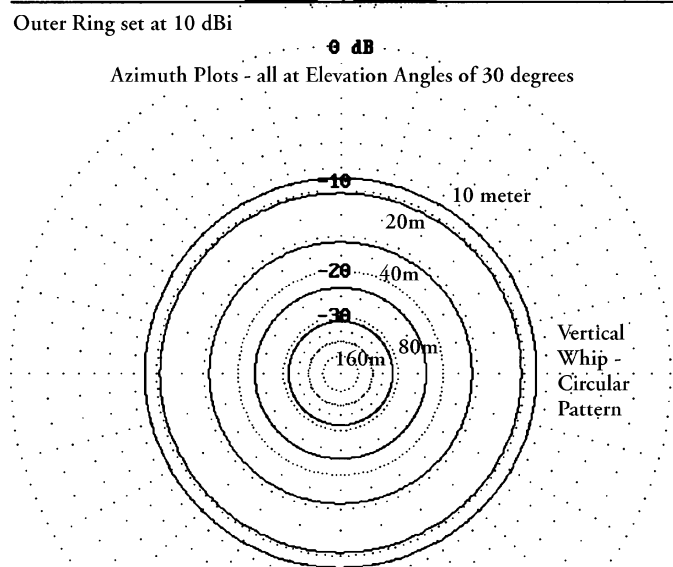
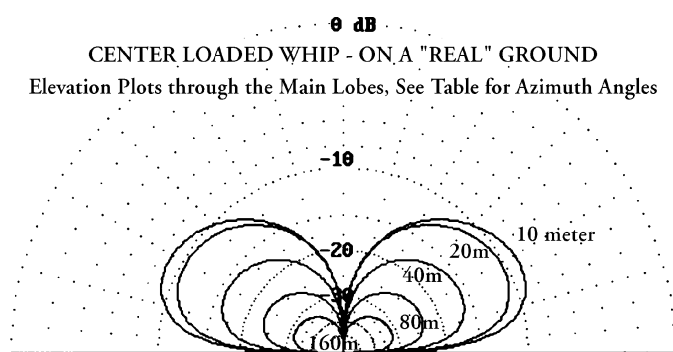


Fig 1—Center-loaded whip over a “real” ground. See Table 1.

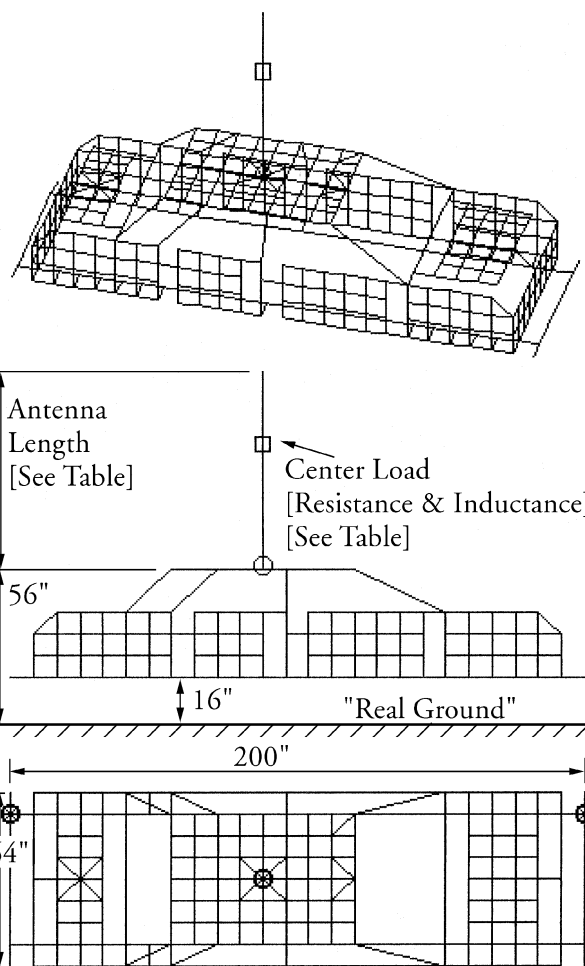


Fig 2—The car model. See Table 2.

The upper part of Fig 1 shows the elevation plots for all five frequencies. All of these have the expected vertical null for a whip antenna directly mounted on the ground. The lower part of this figure shows the azimuth plots at elevation angles of 30°, which I chose as being of interest for DX. Of course, since the “real” ground extends symmetrically in all horizontal directions, the azimuth plots are all circular, as shown in the lower portion of the figure.

The outer ring of all plots throughout this article is set at 10 dBi for consistency. This helps the reader compare one curve set with another. Therefore, all plotted values must be adjusted upward by 10 dBi.

Table 1 shows the data from these runs. For each of the five frequencies, a column shows the antenna length (height) needed to minimize the input impedance. I did not bother with length changes of less than 0.1 inches—who would believe such minute changes or the purported accuracy anyway? The table also shows the center-load resistance and inductance used, and then the calculated input resistance and reactance that resulted. The maximum gain (dBi) is followed by its take-off angle and azimuth angle. For these simple whips on ground, the azimuth angles are simply shown as circular. For most of the other data tables in this paper, the maximum gain occurs at some specific azimuth angle because the vehicles are anything but circular. The table shows the maximum gain and front-to-back ratio at elevation angles of 20° and 30°, although the 20° curves are omitted to save space.

Maximum gains of 1.1 dBi at 10 meters through -21.1 dBi

at 160 meters seem reasonable, as do the input-resistance values. I used these antennas at various locations on various vehicles, adjusting their heights for minimum input reactance in each case, but changing nothing else.

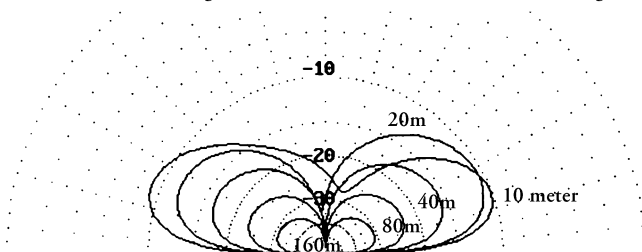
The Car Model

Fig 2 shows a slightly modified version of the same car model I used in my previous article, which concerned the 2-meter band only. Patterns were plotted with HF whips located at the center of the roof, at the left front bumper-mounting bracket, and at the left rear bumper-mounting bracket, as shown by the three black circles on the diagram.

Table 1—Modeled Performance of Ground Mounted HF Vertical Antennas

HF Band	Parameter	10m	20m	40m	80m	160m
Frequency		29.0Mhz	14.2 Mhz	7.2 Mhz	3.8 Mhz	1.8 Mhz
Length	Inch	99.6	79.8	76.2	75.2	73.5
Load Resis	Ohm	N/A	2.5	6.0	12.0	23.0
Load Induct	micro-Henry	N/A	8.6	40.0	150.0	700.0
Input Imped	Resist, Ohm	26.5	9.6	9.6	16.8	32.0
	React, Ohm	+j0.7	+j0.9	+j0.9	+j2.3	+j1.7
Maximum	MaxGain dBi	1.1	-0.3	-5.7	-13.0	-21.6
	at Elev, deg	27.0	29.0	29.0	28.0	25.0
	Azimuth, deg	Circular	Circular	Circular	Circular	Circular
20 deg Elev	MaxGain, dBi	0.8	-0.8	-6.2	-13.4	-21.7
	F/B Ratio, dB	Circular	Circular	Circular	Circular	Circular
30 deg Elev	MaxGain, dBi	1.1	-0.3	-5.7	-13.1	-21.1
	F/B Ratio, dB	Circular	Circular	Circular	Circular	Circular

Fig 3—Whip at center of car roof. See Table 2.
 CENTER LOADED WHIP - AT THE CENTER OF A CAR'S ROOF
 Elevation Plots through the Main Lobes, See Table for Azimuth Angles



Outer Ring set at 10 dBi

Azimuth Plots - all at Elevation Angles of 30 degrees

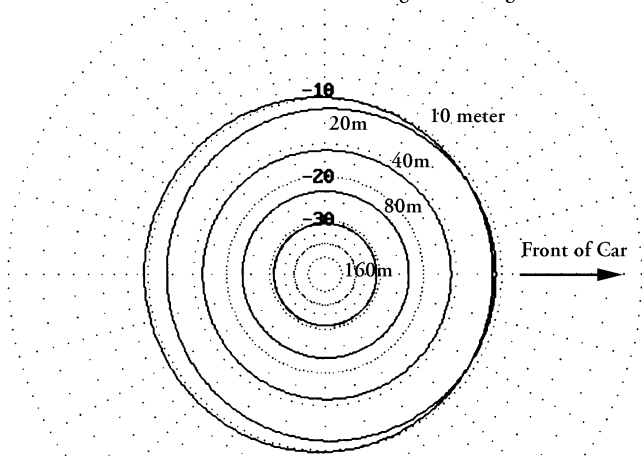
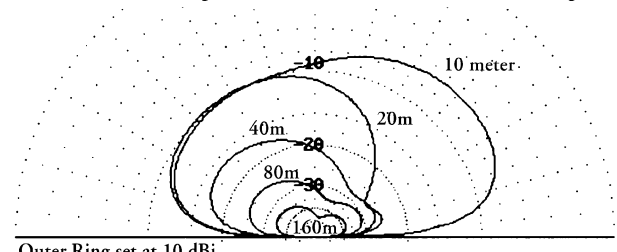


Fig 4—Whip on car front bumper. See Table 2.
 CENTER LOADED WHIP - LEFT END OF A CAR'S FRONT BUMPER
 Elevation Plots through the Main Lobes, See Table for Azimuth Angles



Outer Ring set at 10 dBi

Azimuth Plots - all at Elevation Angles of 30 degrees

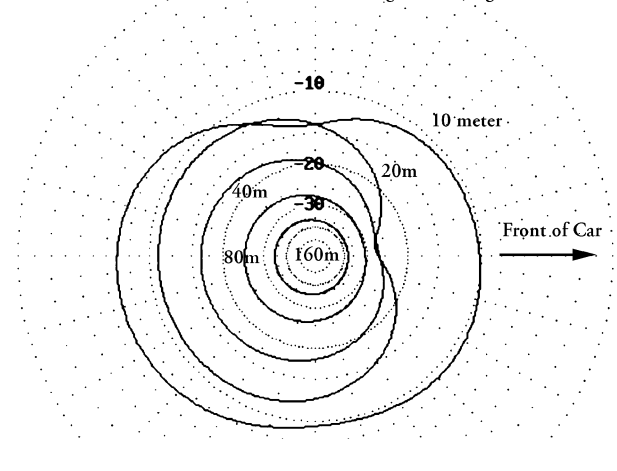


Fig 3—Whip at center of car roof. See Table 2.

Fig 4—Whip on car front bumper. See Table 2.

The modifications included opening nonconductive gaps around the doors, hood, and trunk lid, leaving them connected to the rest of the body only by a pair of hinges on one edge and a latch on the opposite edge. I discussed the possible effect of these restrictions on the flow of currents over the car body previously (see [Note 1](#)). I show the resulting radiation patterns later in this article. Because these gaps resulted in near open-circuits from front to back on the car along the lower edges of the doors, I added a front-to-back member under both sides of the car. These simulate the continuous conducting path provided by the lower edge of a real car body via the doorsills and frame members. This analysis assumes, of course, that a real car body actually has electrically conductive joints between its many metal panels. The real world is full of unknowns, and one can only model features that are known! Who knows what lies under the glossy paint of any specific automobile? $[(\text{Fe}_2\text{O}_3)_3 \cdot \text{H}_2\text{O}]$ under mine.—*Ed.*

Since this modified model was designed for frequencies of 29 MHz and lower, it did not need as great a resolution as when it was used at 2 meters. Rather than develop a completely new and mathematically smaller model with greater spacing between fewer wires, I reduced the number of sections from two to one per eight-inch wire element. This however still uses wires no longer than $\lambda/50$, which is more than adequate. Since two-dimensional matrix solutions apply, reducing the number of sections to about half reduced the computer run time to about one-fourth. This article required more than 800 runs of up to 16 minutes on a 200-MHz machine, so every little bit helps. The previous model, used at 2 meters, was a compromise between the

desirable resolution of 4 inches ($\lambda/20$) and a practical number of total model segments (678 eight-inch wires; 1456 four-inch segments). That model was marginally adequate for 2-meter analysis.

Whips on Car Roofs and Bumpers

[Figs 3, 4](#) and [5](#) show the radiation patterns for whip antennas located on the roof, front bumper and rear bumper of a car, respectively. [Table 2](#) consolidates the data in written form.

With the whip mounted at the center of the roof ([Fig 3](#)), the gains at all five frequencies are within a few tenths of a dB of those for the same antennas directly mounted on the “real” ground. The azimuth patterns approach circles, I presume because the car is fairly symmetrical from front to back.

With the whip at the front or the rear of the car ([Figs 4](#) and [5](#)), the patterns are decidedly asymmetrical, particularly at 20 meters, where the car is approximately $\lambda/4$ long. These patterns are tilted forward for the rear-mounted antenna, rearward for the front-mounted one, and have a shallow null in the opposite direction in both cases. At 20 meters, the car seems to be acting as a very fat, resonant, quarter-wave ground radial, and the maximum radiation is in the direction in which it points. At lower frequencies, the tilt is still somewhat evident. High-angle lemon-shaped upward lobes are seen in the elevation plot. A clue: Similar strange behavior was uncovered when I plotted patterns for the camper and the RV, as reported below. I became increasingly curious until, eventually, I explored some of the issues further and found hints as to some of the behavior. The final sections of this article delve

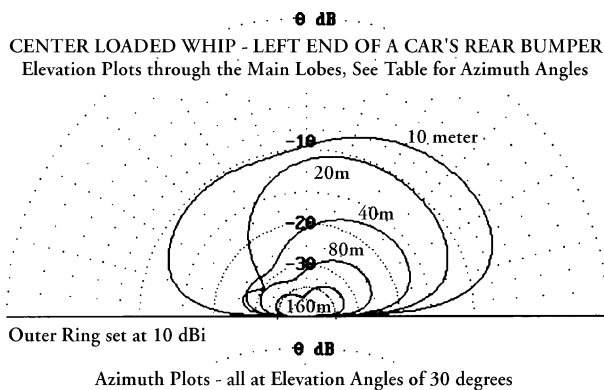


Fig 5—Whip on car rear bumper. See [Table 2](#).

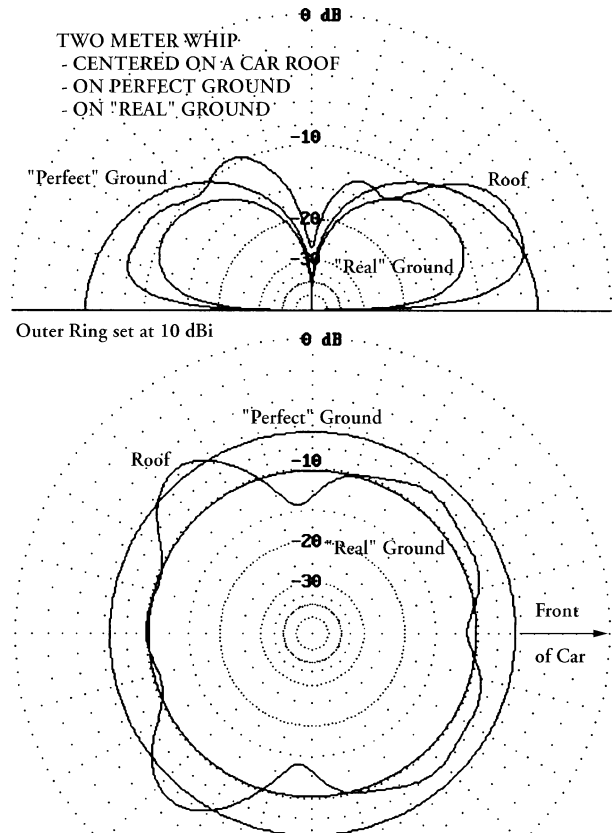


Fig 6—2-meter whip at center of car roof and on ground.

Table 2—HF Whip Performance on a Car

29.0 Mhz, 10 meter Whip		CentRf	FrtBmp	RrBmp
Length	Inch	96.7	102.4	102.0
Input Imped	Resistive, Ohm	52.2	33.1	27.7
	Reactive, Ohm	+j0.3	+j0.2	+j0.1
Maximum	Max. Gain dBi	0.9	3.4	3.6
	at Elev, deg	22.0	41.0	36.0
	Azimuth, deg	0.0	193.0	348.0
20 deg Elev	Max. Gain, dBi	0.9	2.4	2.8
	F/B Ratio, dB	1.0	3.8	5.1
30 deg Elev	Max. Gain, dBi	0.4	3.2	3.5
	F/B Ratio, dB	1.2	3.6	4.7
14.2 Mhz, 20 meter Center Loaded Whip				
Length	Inch	80.0	78.4	78.5
Load Resis	Ohm	2.5	2.5	2.5
Load Induct	micro-Henry	8.6	8.6	8.6
Input Imped	Resistive, Ohm	19.7	18.2	18.0
	Reactive, Ohm	j0.51	+j0.11	j.69
Maximum	Max. Gain dBi	-0.6	-0.1	-0.2
	at Elev, deg	28.0	66.0	63.0
	Azimuth, deg	0.0	6.0	352.0
20 deg Elev	Max. Gain, dBi	-0.9	-1.9	-1.9
	F/B Ratio, dB	1.1	13.4	14.4
30 deg Elev	Max. Gain, dBi	-0.6	-0.9	-0.9
	F/B Ratio, dB	1.3	16.4	18.6
7.2 Mhz, 40 meter Center Loaded Whip				
Length	Inch	76.7	76.3	76.3
Load Resis	Ohm	6.0	6.0	6.0
Load Induct	micro-Henry	40.0	40.0	40.0
Input Imped	Resistive, Ohm	17.7	13.2	13.4
	Reactive, Ohm	-j1.1	-j0.5	+j1.1
Maximum	Max. Gain dBi	-5.8	-6.2	-6.4
	at Elev, deg	29.0	36.0	35.0
	Azimuth, deg	0.0	14.0	344.0
20 deg Elev	Max. Gain, dBi	-6.2	-7.0	-7.2
	F/B Ratio, dB	0.5	9.6	9.2
30 deg Elev	Max. Gain, dBi	-5.8	-6.3	-6.5
	F/B Ratio, dB	0.5	10.5	10.0
3.8 Mhz, 80 meter Center Loaded Whip				
Length	Inch	75.7	75.4	75.4
Load Resis	Ohm	12.0	12.0	12.0
Load Induct	micro-Henry	150.0	150.0	150.0
Input Imped	Resistive, Ohm	28.5	24.3	24.6
	Reactive, Ohm	+j1.2	-j0.6	-j3.2
Maximum	Max. Gain dBi	-12.7	-14.5	-14.7
	at Elev, deg	28.0	32.0	31.0
	Azimuth, deg	355.0	15.0	345.0
20 deg Elev	Max. Gain, dBi	-13.0	-15.0	-15.2
	F/B Ratio, dB	0.3	5.8	5.7
30 deg Elev	Max. Gain, dBi	-12.7	-14.5	-14.7
	F/B Ratio, dB	0.3	6.3	6.1
1.8 Mhz, 160 meter Center Loaded Whip				
Length	Inch	74.0	73.8	73.8
Load Resis	Ohm	23.0	23.0	23.0
Load Induct	micro-Henry	700.0	700.0	700.0
Input Imped	Resistive, Ohm	52.5	49.0	50.2
	Reactive, Ohm	-j0.9	+j1.7	-j1.7
Maximum	Max. Gain dBi	-21.0	-24.1	-24.4
	at Elev, deg	25.0	27.0	27.0
	Azimuth, deg	344.0	15.0	0.0
20 deg Elev	Max. Gain, dBi	-21.8	-24.3	-24.6
	F/B Ratio, dB	0.2	3.6	3.5
30 deg Elev	Max. Gain, dBi	-21.1	-24.1	-24.3
	F/B Ratio, dB	0.2	3.9	3.7

into these issues, but first, onward to more basic plots for the car, camper and RV.

A 2-meter Whip on a Car

Before dealing with the camper and RV, I explored how the modified car model behaved at 2 meters. The version of the model used for these 2-meter plots differs from the one I used in my previous article. I included gaps around the doors, trunk lid and hood, front-to-back frame members, and I tuned the 2-meter whip for minimum input reactance for each mounting location. Previously I fixed its height at 19.6 inches. I wanted to see what difference the modeling changes made to my previous results before continuing to modify the model by reducing the number of segments from two to one per eight-inch wire element. So, I made these runs before completing the model changes, and before running the above-reported 10 through 160-meter analyses.

Fig 6 shows the elevation and azimuth plots for the 2-meter whip at the center of the car roof. The figure also shows the elevation and azimuth plots for the 2-meter whip mounted directly on a “real” and on a perfect ground. It is interesting to see that the performance of the 2-meter whip on the car roof lies somewhere between the others. That the car roof is 56 inches above ground level obviously contributes to the complex multilobed pattern in addition to whatever effects are caused by the shape and size of the car body. Clearly, larger local currents are induced in the higher conductivity of the roof’s metal by the antenna’s near fields than are induced in the lower conductivity of the “real” ground in the immediate vicinity of the whip when it is mounted on the ground. This gives rise to larger radiated fields at the higher

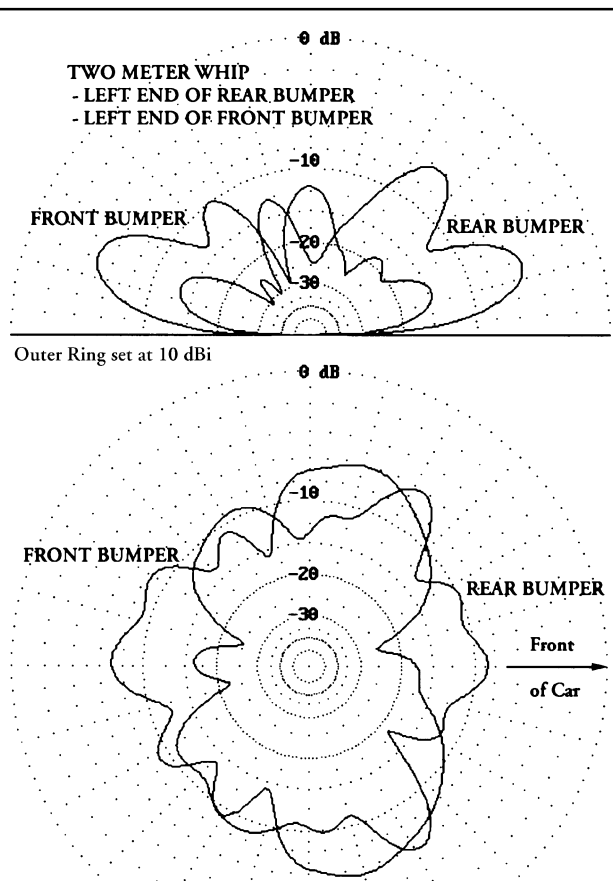


Fig 7—2-meter whip on front and rear bumpers of car.

elevation angles from the car roof, since these fields are principally reflected from areas immediately surrounding the antenna. In contrast, the far-field pattern at the lower elevation angles is determined by reflected energy from the low conductivity of the ground.

The car-roof patterns shown in Fig 6 are evidently influenced by both the metal of the roof at high angles and the lower conductivity of the ground at low angles. With the 2-meter whip at the center of the car roof, the input impedance, which was previously $72 + j20$ for an untuned 19.6-inch whip, became $74 + j0.1$ for a tuned 18.8-inch whip in the revised model. The maximum gain was 4.3 dBi at a 13° elevation angle (see Fig 5 in Note 1). It changed to 5.0 dBi at 23° in the revised model. Table 3 shows these numerical values. In general, the patterns were similarly complicated, remained within a few dBi in most directions and showed that the gaps around the doors, etc, had small but discernible effects.

As I told myself before running the models, nobody would waste their time mounting a 2-meter whip on a front or rear car bumper. Who, I asked myself, would even try such a silly position for an itchy-bitsy whip that would be hidden by a great-big car? Well, surprise, surprise—the performance in the directions of maximum gain is not that different from the mounting on the roof, which everyone knows is a better location! Fig 7 shows the results.

I have not actually tried a 2-meter whip on a bumper. Perhaps someone can tell me what really happens, if anyone really cares. The model suggests that, when front bumper mounting is used, a lobe with about 5 dBi gain occurs at an elevation angle of 21° over the rear of the car. Similarly, using a rear bumper mount, a lobe with a gain of about 4.5 dBi occurs at an elevation angle of 34° over the front of the car. The input resistances for these two cases did tune to low reactance values, but would be somewhat difficult to match to feed lines; they have unexpectedly high input-resistance values of 198 and 136 Ω , respectively. These patterns are far from circular, have lower gain in other directions and are generally not very useful—but they intrigue me nonetheless. They result from fields radiated from the currents induced in the car body.

A Pickup with a Camper Shell

In a style similar to the car, Fig 8 shows my model for a pickup truck fitted with a camper shell. For want of more detailed structural information and with the knowledge that many variations exist in vehicle construction, my model assumes that the exterior surface is continuously conductive and has no joints, breaks or other imperfections except for a single aperture representing the windshield. Since this model was developed for frequencies of 29 MHz and lower, I

Table 3

146.0 Mhz		Whip on Gnd		Car		
2 meter Whip		Real	Perfect	CentRf	FrtBmp	RrBmp
Length	Inch	19.1	19.1	18.8	14.6	12.1
Input Imped	Resistive	35.7	35.7	74.4	197.7	136.4
	Reactive	+j1.4	+j1.4	+j0.1	+j0.7	+j0.4
Maximum	MaxGain	-0.1	5.2	5.0	5.2	4.5
	at Elev	27.0	0	23.0	21.0	34.0
	Azimuth	Circular	Circular	231.0	0.0	303.0
20 deg Elev	MaxGain	-0.5	4.3	5.0	5.2	4.9
	F/B Ratio	Circular	Circular	2.8	9.8	8.1
30 deg Elev	MaxGain	-0.2	3.5	4.8	4.6	4.4
	F/B Ratio	Circular	Circular	3.0	7.1	3.8

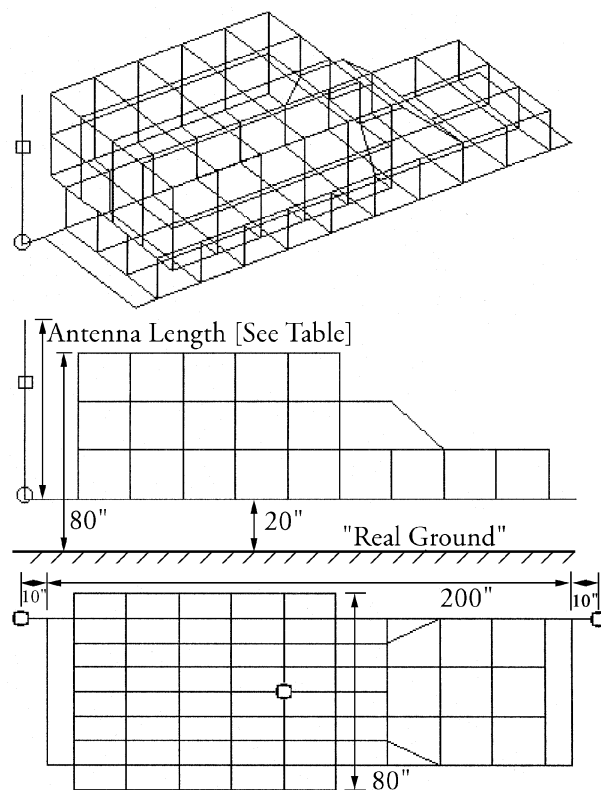


Fig 8—The pickup truck model. See Table 4.

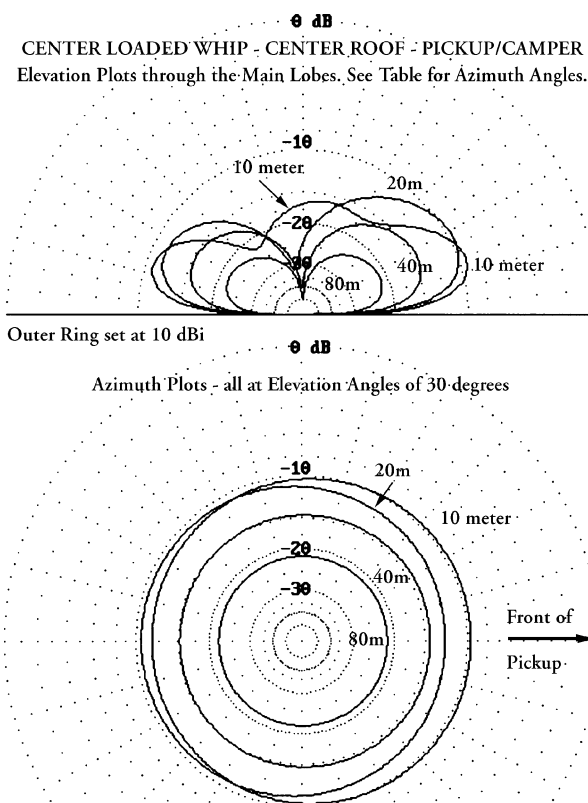


Fig 9—Whip on pickup w/camper roof. See Table 4.

used 20-inch wires comprised of a single section each, spaced 20 inches apart. The top of the camper shell is 80 inches—and the chassis 20 inches—above the ground. A full underpan is included. The front and rear bumpers are simply single wires 80 inches long, divided into four 20-inch segments. They are joined to the pickup body by a 10-inch-long wire at each end. Figs 9, 10 and 11 show the patterns produced by an HF whip mounted on the roof, front bumper and rear bumper, respectively.

The results for the roof-center mounting at all frequencies were roughly similar to those of the car. However, strange behavior was found at 29 MHz when the antenna was mounted on the front or rear bumper. As I incrementally increased the antenna height from an initially too-short dimension, the reactive component of the input impedance changed from a large negative value to a smaller negative value as one would expect. It then reached a minimum—but not zero—and became progressively more negative as the height increased. It *never* became positive, as I expected for a longer-than-tuned length. My immediate reaction was that a portion of the input reactance was the large capacitance between the antenna and the pickup body. I moved the antenna 10 inches farther from the pickup body by adding a stand-off, reran all data for the bumper mounts and obtained what appear to be understandable data as shown in Table 4. “Bingo!” I thought. That agrees with what my friend Ron, W6VCF, has been telling me: “Whips must not be mounted too near large vertical conductive surfaces.” That seemed true, but little did I know that vehicle length also played a part in the story, as we will explore later.

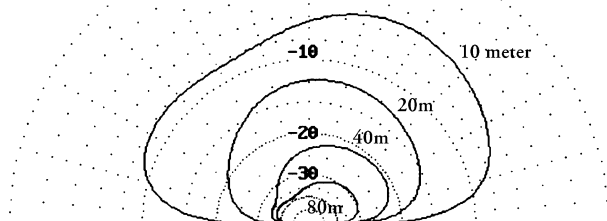
A Recreational Vehicle

Fig 12 shows my RV model. It is constructed similarly to that of the pickup truck, but the height is increased to 96 inches, the length to 300 inches and the shape of the front end is different. In a once-bitten-twice-shy approach, I made some initial runs with a whip mounted directly on the end of the bumpers, and rapidly decided to add 10-inch-long stand-off brackets to space the antennas a full 20 inches from the front and the rear of the RV body.

Table 4—HF Whip Performance on a Pickup Truck

29.0 Mhz, 10 meter Whip		CentRf	FrTBmp	RrBmp
Length	Inch	84.0	109.0	89.6
Input Imped	Resistive, Ohm	46.4	40.5	13.6
	Reactive, Ohm	-j1.0	+j0.2	+j0.1
Maximum	Max. Gain dBi	0.7	5.0	2.8
	at Elev, deg	19.0	63.0	56.0
	Azimuth, deg	180.0	206.0	3.0
20 deg Elev	Max. Gain, dBi	0.7	2.4	1.7
	F/B Ratio, dB	1.5	1.6	5.4
30 deg Elev	Max. Gain, dBi	-0.5	3.5	2.3
	F/B Ratio, dB	2.0	2.1	6.4
14.2 Mhz, 20 meter Center Loaded Whip				
Length	Inch	61.9	77.2	75.8
Load Resis	Ohm	2.5	2.5	2.5
Load Induct	micro-Henry	8.6	8.6	8.6
Input Imped	Resistive, Ohm	19.7	34.0	13.5
	Reactive, Ohm	-j0.3	+j0.0	+j0.3
Maximum	Max. Gain dBi	0.4	-2.1	-1.7
	at Elev, deg	27.0	80.0	75.0
	Azimuth, deg	0.0	234.0	0.0
20 deg Elev	Max. Gain, dBi	0.0	-5.9	-4.5
	F/B Ratio, dB	1.7	7.4	13.3
30 deg Elev	Max. Gain, dBi	0.3	-4.7	-3.3
	F/B Ratio, dB	0.0	5.2	8.7
7.2 Mhz, 40 meter Center Loaded Whip				
Length	Inch	59.0	75.1	73.7
Load Resis	Ohm	6.0	6.0	6.0
Load Induct	micro-Henry	40.0	40.0	40.0
Input Imped	Resistive, Ohm	14.8	31.9	11.2
	Reactive, Ohm	-j0.1	+j1.2	+j0.5
Maximum	Max. Gain dBi	-4.4	-10.7	-9.8
	at Elev, deg	29.0	39.0	39.0
	Azimuth, deg	0.0	199.0	343.0
20 deg Elev	Max. Gain, dBi	-4.8	-11.7	-10.8
	F/B Ratio, dB	0.8	13.0	13.8
30 deg Elev	Max. Gain, dBi	-4.4	-10.9	-10.0
	F/B Ratio, dB	0.8	13.7	14.6
3.8 Mhz, 80 meter Center Loaded Whip				
Length	Inch	58.1	74.4	73.0
Load Resis	Ohm	12.0	12.0	12.0
Load Induct	micro-Henry	150.0	150.0	150.0
Input Imped	Resistive, Ohm	23.6	65.0	23.0
	Reactive, Ohm	-j1.4	-j1.3	+j3.6
Maximum	Max. Gain dBi	-11.3	-19.4	-18.9
	at Elev, deg	28.0	33.0	33.0
	Azimuth, deg	0.0	197.0	342.0
20 deg Elev	Max. Gain, dBi	-11.6	-20.0	-19.5
	F/B Ratio, dB	0.5	7.1	8.1
30 deg Elev	Max. Gain, dBi	-11.3	-19.4	-19.5
	F/B Ratio, dB	0.5	7.5	8.1

0 dB
CENTER LOADED WHIP - FRONT BUMPER- PICKUP/CAMPER
Elevation Plots through the Main Lobes. See Table for Azimuth Angles.



Outer Ring set at 10 dBi

0 dB
Azimuth Plots - all at Elevation Angles of 30 degrees

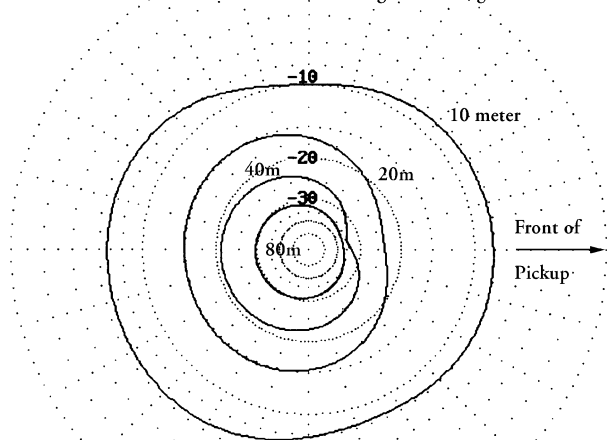


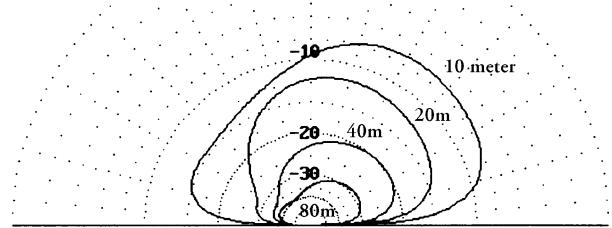
Fig 10—Whip on pickup w/camper front bumper. See Table 4.

While developing this model, I became curious about the potential effect of windows at the sides and rear. The wide slot for a windshield was the only opening in place when I first ran the model with a 29-MHz HF whip centered on the roof. I then cut a pair of windows into each side, and another window into the rear face, and ran the model again. I found it interesting that, without windows, a 97-inch-high whip was needed to give a 3.2-dBi maximum gain, and an input impedance of $52.1 + j0.7$. With the windows, the

Table 5—HF Whip Performance on an RV

29.0 Mhz, 10 meter Whip		CentRf	FrtBmp	RrBmp
Length	Inch	95.6	81.0	82.7
Input Imped	Resistive, Ohm	56.9	149.1	42.1
	Reactive, Ohm	+j0.3	-j1.9	+j0.8
Maximum	Max. Gain dBi	3.0	2.3	3.6
	at Elev, deg	21.0	56.0	56.0
	Azimuth, deg	0.0	186.0	4.0
20 deg Elev	Max. Gain, dBi	3.0	-2.6	-0.2
	F/B Ratio, dB	2.3	1.7	3.9
30 deg Elev	Max. Gain, dBi	2.7	-0.3	1.7
	F/B Ratio, dB	2.1	3.1	3.8
14.2 Mhz, 20 meter Center Loaded Whip				
Length	Inch	77.8	79.3	76.7
Load Resis	Ohm	2.5	2.5	2.5
Load Induct	micro-Henry	8.6	8.6	8.6
Input Imped	Resistive, Ohm	17.8	412.5	45.0
	Reactive, Ohm	+j0.6	+j2.9	-j0.3
Maximum	Max. Gain dBi	0.1	-5.7	0.4
	at Elev, deg	25.0	75.0	77.0
	Azimuth, deg	96.0	196.0	351.0
20 deg Elev	Max. Gain, dBi	-0.2	-10.9	-4.6
	F/B Ratio, dB	0.0	2.1	3.6
30 deg Elev	Max. Gain, dBi	-0.1	-9.1	-2.9
	F/B Ratio, dB	0.0	2.2	3.0
7.2 Mhz, 40 meter Center Loaded Whip				
Length	Inch	74.8	76.2	76.0
Load Resis	Ohm	6.0	6.0	6.0
Load Induct	micro-Henry	40.0	40.0	40.0
Input Imped	Resistive, Ohm	13.9	946.4	13.6
	Reactive, Ohm	+j2.1	-j1.3	-j1.6
Maximum	Max. Gain dBi	-4.3	-21.7	-7.3
	at Elev, deg	152.0	79.0	80.0
	Azimuth, deg	97.0	191.0	355.0
20 deg Elev	Max. Gain, dBi	-4.6	-25.3	-11.3
	F/B Ratio, dB	0.0	10.8	7.3
30 deg Elev	Max. Gain, dBi	-4.3	-24.0	-10.0
	F/B Ratio, dB	0.0	7.6	5.6
3.8 Mhz, 80 meter Center Loaded Whip				
Length	Inch	74.0	76.0	76.0
Load Resis	Ohm	12.0	12.0	12.0
Load Induct	micro-Henry	150.0	150.0	150.0
Input Imped	Resistive, Ohm	21.6	3825.5	22.8
	Reactive, Ohm	+j2.0	-j5.7	-j4.6
Maximum	Max. Gain dBi	-11.1	-36.1	-19.0
	at Elev, deg	153.0	43.0	52.0
	Azimuth, deg	96.0	196.0	344.0
20 deg Elev	Max. Gain, dBi	-11.1	-37.2	-20.3
	F/B Ratio, dB	0.1	10.3	11.8
30 deg Elev	Max. Gain, dBi	-11.1	-36.4	-19.4
	F/B Ratio, dB	0.1	9.3	9.8

0 dB
CENTER LOADED WHIP - REAR BUMPER - PICKUP/CAMPER
Elevation Plots through the Main Lobes. See Table for Azimuth Angles.



Outer Ring set at 10 dBi

0 dB
Azimuth Plots - all at Elevation Angles of 30 degrees

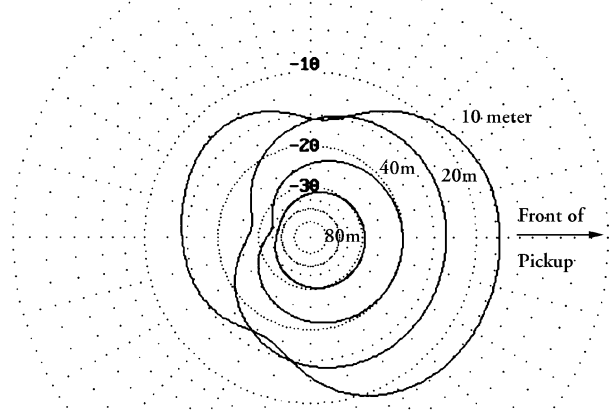


Fig 11—Whip on pickup w/camper rear bumper. See Table 4.

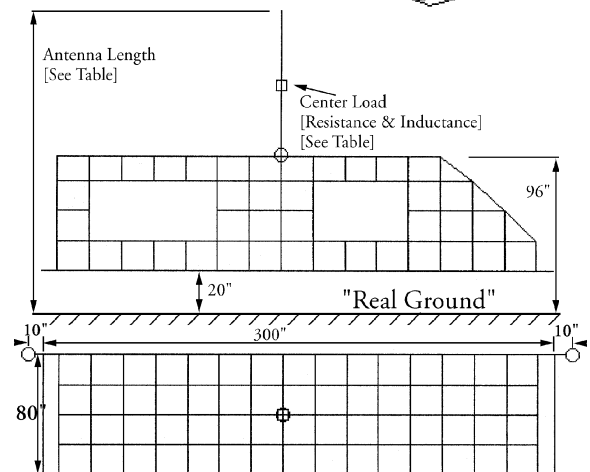
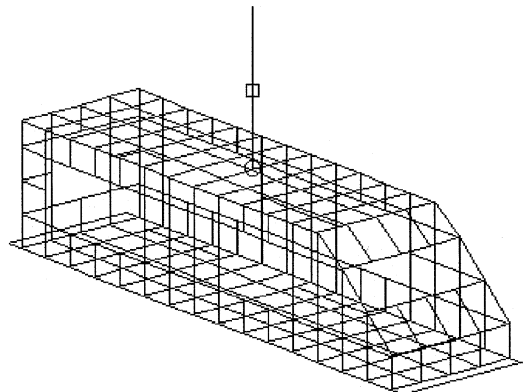


Fig 12—The RV model (see Table 5).

antenna height needed was reduced to 95.6 inches, the gain decreased to 3.0 dBi and the impedance increased to $56.9 + j0.3$. These small differences seem to indicate that this modeling is not unduly sensitive to minor things like window openings and echo the findings of the similarly minor effects of gaps around the doors in the car model. Figs 13, 14 and 15 show the radiation patterns for roof, front-bumper and rear-bumper mounting locations, respectively. The greater length of the RV (about $3\lambda/4$ at 29 MHz) appears to cause the unusual elevation patterns seen at this frequency. Even the 20-inch spacing of this model, yields unusually large values of input resistance, particularly for the front-bumper mounting location, as shown in Table 5.

Input Resistance

The values for input resistance seen in Tables 3, 4 and 5 include a few which, to me if no-one else, appear unusually high. The values of 198 and 136 Ω mentioned above for the 2-meter whip on the car bumpers are joined by values of 65 Ω for the front bumper location of the camper at 3.8 MHz and by 149, 412, 946 and 3825 Ω on the other bands for the front-bumper location on the RV.

“What is happening?” In my ignorance about real practice, I was prepared to accept input resistances as low as 9 Ω and as high as 50 Ω for most of the situations modeled. Why did the values seem to jump around so much among locations and frequencies, and what caused these abnormally high values?

Effects of Length: The One-Radial Model

As I mentioned above, some of the patterns appeared to show unexpected performance when the length of the vehicle was some particular fraction of a wavelength. “Bingo!”

CENTER LOADED WHIP - LEFT END OF AN RV'S FRONT BUMPER
Elevation Plots through the Main Lobes, See Table for Azimuth Angles

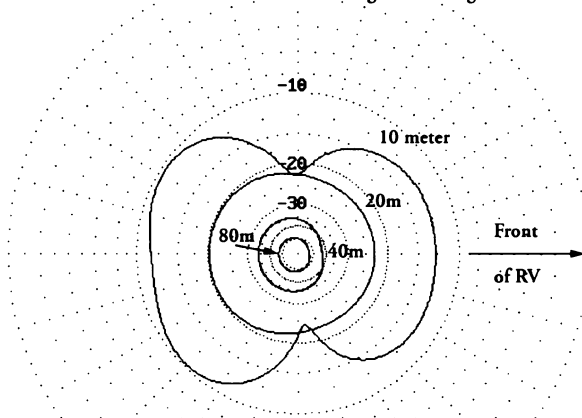
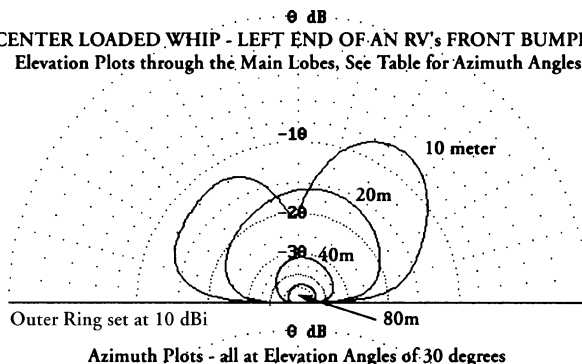
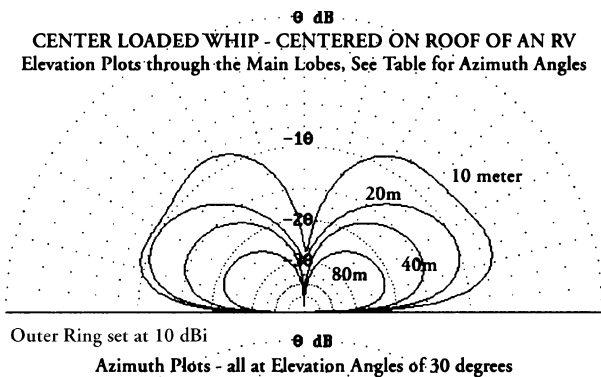


Fig 14—Whip on front bumper of RV. See Table 5.

CENTER LOADED WHIP - CENTERED ON ROOF OF AN RV
Elevation Plots through the Main Lobes, See Table for Azimuth Angles



CENTER LOADED WHIP - LEFT END OF AN RV'S REAR BUMPER
Elevation Plots through the Main Lobes, See Table for Azimuth Angles

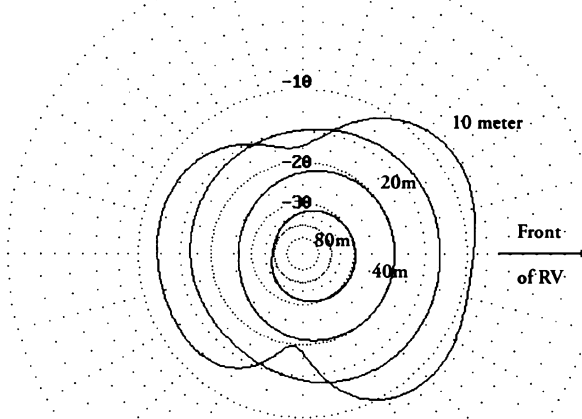
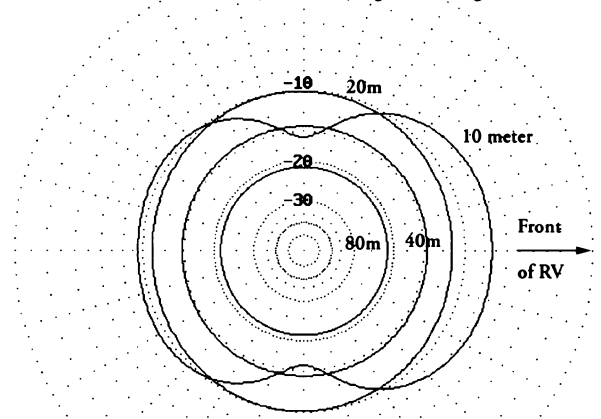
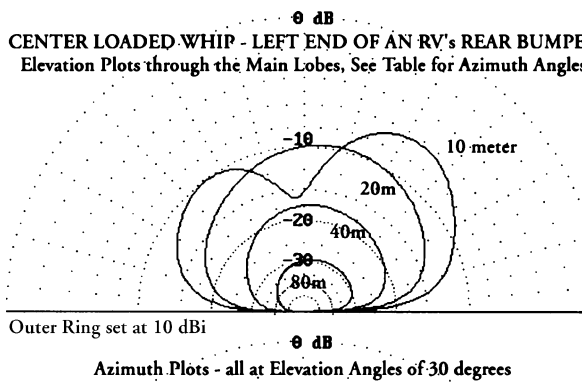


Fig 13—Whip at center of RV roof. See Table 5.

Fig 15—Whip on rear bumper of RV. See Table 5.

I thought. Let's see if vehicle length by itself—regardless of width and height—has some understandable effect.

As an extreme case, I visualized a vehicle as a very fat transmission line lying parallel to the ground with an antenna at one end. As an even more-extreme case, I visualized a wire-like transmission line—in fact a single, above-ground radial—with a vertical whip at one end. If the antenna were not present, the following can be said of the radial:

- It will resonate at certain frequencies, ie, at multiples of $\lambda/2$.
- High-impedance (voltage) nodes will form at each end at these frequencies, making it difficult to force current to flow into the ends.
- Whatever current flows into the bottom of a whip antenna must also flow from the structure on which it is mounted. If the end of the radial exhibits a high-impedance node, then matching the antenna becomes impossible!

To test this, I modeled a very simple case with a 29-MHz whip sticking straight up from one end of a single horizontal ground radial 20 inches above a “real” ground and of adjustable length. I gradually changed the length of this radial, covering a range from about 28 inches (less than $\lambda/10$ at 29 MHz) to 400 inches (λ). I used a simple 10-meter whip and tuned its height for minimum input reactance for each length of the radial.

This simple L-shaped model is shown in the top portion of Fig 17. It generates a variety of radiation (elevation) patterns, a selected set of which is shown in the upper and lower portions of Fig 16. Each pattern is annotated with its associated radial length.

The lower portion of Fig 17 graphs the values of four different calculated parameters against the length of the radial. The left scale is used for the length of the whip (above the radial), the take-off-angle and the gain (multiplied by 10 to better fit the scale). The right scale is used to plot the resistive component of the input impedance. All maximum-

gain lobes point toward the far end of the ground radial.

At radial lengths near 400 inches—approximately λ —the input reactance could not be minimized, the input resistance tended toward infinity and the antenna height became very small, just a few inches. Clearly, the formation of high-impedance nodes at the ends of the ground radial prevented current from flowing into or out of the antenna base. Owners of 400-inch-long RVs (of negligible height and width) will not be able to drive 10-meter whips mounted at the ends of their vehicles, no matter what kind of matching circuit they try!

The model became tractable for lengths of 387 inches and less. The input resistance decreased from some 1001 Ω to a low of 18.8 Ω as the radial length decreased to 326 inches. Decreasing the radial length even further caused the input resistance to turn around and rise until tuning for minimum input reactance again became impossible at a radial length of 225 inches (close to $\lambda/2$). Over this entire range of radial lengths, the antenna height steadily increased, reaching 180 inches for a radial length of 225 inches. The gain and take-off angle also steadily changed over this range. A maximum gain of 7.75 dBi was achieved for a radial (vehicle) length of 326 inches. Between radial lengths of 225 and 187 inches, on either side of $\lambda/2$, the model again proved impossible to tune.

With radial lengths from 187 to 28 inches, the values for antenna height and input resistance roughly repeated the behavior described above. The take-off-angle plot shows a relatively abrupt change from the 80°-90° range to the 20°-30° range at a radial length of around 130 inches. This can best be seen by viewing the changes in the shape of the elevation plots shown in the upper and lower portions of Fig 16. High-angle lobes give way to lower-angle butterfly-shaped lobes.

The whole behavior is obvious—once I found it. I asked myself: “Why didn't I think of this? Has it been discovered before? Am I reinventing the wheel?”

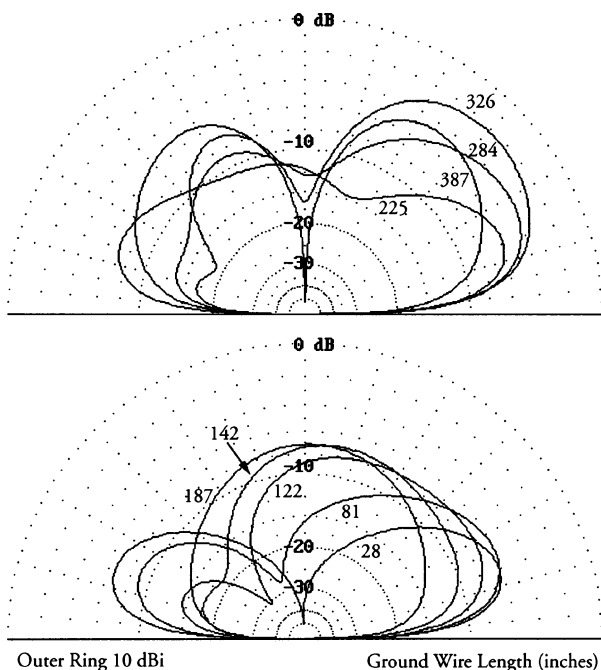


Fig 16—Ten-meter whip with single ground radial.

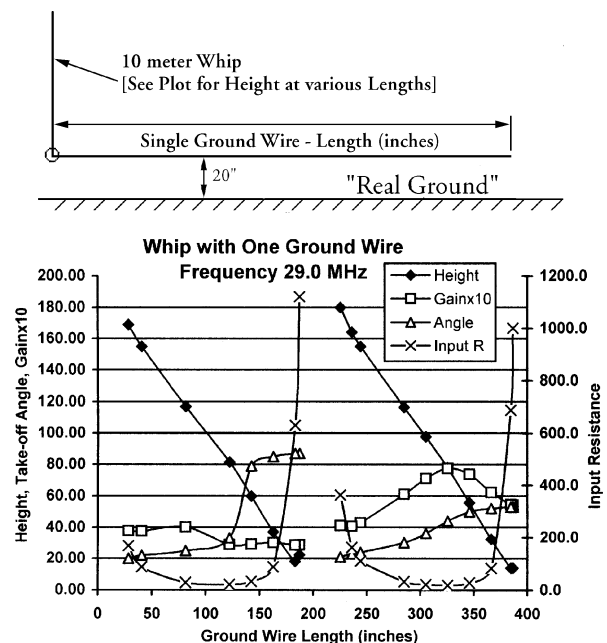


Fig 17—Effect of length of single radial.

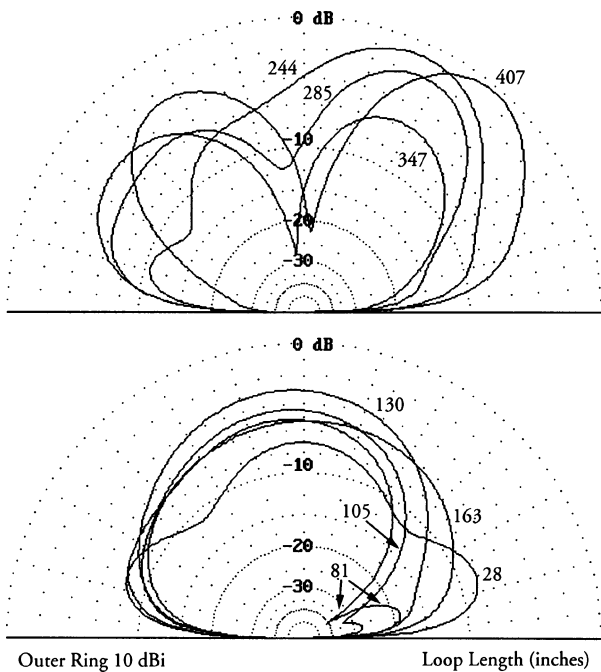


Fig 18—Ten-meter whip spaced 20 inches from a large loop.

Generally, if one mounts an antenna at some point on a vehicle that becomes a high-impedance node at some particular frequency, then one will not be able to drive power into that antenna!

Effects of Length of a Conducting Loop

The final step for this article was prompted by thought about the currents induced in the vertical end of a vehicle near a vertical antenna. An electrically large conductive box, such as an RV, can act as a short-circuited loop. Current induced by a whip located near one end flows up that end, along the top surface, down the other end and then returns along the lower edge. Resonances around this loop will not occur at exactly the same frequencies as resonances along the horizontal length of the vehicle. Fields from these different currents will combine in some complex way to form equally complex radiation patterns. I reintroduced height into the model by replacing the single ground radial with a vertically oriented loop of wire. The loop is 76 inches high by “loop-length” long, as shown in the upper portion of Fig 19. A second, parallel ground radial, 76 inches above the original ground radial, was added. Their ends were joined by two 76-inch vertical wires. The whip antenna was moved 20 inches to the left, and a 20-inch horizontal extension was added to space the antenna away from the loop.

In this situation, two electrical conditions must be met simultaneously. Not only must any current driven into the base of the antenna from the feed lines be balanced by an equal and opposite current out of the corner of the loop to which it is attached, but also any antenna current induces an opposing current in the nearby vertical portion of the loop. Some combination of these two currents will resonate around the loop and the antenna. Fig 18 shows the radiation patterns for this model. The lower portion of Fig 19 graphs the calculated parameters.

This model shows a somewhat similar behavior to that of the single ground radial, but without the extreme values of

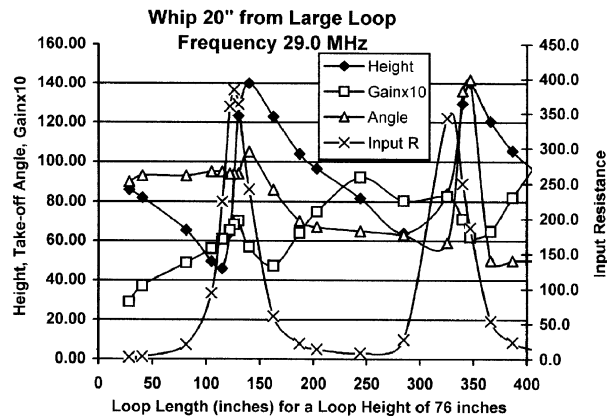
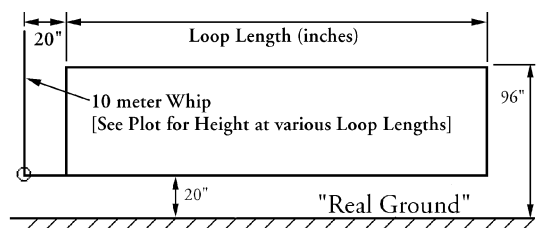


Fig 19—Effect of length of large loop.

input impedance. The whip could be tuned at all frequencies. Strong resonant behavior—including high values of input resistance—is evident at lengths of about 326 inches (326 plus the loop height of 76 inches equals λ) and 126 inches (126 plus 76 equals $\lambda/2$). Clearly, the resonances of this short-circuited loop are following the long-known rule of thumb for microwave cavities: The circumference of the object (cavity) is the primary factor in determining the resonant frequency. The shape, whether cylindrical, rectangular, or otherwise, is significant but only of secondary importance.

Conclusion

HF whip antennas mounted on vehicles are often inexplicably difficult to match to antenna feed lines. This article explored a selected set of vehicles and mounting locations, then investigated some of the factors that cause problems. The length and height of the vehicles, measured in wavelengths, play a major part.

Notes

- ¹P. Madle, KE6RBV, “The Car—As a Contoured Ground Plane,” *QEX*, Jan/Feb 1998, pp 3-8.
- ²R. Schetgen, KU7G, Editor, *The 1995 ARRL Handbook* (Newington, Connecticut: ARRL), p 20.46.

Peter Madle, KE6RBV, graduated from London University, England, in 1948 as an electronic engineer (BS). Almost all his career has been spent in the field of military electronics, missiles and satellites. First in England, then in Canada and after entering the United States in 1957, at various major defense contractors on the East and West Coasts.

Before leaving England he was an active SWL and “really tried” to achieve the required 13 WPM in code, but never “made the grade” before shipping out. His interest in Amateur Radio revived after his retirement in 1992—at least as far as becoming a no-code Tech, but the thought of learning code now is quite daunting. Will the future include moon-bounce, ATV or satellites? Time will tell. □□

Performance Specifications for Amateur Receivers of the Future

What constitutes an ideal receiver? Don't just sit and wait for the features to appear. Join this discussion and help determine your own future.

By Ulrich Graf, DK4SX

The increasing severity of EMC problems in Europe, especially in Germany, may lead in the near future to a requirement that amateurs reduce output power. In so doing, the strength of desired signals would be much lower in our receivers. Achieving the same signal quality as before—with unchanged signal density and levels from commercial stations—will require that receiver strong-signal performance be significantly increased. This means improvements that have not yet been addressed in most equipment presently on the market.

Forty years ago, the DARC (Deutscher Amateur Radio Club)

defined a technical standard with the development of the RX57 and RX60, and demonstrated to amateurs how to homebrew proven top-technology receivers. Today, this task has been ceded entirely to industry. Nevertheless, according to the “Future of Amateur Radio” workshop, the demand from commercial customers for shortwave communications equipment will soon decrease dramatically. To the amateur, this means fewer manufacturers and reduced variety in the foreseeable future. In my opinion, radio amateurs are forced to define the receiver of the future before this situation occurs. Decreased competition among only a few brands will offer little chance to influence specifications. It's time for amateurs to define the functionally critical parameters of top-of-the-line radios themselves, rather than leave

this essential task to Far East marketing strategists.

The following specification proposal can be thought of as a platform for discussion. It should serve to stimulate dialogue about the performance levels required. It illustrates some of the deficiencies in actual implementations, and—I hope—encourages criticism of outdated standard solutions. I will define terms and explain criteria for certain performance numbers.

Modes of Operation

An amateur HF receiver must operate in SSB and CW modes. Even though AM is only of historic value technically, many shortwave listeners value a good AM detector. For narrow-band FM, the necessary limiting IF amplifier and demodulator could

Seidlheck 19
D-89081 Ulm, Germany
ulrich.graf@ulmail01.europe.nokia.com

be realized on an optional plug-in module. Digital modes could be demodulated in SSB mode within an appropriate IF bandwidth.

The BFO must be tunable. A tuning range—either continuous or in 10-Hz steps—of ± 2 kHz seems to be adequate.

Sensitivity versus Noise Figure

In the past, and even today, much attention (perhaps too much) has been focused on receiver sensitivity. This may be explained by the historic evolution of receivers. Today, with modern parts and circuitry, virtually any reasonable—or unreasonable—sensitivity is possible. As long as it is treated outside the context of total dynamic range, sensitivity is not an important quality specification for a receiver any more!

Defined as the voltage across the receiver's input terminals for a set signal-to-noise ratio, sensitivity is determined by the gain and noise figure of front-end components (like filters, preamps, mixers and their following amplifier) and by IF filter bandwidth and audio-passband shape. Different audio responses and an irritating variety of IF filters in multiple IF conversions make sensitivity specification an ambiguous task. It is difficult to find sensitivity numbers in test reports or data sheets referenced to a standardized test bandwidth that allows immediate comparison. Because many amateurs are not aware of its impact on sensitivity, bandwidth is often manipulated to obtain better sensitivity numbers. As a result, most of these data are unusable and don't allow objective comparisons of receiver quality overall.

Sensitivity measurements are even more difficult to compare in modern transceivers with digitally processed audio. A usual single-tone sensitivity measurement of a radio having DSP noise cancellation leads the DSP to use the narrowest available bandwidth. It does not take the noise power usually present within the average voice bandwidth (300 Hz to 3 kHz, 2.7 kHz bandwidth) into account. Measured in this way, a DSP receiver exhibits up to a 20-dB increase in sensitivity over its analog counterpart, even though front-end components and circuitry might all be the same, and the IF bandwidth switch is in the same (eg, SSB) filter position! The difference is not caused by improved front-end construction, but only by dramatically reduced bandwidth. Yet, this reduced bandwidth is irrelevant for SSB. Because noise-canceling

bandwidth reduction operates automatically and independently of the actual IF bandwidth, this phenomenon is not even uncovered by many testers and readers of their papers.

The dilemma is obvious. Why not throw the classic bandwidth-dependent measurement overboard and introduce a bandwidth-independent sensitivity criterion to Amateur Radio tests? Noise-figure evaluation is a professional, standardized procedure that is simple to perform, needs little equipment and results in reliable numbers always comparable to those of other devices.

At HF, a receiver noise figure of 15 dB is adequate. Nearly all (95%) receiving situations on all shortwave bands will be managed with ease, since receiver noise plus usual feed-line loss will not exceed atmospheric noise. Accounting for average input-filter loss, a 15-dB noise figure can be realized practically with a passive mixer for highest signal capability. In remote areas with low man-made noise levels, a noise figure of 10 dB is low enough for DX work on the higher bands, even with a simple dipole or vertical antenna. This is easily accomplished with a switchable preamplifier. A linear amplifier with a 3-dB noise figure and 10 dB of gain is more than adequate for up to 3 dB input filter loss. Multiple preamplifiers in a receiver front-end give the impression of sub-optimum design and only add avoidable cost.

For comparison purposes, we can look at the relationship between noise figure and sensitivity as a function of bandwidth in [Table 1](#).

Bandwidth

Different operating modes require different receiving bandwidths. Bandwidth selection (filtering) should take place at a point as close to the front end as possible. This gives the greatest immunity against strong adjacent signals. In multiconversion systems with channel selection on the lowest IF frequency, only filters in all previous IFs having the maximum necessary bandwidth for the mode in use should be permitted. The roofing filter

on the first IF and the filters in the second IF must be designed to about 3 kHz maximum bandwidth for SSB. In a third IF, only the selection between, for instance, 1.8 kHz, 2.1 kHz and 2.4 kHz is to be performed by DSP with the lowest-possible shape factors. Roofing and second-IF filters should *not* be designed for AM—or still worse, FM—as in actual designs, with narrow CW bandwidths then selected by DSP at a low-frequency IF!

With an AM or FM-mode option, not only demodulators but also wider filters must be installed. This seems to me the only way that a receiver can have optimum interference immunity in its basic configuration. For best CW operation, the mentioned filters should exhibit an even smaller bandwidth: 1.0 to 1.5 kHz bandwidth in the first IFs would allow pleasant frequency-search operation and satisfyingly rapid AGC action.

Conclusion: Optimum interference immunity of a modern multi-mode amateur receiver is obtained only with selectable filters optimized for specific modes of operation in both the first and second IFs.

This prohibits receiver systems with a first LO tuned in several-kilohertz steps and fine tuning performed with the second LO. With those architectures, the bandwidth of the first IF filter must always be at least the sum of the bandwidth needed for the mode in use and first LO step size. Such a receiver will never perform ideally under large-signal operating conditions!

Selectivity

For optimum adjacent-channel selectivity, the shape factor and ultimate attenuation values of the filters in use are most critical. Shape factor is defined as the ratio of -60 dB bandwidth to -6 dB bandwidth, and should be two, or less, for a good filter. The best mechanical filters offer shape factors as low as 1.3, and DSP offers almost rectangular selectivity curves, with

1.1 shape factors obtainable. The best ultimate attenuation is strongly dependent on filter mounting and the circuit layout associated with it. Utmost care and skill is necessary in

Table 1—Noise Figure versus Sensitivity/Bandwidth

Noise Figure	Sensitivity, $V_i / 50$ Ohms for 10 dB S+N/N ((V)		
	Bandwidth 500 Hz	Bandwidth 2400 Hz	Bandwidth 4000 Hz
10 dB	0.10	0.22	0.28
15 dB	0.18	0.39	0.50

layout and shielding design to reach the necessary -90 dB ultimate attenuation for a single filter, or a minimum of -120 dB for a filter cascade. Shape factors of installed filters must be evaluated during tests, and should be mentioned in the data sheets! Measurement of image rejection gives an indication of the ultimate attenuation of the roofing filter.

Ultimate attenuation of a DSP implementation is usually limited by the A/D converter's dynamic range. Actual values are about -80 dB, maximum. Additional preselection is therefore required.

Low-cost ceramic filters are not always available in optimum bandwidths for given modes, and there are very few manufacturers offering ceramic filters with sufficient ultimate attenuation and satisfactory shape factors. So the receiver must be equipped with crystal or mechanical filters. Double-conversion receivers with DSP filtering in a second IF require selectable eight-pole filters with low shape factor as roofing filters.

If the shape factor and ultimate attenuation can be realized according to these recommendations, real selectivity will be limited only by LO sideband noise. Requirements such as those given below under "Blocking Dynamic Range" allow the use of narrow-band crystal filters with low shape factors. Selectivity is one of the very important specifications. So we *must* have the measured shape factor and ultimate attenuation of the IF path in the receiver's datasheet.

Tuning

Tuning may be realized using either analog or digital means. Tuning should vary frequency at a rate of 5 to 25 kHz per knob revolution to tune sensitively enough in SSB or CW mode, even with narrow-band IF filters. Fine resolution of digitally synthesized or DDS-generated LO signals is preferably done in 10-Hz steps or less. Only this minimum fine resolution results in quasi-continuous tuning and easy listening. The tuning rate must be adjustable to larger frequency steps, ie, 100 Hz and 1 kHz. The tuning encoder must offer a resolution of at least 100 to 300 bits per revolution, or search operations are too cumbersome because of the continual need to switch between tuning rates.

Frequency Stability

A temperature-compensated crystal oscillator as a receiver frequency reference guarantees ± 1 ppm stability at

acceptable cost. This corresponds to a maximum frequency deviation of ± 30 Hz on the 10-meter band over the full temperature range. Even for data communication during long transmission periods, higher stability is not required. A free-running analog oscillator's absolute drift should be within 100 Hz per hour at room temperature $\pm 10^\circ\text{C}$ (including warm-up).

Absolute frequency accuracy is only required in unsupervised automatic use. Band-edge limits require a safety offset determined by the mode in use. Since amateurs are able to recalibrate their radio's frequency reference regularly by comparison to WWV, absolute accuracy of the internal reference plays only a secondary role. A typical aging value of ± 2 ppm per year should be adequate.

IF-Shift and Variable Bandwidth Tuning

Parallel shift of mixer injection signals before and after one or more filter chains moves the passband of these filters without affecting the receiver's frequency. If this manipulation keeps the passband width unchanged, it is a typical case of IF-shift. (Although Drake and Collins called this technique *passband tuning*.) IF-shift can help suppress interference on one side of the desired signal.

The process of variable-bandwidth tuning (VBT) varies IF bandwidth by effectively moving filter edges individually. Like IF-shift, VBT helps suppress nearby interference, but it can exclude interference on *both* sides of the desired signal. Narrowing the passband can also degrade the intelligibility of the received signal. By individual manipulation of filter edges, you can indeed react more flexibly to interference, but handling tends to be a little complicated. To avoid mistuning of the receiver frequency, definite center positions of VBT and IF-shift knobs must be marked.

With VBT, it is possible to adapt passband width to narrow-band signals with wide filters. You must realize, however, that absolute filter-edge steepness of wide-bandwidth filters tuned to a small bandwidth is much less than that of an individual narrow-band filter, even when filters have equal shape factors! Optimum filter adaptation to received-signal conditions is therefore only possible with individually selectable filters. The best choice of multiple bandwidths of low-

est shape factor at reasonable cost is offered by receivers with DSP.

IF-shift is already possible in single-conversion superhet receivers, VBT needs multiple conversions. With a digitally processed IF, you are not only able to implement specific bandwidths, but also individual filter center frequencies.

Notch Filters

Notch filters permit the rejection of steady or pulsed single-tone interference. They are most efficiently realized at low IFs. Notch filtering can be implemented by tuning an analog trap or bridge circuit, or digitally, with DSP. Using adaptive DSP algorithms, several interfering signals may even be suppressed simultaneously. In addition, it is possible to weigh signals so that short pulses like CW signals are suppressed in one case, or only continuous tones are affected in another.

Strong interference tends to overload previous IF stages if notch suppression takes place in the last stages. An effective design should have a compromise between highest notch suppression and satisfactory overload characteristics. Such a compromise prohibits the use of less-efficient audio notch filters.

Desired-Signal Dynamic Range

Dynamic range is the difference between the weakest detectable signal and the strongest linearly processed signal in a receiver. The weakest detectable signal is determined by the receiver's noise figure. It is also measurable as the $(S + N) / N = 3$ dB level, referred to as the minimum discernible signal (MDS). It represents an input signal power equal to the receiver noise floor. When measuring MDS, all of the factors mentioned about sensitivity above must be considered! This measured MDS must be cross-checked with the value computed from noise figure because, as the reference for all dynamic-range definitions, it effects other measurement results. Differences must be within 1.5 dB.

Most important for dynamic-range measurements is the definition of a standardized IF bandwidth. I would suggest a bandwidth of 2.4 kHz because it is used in most amateur communications receivers. In addition, all sensitivity and MDS evaluations must be performed with a linear audio response of from 0.3 to 3 kHz ± 3 dB. Any measurement results that are not clearly related to this IF bandwidth

and audio response are questionable.

The strongest manageable signal is determined by a certain level of distortion, or by audio-gain reduction caused by front-end or IF overload. Goals for dynamic range are given below.

Gain Control (AGC)

The gain-control range should come close to desired signal dynamic range. Gain control must react even to very small input signals. In many modern receivers, this point is neglected in favor of a subjectively “quiet” output when input signals are weak. Insufficient IF gain has then to be equalized with increased audio gain. Better IF AGC circuits affect weak signals, so that they are reproduced with constant audio power and shown accurately on the S-meter.

A good AGC will have little overshoot, no sign of oscillation and rise and decay times optimized for the different modes. Real difficulties are caused by the delay that signals experience while passing through narrow-band IF filters, which makes short attack times a significant design problem. For a similar reason, processing times in a DSP receiver sometimes lead to unacceptable control characteristics. Even some professional radios—analogue and digital—exhibit control characteristics with intolerable overshoots in CW with short hold times and distorted audio response in SSB that can only be corrected with additional manual control. In a system with multiple cascaded filters at different IFs, it is very desirable to have a fast-acting AGC for initial adaptation, say after the narrow-band roofing filter. This is also recommended for DSP receivers. Nevertheless, correct operation of such an AGC is only achieved when the roofing filter’s bandwidth is close to that of subsequent filtering. That means, of course, that filters preceding derivation of the AGC signal must be mode-selectable.

Optimum AGC design makes a manual gain control superfluous. In other words, a receiver that performs best only with manual gain control has a deficient AGC. If masking of weak interfering signals is desired, selection of a long AGC hold time is always the better way of operation.

IMD Dynamic Range

Intermodulation dynamic range is the difference between the MDS and the levels of two interfering signals causing an IMD product just equal to the MDS. IMD products of second, third

or higher orders are usually characterized. All of them count equally, and I can’t repeat it often enough: Measurement results without reference to IF bandwidth and audio response are meaningless! IMD dynamic range best shows the large-signal capabilities of your receiver—how it behaves under real-world conditions on a big antenna.

From the IMD dynamic range and the level of interference, you can calculate the intercept point (IP). Along with noise figure, it is one of the most important quality criteria of a modern receiver. For easiest comparison, it is best related to the input level at the tested receiver or module, and given for at least the second and third orders. [IP is the extrapolated input level at which the distortion product’s level just equals that of the interference. The IP of a receiver is calculated from the upper IMD dynamic-range measurement by assuming a distortion product of order n increases n dB for every decibel the interference is increased.—*Ed.*]

Intercept point is bandwidth-independent! It may be shifted to higher values with an attenuator at the receiver input. Thus, the unchanged dynamic range will be shifted toward higher levels at the expense of sensitivity. Activating a preamplifier reverses the situation. However, the IP is even further decreased because of the distortion added by the preamplifier. For quickly comparing large-signal capabilities of a receiver, preamplifier or mixer, the input IP specification is very helpful. To quantify the characteristics of a receiver overall, IP must be given with the corresponding noise figure! These data reveal IMD performance and sensitivity at a glance.

IMD immunity of a receiver is determined by the limits of its linear signal capability; ie, by the limiting effects of active circuitry such as the preamplifier, mixer and first IF amplifier. Passive components may also exhibit such limiting effects. Diodes for filter selection, receive/transmit switching or preamplifier or attenuator activation very often causes additional IMD in actual designs. Further, overload of varactor diodes in automatically tuned preselectors, subminiature chip inductors and monolithic two-pole filters (duals) in the first IF, right behind the first mixer, may take their part in IMD generation.

Meanwhile, you can easily find circuit suggestions for very linear preamplifiers in the literature. Mixers should be constructed as super-high-level switching types using MOSFETs.

To select front-end filters, subminiature relays are a prized substitute for PIN diodes, without any danger of overload. With these modifications, the rather poor IMD performance of Far East active circuitry could be overcome. When it comes to passive components, replacing chip coils with toroids increases the size of front-end circuitry. You won’t carry your receiver of the future around in your jacket pocket! These kinds of changes have a deep influence on system architecture. Unfortunately, most Amateur Radio manufacturers are afraid to invest in these design improvements.

Reducing transmit output power from 750 W (the legal limit in Germany) to 100 W equals a reduction of receiver input voltage of 8.75 dB. To increase the IMD dynamic range of a top amateur receiver by the same amount means an increase from 100.1 dB to 108.9 dB, and an increase of the IP_3 from about +25 dBm to +38 dBm if all the extension comes at the high end. Relate these numbers to a noise figure of 15 dB and a 2.4 kHz SSB bandwidth. This is the real challenge to receiver-development engineers! A receiver with this IP_3 does not need an input attenuator any more. Multi-step selectable attenuators are inefficient and only witness careless RF development and in-advance acceptance of deficiencies.

If the second-order IMD dynamic range should be equal to the third-order range, the equivalent IMD equation gives an IP_2 of almost +93 dBm. This can be obtained with additional front-end filtering only.

The measurement of high IMD dynamic range is made difficult by poor blocking or reciprocal mixing characteristics. Especially during third-order IMD evaluation with small frequency offsets, you find IMD products covered by increasing noise. Then it’s possible to obtain values that are too good to be true. This is always the case when blocking dynamic range is measured lower than IMD dynamic range. Comparison with experience quickly exposes unrealistic test results and methods.

In-band IMD

Distortion at baseband (audio) must have a maximum value of –40 dB. This value must not be exceeded by in-band IMD for all RF input signal levels and AGC conditions.

Blocking and Reciprocal Mixing

The term *blocking* is often used for

two mechanisms with comparable effects: compression and reciprocal mixing. Compression, or drive of active circuits into limiting, theoretically occurs only in front-end modules like preamplifiers, mixers and first IF amplifiers as long as the AGC range is larger than the blocking dynamic range. You'll find a definite, calculable relationship between all effects based on limiting, such as IMD, cross-modulation and compression. In other words, a receiver with sufficient IMD immunity will have sufficient cross-modulation and compression immunity. Testing and quality evaluation may therefore be restricted to IMD measurements.

When driving a receiver with high-level interference offset from a center-channel, desired signal, the interference mixes part of the sideband noise spectrum of the LO into the IF. There it covers up the desired receive signal. This is the reciprocal-mixing effect. Because of this noise increase in the passband, the receiver gets less sensitive; the result is called desensitization. Using narrow-band CW filters adjacent to strong signals—as in typical CW contest operation on 40 meters, or with multiple stations in proximity—makes this effect very evident, and argues for lowest-possible LO sideband noise. Actual blocking dynamic ranges should be > 110 dB, for an interference offset of 20 kHz, and measured in the SSB bandwidth. This gives you the chance to efficiently use a narrow-band filter with good ultimate attenuation in the first IF. In CW mode, this value should be maintained for offsets of < 10 kHz.

To use the wanted IMD dynamic range of about 109 dB (SSB bandwidth) in the presence of strong signals, the blocking dynamic range must be a minimum of 10 dB better, or 119 dB. This is essential to prevent desensitizing the receiver with any strong signals appearing near the front-end filter's passband.

A blocking dynamic range of 119 dB, measured in a 2.4 kHz bandwidth with a 20 kHz offset means the sideband noise of the LO signal has a maximum of $119 \text{ dB} + 33.8 \text{ dB}$ (bandwidth factor) = 152.8 dBc/Hz . This value isn't offered by any amateur receiver, at present. Modern radio development must make energetic progress to reach these specifications.

With small steps, synthesized LO signals are preferably created with direct digital synthesis (DDS) today. Because of the generation system and limited resolution of the D/A converter,

a DDS produces a discrete and predictable S/N ratio. The simple statement that a synthesizer can be noise-free only by application of DDS is strongly misleading. The LO might contain quite small amounts of close-in phase and amplitude noise, but unavoidable phase errors cause a dense floor of discrete, non-harmonic spurs. This limits receiver-blocking characteristics in a way comparable to sideband noise effects. A DDS reference in a LO synthesizer must therefore be band-pass filtered to gain a low-noise reference for use in a hybrid PLL-DDS system. Maximum filter bandwidth is determined by the tuning range for fine resolution, and should be less than ± 1 kHz. For wider tuning ranges, the broader noise floor causes blocking effects by strong signals close to your channel. A main PLL step size less than 2 kHz in this case probably brings the compromise of higher settling time. All this affects only full-break-in operation at the highest CW speeds and large TX/RX frequency offsets. Frequency hopping and high-speed scanning is of no importance to Amateur Radio.

Blocking dynamic range is as significant as IMD dynamic range, and must not be omitted in any test report.

Spurious Responses

A spurious response is the unwanted sensitivity of a receiver to image responses, to strong signals being mixed with spurs on the various LOs, or to signals appearing directly at the IFs. Interference in any IF is deleterious to reception on all RF bands. Signals at image frequencies lead to interference only when exact mathematical relationships are true. Their interference potential is not great as blocking. All receivers with a first IF higher than the highest receiving frequency limit (30 MHz) need nothing but a low-pass filter for image rejection. This is best realized by two separate, shielded low-pass filters of lower order for better ultimate attenuation. For utmost signal capability, use air-wound coils or toroids with 10-mm minimum diameter to avoid core-saturation effects.

Even in high-dynamic-range receivers, a detectable spurious response results from the first LO's second harmonic being mixed with a strong interfering signal's second harmonic. This interference always appears with an offset of $IF / 2$ from the receive frequency. To get rid of this response, some manufacturers choose a first IF frequency greater than 2×30 MHz. These high first IFs require careful selection

of crystal filters for maximum IP. Otherwise, only lower IFs and front-end filters with bandwidths less than $IF / 2$, could offer a satisfactory solution. However, those filters are required anyway to improve the IP_2 as outlined above. Ultimate attenuation of such filters may be relatively low; theoretically, 20 dB is adequate. Second-order IMD immunity requires sub-octave front-end filter bandwidths.

Inductive parts of these filters must also be wound on toroids or adjustable pot cores with large ferrite cross-sections.

Unusable Frequencies

All signals created internally and falling on a receive frequency can cause that frequency to be unusable. Amateurs know them well as "birdies." They must be suppressed (preferably to inaudibility) or mentioned in the datasheet if their strength is equal to or higher than a certain equivalent input level, say of $1 \mu\text{V}$ (-107 dBm).

In receivers that use digital circuitry for signal synthesis, IF and audio processing, a lack of circuit decoupling, insufficient shielding or careless filtering can result in audible internal signals. DDS tuning clicks, processor noise or DSP "space sounds" must be suppressed to a minimum S/N of 40 dB.

Signal-Strength Indicator

A signal-strength indication is usually derived directly from the AGC signal. If the AGC begins to act at very small RF voltages, the display range might reach 120 dB. The display should be calibrated in S units, decibels and a common RF level scale. Either $\text{dB}\mu\text{V}$ or dBm seem a suitable choice. Acceptable accuracy is ± 3 dB. The display must be corrected, of course, with the activation of a preamplifier.

Memory

Besides storage of operational settings when the receiver is switched off, the radio should be able to store a maximum of three other setting memories. Absolute frequency repeatability is seldom required for ham work—usually for specific contest applications or to memorize beacon or net frequencies—not more than 10 additional frequency memory positions are needed.

What is true of memories is valid for computer control and its interface as well. Only operators listening to non-amateur frequencies probably need an interface for PC decoding and processing of transmissions. In Amateur Radio, I don't know of any necessity for

PC control. Finally, few amateur radios must have a PC interface because only one in a thousand will be used as an unmanned beacon station. Unnecessary capabilities do nothing but increase cost instead of improving performance parameters or operational ergonomics.

Spectral Purity

LO signals must not be radiated from the equipment. These emissions must be suppressed to below the maximum-permitted FCC levels by adequate shielding and RF low pass and band-pass filters. LO radiation from modern receivers with first IFs above the highest receive signal frequency must be evaluated at the antenna connector.

Audio Response

For superior audio reproduction, a flat (± 3 dB) audio response from 300 Hz to 3 kHz is necessary. It is desirable to narrow or widen this response

by individual variation of upper and lower filter-cutoff frequencies. This may be accomplished by either analog techniques or digital audio processing.

Audio Output Power

A typical value for audio output power is shown in Table 2 below. Connections for a 4 to 8- Ω external speaker, 600- Ω headphones and a 10- Ω auxiliary load must be provided.

General Evaluation and Operational Ergonomics

The most prominent feature of today's standard and high-end equipment is operational complication. Who is still able to operate a top transceiver only infrequently or after a holiday period without the instruction manual? Who could say what function is hidden in which submenu, and which memory contents must be activated in which mode? The unspoken desire of many radio amateurs is a radio with

self-explanatory operation. Why is the Collins KWM-380, almost 20 years after its introduction into the market, still valued at second-hand prices hardly 30% lower than its original list price? The answer is simple: This transceiver provides both experts and amateurs respectable, top-quality RF performance and unbeatable audio quality. Its operation requires only a brief front-panel study. Tuning elements, mechanical design and modular construction are robust and easy to use and service.

Large-signal capabilities of the somewhat less-prized Drake TR-7A, introduced about 17 years ago, are still unsurpassed. The AGC characteristics, the expert design of the crystal filters, and their mounting on the PC board are exemplary. Only a few additional features offered by modern transceivers were not realized in these rigs. That leads to a provocative question: Is this all we have achieved from

Table 2—Proposed Technical Specifications for an Amateur Receiver of the Future

<i>Parameter</i>	<i>Specification</i>	<i>Remarks</i>
Modes of Operation	SSB, J3E, LSB and USB individually selectable; CW, A1A	Optional: AM, A3E; narrow band FM, F3E
Noise Figure	15 dB without preamp; 10 dB with preamp	
Bandwidth	SSB: 2.4 kHz nominal, 3 kHz maximum CW: 500 Hz nominal, 1 kHz maximum	Maximum bandwidths for filters in first and second IF! Provision for additional plug-in filters
Selectivity	Shape factor: ≤ 2 ; ultimate selectivity / filter > 90 dB; ultimate selectivity/ cascade ≥ 120 dB	Valid for roofing filter, too!
Tuning	Continuously or stepwise with ≤ 10 Hz resolution and ≥ 100 steps per revolution	Step size selectable in factors $\times 10$, $\times 100$, $\times 1000$ or $\times 30$, $\times 1000$
Frequency Stability	± 1 ppm 0°C to 45°C , TCXO	Aging ± 2 ppm/year
IF Shift	Center frequency ± 1.5 kHz	Constant bandwidth
Passband Tuning	Bandwidth 0 Hz (-6 dB) to maximum	Variable bandwidth
Notch Filters	Depth 40 dB minimum width 100 Hz -6 dB minimum	
Desired-Signal	120 dB minimum	Target: noise floor to 0.5 V (-125 dBm to $+7$ dBm)
Dynamic Range		
Gain Control (AGC)	Target: 120 dB -60 dB step: 100 ms To 5 s, preferably continuously	AGC time constants: $+60$ dB step: 15 ms maximum
IMD Dynamic Range	Target: 110 dB IP3 + 38 dBm (NF = 15 dB); IP2 $> +92$ dBm (NF = 15 dB)	IF bandwidth 2.4 kHz; Audio response 0.3 to 3 kHz (-3 dB)
In-band IMD	< -40 dB	Within total AGC range
Blocking Dynamic Range	Target: 110 dB at 5 kHz offset; 120 dB at 20 kHz offset	IF bandwidth 2.4 kHz; Audio response 0.3 to 3 kHz (-3 dB)
Spurious Responses	IF suppression > 100 dB image suppression > 80 dB IF/2 suppression > 80 dB	If IF < 30 MHz, image suppression > 100 dB
Unusable Frequencies	RF: interference $<$ noise floor; Audio: S/N > 40 dB	If interference > -107 dBm, then remarks in datasheet
Signal-Strength Indicator	According to AGC range, display S units, dB and dBm (or dB μ V)	Display accuracy within ± 3 dB with correction for preamp gain
Memory	Operation settings: 3; Frequencies: 10	Operation settings: mode, frequency, filter(s), preamp
Spectral Purity	to FCC specifications	
Audio Response	300 Hz to 3 kHz (-3 dB); nominal filter skirts -20 dB per octave	Pass-band response adjustable, marks for nominal bandwidth
Audio Output Power	1 W minimum at 4 Ω 200 mW at 600 Ω	

almost 20 years of Amateur Radio development? Of course, you can't make it right for everyone, but we are invited to think about all the money we've invested in the realization of questionable "gimmicks" instead of definite RF parameter improvements.

I really want to question the necessity of four controls for a station receiver's noise blanker now that the *woodpecker* is gone. Scan functions are nonsense *par excellence* in an amateur receiver, as are hundreds of memories. The squelch control, RF/IF manual gain controls and multiple-step RF attenuators are obsolete as well. Nobody could convince me so far, that a PC-controlled transceiver can be more ergonomically operated than one with only a handful of discrete knobs.

For simple handling in a future top receiver, the mode, selectivity, tuning rates, AGC time constants and memories could be chosen by individual keys. Selected parameters could then be shown on the display. Double or even multifunction keys must be strictly avoided! Besides a stripped-down keyboard, it would have elements for frequency tuning, audio volume, passband tuning, IF shift and DSP audio-response adjustment. Standardized terms for control functions would yield self-explanatory handling.

Correct use of DSP and DDS technology holds a great potential to revolutionize large areas of RF technology, while modern microprocessor control eases handling and operational convenience. Many remarkable improvements will be expected with these developments. Unfortunately, too many recent equipment "improvements" were obviously oriented toward marketing arguments rather than performance. Just remember the still-used, now-more-than-20-years-old JFET mixer technology, and those useless spectrum displays!

Finally, an important note: Data-sheets and test reports serve—besides displaying pretty pictures—to present an understandable explanation of a new product's performance so it can be compared to other products. Great stock is put in comparability! It would be best if specifications were based on internationally standardized measurement procedures. In case of any doubts, the amateur should not hesitate to look into professional "specs" for comparisons. You will quickly learn that good performance has always been a good reason for exposure, and that bad performance will be glossed over.

□□

A Better Mousetrap?

Although we don't often run this kind of article, we feel that the author's main point about dynamic range justifies the discussion. HF receivers operating in Europe suffer from extremely high levels of international broadcast interference. The cry for better strong-signal capability is echoed across the continent and in Great Britain. In the interest of promoting further dialogue about the problem, we offer some additional thoughts.

Receiver design involves conflicting goals. For example, the high-level mixer needed for dynamic-range extension requires more LO energy, which potentially means increased phase-noise and birdy difficulties. Multiple narrow bandpass filters in the first IF of an up-converting HF receiver seem to strain the trade-offs between performance, cost and reproducibility. Many experimenters have set their sights on digital-direct conversion (DDC), since this architecture addresses most of the desires mentioned while avoiding many of the pitfalls.

The number-crunching horsepower for DDC can be mustered even today, but ADCs with 119 dB of dynamic range and sufficient conversion speed are still a ways off. Until they appear, designers are hard-pressed to improve on the superhet. Practical matters in the design and operation of receivers mean that you are likely to agree with some of the author's points and disagree with others. We expect to hear from some of you on this one.—Ed.

Without Tears ®

Multimedia Interactive CD-ROM

Get all three CDs for \$1299 +S/H

Receive a free bonus Technical Book while
supplies lasts

Call Z Domain Technologies 1-800-967-5034 or 707-591-9620.

Hours: 9 - 5 PST. Or E-mail dsp@zdt.com

Ask for a free demo CD-ROM.

We also have live on-site 3-day seminars: DSP Without Tears,
Advanced DSP With a few Tears & Digital-Communications
<http://www.zdt.com/~dsp>

A 300-W MOSFET Linear Amplifier for 50 MHz

Everyone is looking to go QRO on 6 meters. Build this “almost a brick” to boost your signals from 15 to 300 W.

By Richard Frey, K4XU

In an earlier article, I described a 50 MHz, 125 V, 250 W, class-C amplifier using ARF448A/B high-voltage MOSFET devices.¹ This paper describes an improved version of an amplifier that is capable of class-AB linear operation. The design changes required and the procedures involved are explained and demonstrated. Complete descriptions of the amplifier and its construction are presented, as well as the measured performance.

High-voltage, high-power MOSFETs have been shown to be very capable RF

power amplifiers.² The metal-gate architecture of the ARF series from Advanced Power Technology has raised the frequency limits for this type of device to 100 MHz. The APT448A/B is typical of the series. It has a 68,000-square-mil die with a breakdown voltage rating, BV_{dss} , of 450 V. The device is provided in the inexpensive TO-247 plastic package, and is available in common-source symmetric pairs. Like all MOSFETs, the gate threshold voltage, V_{th} , has a negative temperature coefficient. This makes operation as a linear amplifier difficult or impossible without compensation.

When forward biased with a constant gate voltage, the quiescent drain current rises as the temperature of the die increases. Operating at the typical drain voltage for these parts, about

one third of the rated BV_{dss} , the power dissipation caused by the increasing I_{dq} results in “hot spotting” and subsequent thermal runaway. This is an unstable system. The dissipation increases so rapidly that the outside surface of the case does not follow internal junction temperature well. As a result, a bias-compensation scheme that uses temperature sensing cannot keep up with the V_{th} shift, and the device is destroyed.

The power dissipation within the die is a direct function of the operating voltage. By lowering the operating voltage, the thermal loop gain can be reduced to a point where the gate-threshold shift can be compensated. Thermal stability can be achieved by sensing the case temperature. Linear operation thus becomes practical at

¹Notes appear on [page 54](#).

100 V and below. While this is less than 25% of the rated BV_{dss} and produces less gain, a very rugged and useful linear amplifier is the result.

Amplifier Description

The following were the design goals for the amplifier:

- Frequency range 50 to 51 MHz
- Input SWR < 1.5:1
- Gain > 13 dB
- Output power 300 W PEP or CW
- Efficiency > 50%
- IMD3 > 25 dB below PEP

A push-pull topology was chosen for best output power and minimum harmonic content. The previously reported class-C design used $V_d = 125$ V. Since this is too high for reliable class-AB operation, 80 V was eventually chosen for this design. This is a compromise between gain, efficiency and thermal stability.

Since the gate input impedance is very low, it magnifies the effects of any stray inductance in the gate matching circuit. In a push-pull design, it is critical to maintain absolute symmetry between the two sides. This fact was demonstrated during the initial design work. One preliminary design had a slight asymmetry in the PCB artwork. The amplifier exhibited low efficiency, hot ferrite in the output transformer balun and poor distortion characteristics with asymmetrical IMD product amplitudes. This clearly demonstrates the benefit of symmetrically packaged devices.

A multiple-aperture ferrite bead was chosen for the input transformer. Brass tubing was used for the secondary, and the primary was wound inside the brass tubes to provide a very broadband balanced transformer design with minimum leakage reactance. Several cores and construction methods were evaluated, and this well-tried design proved best.

The typical HF push-pull amplifier employs a bifilar choke to decouple the drain-voltage feed. As frequency and power increase, this feed method becomes less practical because the need to reduce the number of windings to offset the stray capacity and the need to prevent core saturation conflict. In this design, a powdered-iron toroid was chosen for the feed choke core. This proved far superior to any of the ferrite cores evaluated. It is inexpensive and easy to reproduce.

Design

Three main areas must be addressed. The input matching must

provide a balanced feed to a pair of low-impedance gates. The output must be matched to a suitable load impedance, and then transformed to a 50- Ω unbalanced load. The bias must be thermally compensated to track the negative temperature coefficient of the gate bias threshold.

The input is reasonably straightforward. Each gate input is $0.2 + j0.5$, as estimated from the data sheet. The push-pull topology puts these two impedances in series, which makes the matching less difficult. A Smith Chart³ program makes the actual design easy. The program used here is *WinSmith*.⁴ The two gate impedances are added in series, and a network synthesized to transform the resulting impedance up to 50 Ω . The Smith Chart program only works with single-ended circuits, so the center tap was added later. See Fig 1.

The input-transformer design was chosen for its simplicity and relative ease of construction. Of several attempts using different material permeabilities, multiple beads and different conductor types, this proved to be the best and most consistent performer. The core is a Fair-Rite⁵ "multi-aperture" core, part number 2843010402. The type-43 material has a μ_i of 850. At 50 MHz, type-61 material (μ_i of 125) would also be satisfactory. This transformer is essential to provide balanced drive to the gates of the MOSFETs. The secondary wind-

ing is $3/16$ -inch brass tubing. Copper shim stock forms the connections to the brass tubing at each end of the transformer secondary. The two-turn primary is wound inside the tubing. This construction provides a very reproducible transformer with minimum leakage reactance and a very broad frequency response. It would be a suitable input transformer for a broadband amplifier covering 1 to 100 MHz.

The leakage reactance of the input transformer—referred to the secondary—is about 18 nH and is represented as L1 on the simplified input schematic in Fig 1. The gate load is represented by the "Load R," L2 and C3. Using all three parts of the gate impedance allows proper evaluation of the network bandwidth. A pi network consisting of C1, TL1 and C2 is used to step-up the gate load to the 12.5 Ω needed by the transformer and compensates for T1's leakage reactance. Notice that the net stray inductance of the gate is almost enough to effect a match with a single shunt capacitor. This has actually been done, but it was not easy to fit all the parts in the available space; so it was judged unacceptable here. To transform the network into the required balanced configuration, the series TL1 is split into two equal parts; the shunt capacitors remain the same, and a neutral center tap is provided at the transformer secondary.

Because of the high currents circu-

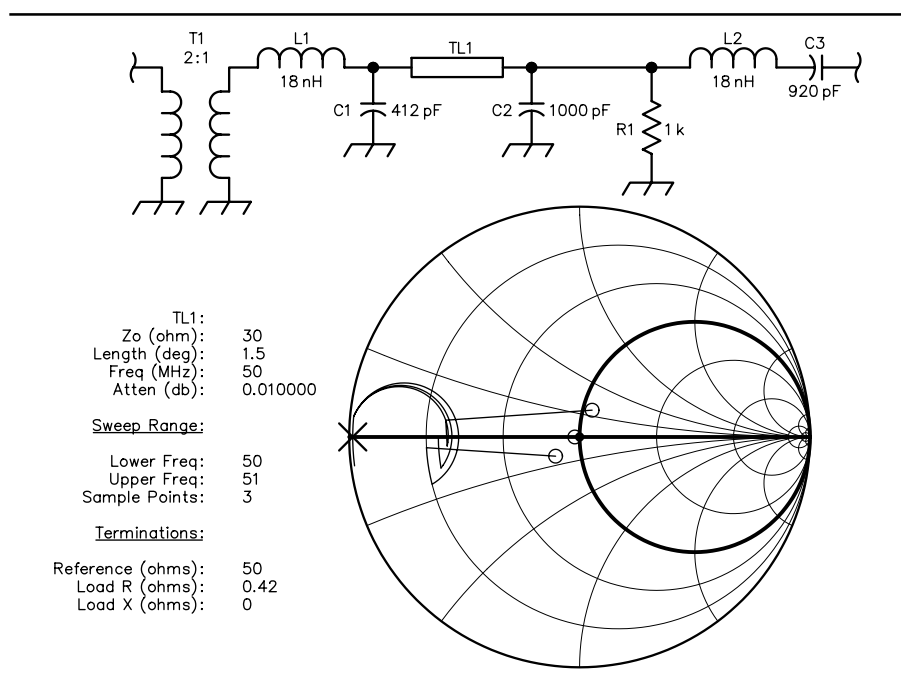


Fig 1—Input matching network and calculation.

lating in the input network, it is imperative that C2 be a larger-sized, class-1 dielectric (C0G or NP0) capacitor. It must be a lead-less, surface-mount chip type, or the value will need to be adjusted. The input tuning capacitor, a 900 pF mica compression trimmer, is mounted directly to the end of the input transformer.

The output network is also straightforward. The proper load impedance for class AB is calculated from the formula:

$$R_L = \frac{0.98V_{dd}^2}{2P_o} \quad (\text{Eq 1})$$

This is the load for each device, and P_o is one half of the total in a push-pull circuit. It is shunted by the output capacitance, C_{oss} . As was done for the gate

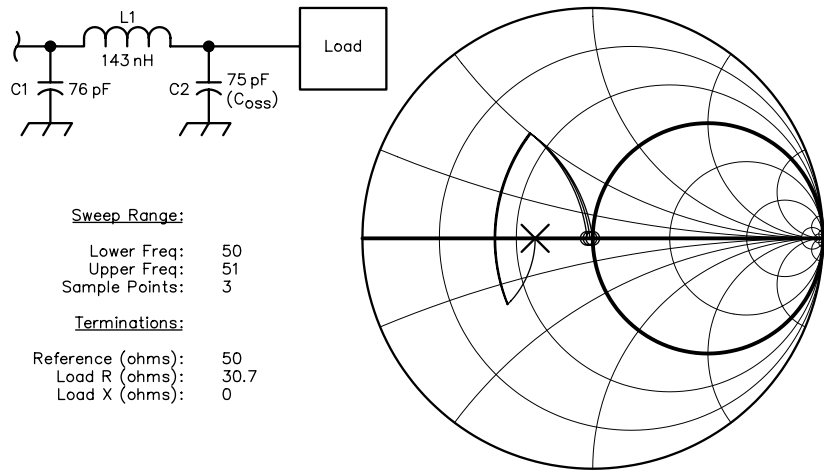


Fig 2—Output2Fig 2--- matching network and calculation.

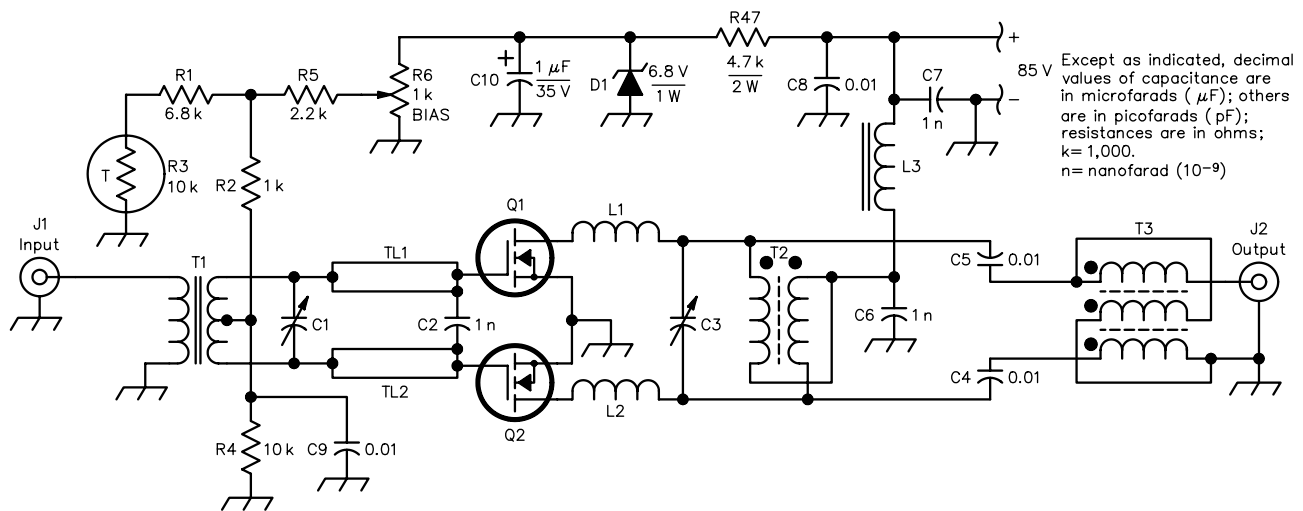


Fig 3—50 MHz amplifier schematic diagram.

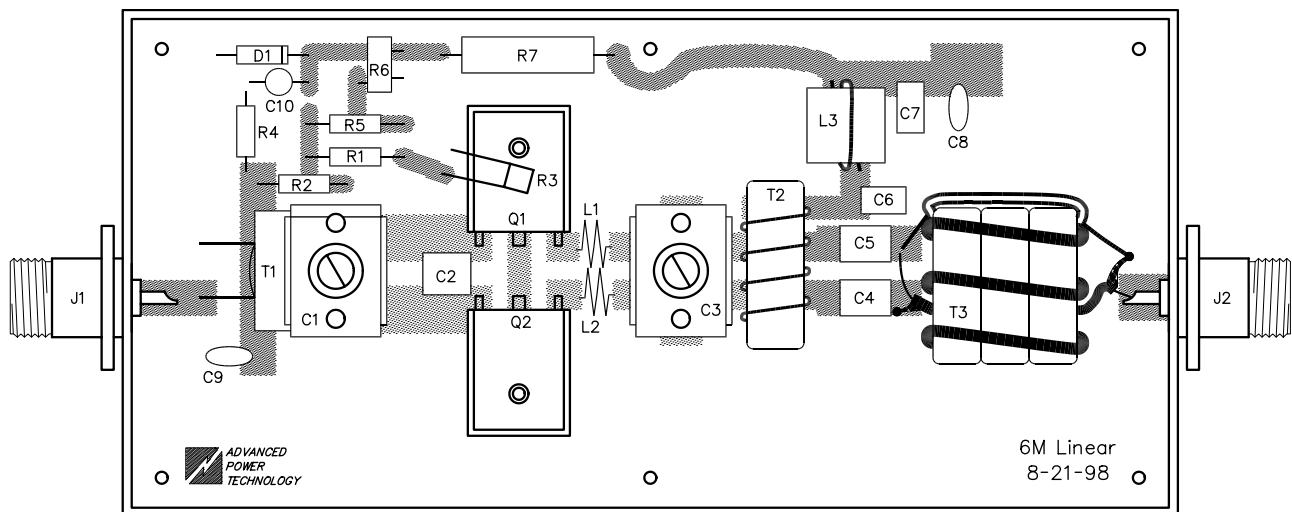


Fig 4—Amplifier parts layout.

circuit, both output impedances are series-connected to represent the total output impedance. The result for both devices in push-pull is $30.7\ \Omega$ in parallel with $75\ \text{pF}$, half the output capacitance of a single device. Though the design goal was $300\ \text{W PEP}$, the amplifier was actually designed for a $400\ \text{W}$ load line. This gives a good compromise between efficiency and linearity.

In a classical design, a suitable transformer would be used to set the load impedance, and either the output power or the operating voltage would be adjusted to fit the available turns ratio. Normally, in a low-voltage HF design, the output capacitance is ignored because it is shunted by a much smaller load resistance. At $50\ \text{MHz}$, the effects of the output capacitance must be compensated, so a slightly different approach was taken in this circuit.

WinSMITH was used again to design the output matching. See Fig 2. The output impedance of $30\ \Omega$ is rotated south by the effect of the shunt output capacitance, C2. Two options present themselves for compensation. Some additional shunt capacitance could be added to further reduce the equivalent series real part to $12.5\ \Omega$, a series L used to resonate the resulting series C, then a 4:1 transformer used to go to $50\ \Omega$. However, building a reproducible low-loss 4:1 balanced transformer was very difficult, and compensating its leakage reactance further complicates the design. The second option was used: The equivalent series output capacitance was resonated first, then more series inductance was added to rotate the load all the way up to the $1/50\text{-mho}$ conductance circle. Finally, a shunt capacitor was used to resonate the added X_L . The extra L and shunt C form an L-network, which transforms the $20\text{-}\Omega$ equivalent series output impedance up to $50\ \Omega$. This results in an easily duplicated design with a smooth, low-Q match.

The dc feed to the drains is provided through a shunt bifilar choke. At this frequency, most ferrite materials exhibit too much loss to be used at this impedance level. A powdered-iron core works famously here.

The balun-transformer function is provided by a simple coax and wire transformer. Two of the windings are provided by $50\text{-}\Omega$ Teflon coax, and the third balancing winding by an additional single wire.

The bias network requires some explanation. Power MOSFETs have normal lot-to-lot variations in gate threshold voltage, V_{th} , forward transconduc-

tance, G_{fs} , and other parameters. A number of devices were checked for V_{th} , and they were all very close. They were all from the same die lot. The die lot number is marked on the package. For comparison, devices from another lot were checked and were uniformly a half a volt lower. Were this the case for the devices to be used in the amplifier, a dc block would need to be added to each side at the transformer, and the bias-feed network duplicated for each device. Since these devices were uniform, the additional complication of individual gate-bias adjustments was omitted in this design.

Because the gate-bias voltage required to maintain a particular value of idling drain current decreases as the temperature of the die increases, it is necessary to thermally compensate the gate-bias source, or the devices will "run away." A commonly available NTC resistor tracks the temperature of the case. (Refer to Fig 3.) This bias circuit has been in the literature for many years.⁶ The ratio of R1 to R3 in part determines the degree of compensation. A smaller value of R1, or a larger value of R5, will increase the thermal sensitivity. A drop of thermally conductive glue keeps the thermistor in contact with the case. Proper operation is indicated when the set value of I_{dq} does not change after the heat sink gets hot from prolonged operation.

Construction

Refer to Fig 4 for the parts layout. A photo master of the artwork is shown in Fig 5. The original size of the artwork is 3.35×7 inches. The circuit board is 1-ounce-copper, double-sided $1/16$ -inch G-10 PCB material. All four

edges of the board and the three sides of the two rectangular cutouts for the transistors are wrapped with copper-foil tape that was soldered in place to provide a low-impedance continuous ground plane. The two cutouts for the transistors and the six mounting holes are the only holes in the board. All of the parts are surface mounted, which permits the board to be mounted directly to the heat sink.

This amplifier was built on a 7-inch length of AAVID #60765 heat-sink extrusion.⁷ It is 3.5 inches wide, 1.5 inches deep and has nine fins. With $50\ \text{CFM}$ of air blown across it, the devices will easily maintain thermal stability in a 30°C environment. The heat sink is not big enough for anything but very intermittent use without a fan to assure adequate airflow across the fins. The input and output connectors are each secured by two #4-40 screws and holes tapped into the base of the heat sink. A cover is recommended for safety; fairly high RF voltages are present.

Power Supply

Power for the amplifier needs to be fairly well regulated, since any ripple will show in the output signal as undesired 120-Hz AM. For on-air testing at the author's home, a very simple power supply was constructed using a $500\ \text{W}$, 120 to 240 V isolation transformer to drive a full-wave, center-tapped rectifier circuit with $50,000\ \mu\text{F}$ of filtering. Under SSB conditions, this is adequate. For CW, it needs some better regulation or the output power will sag over the length of a dash, and there will be some detectable hum. A regulated supply capable of providing $80\ \text{V}$ at $6\ \text{A}$ is needed.

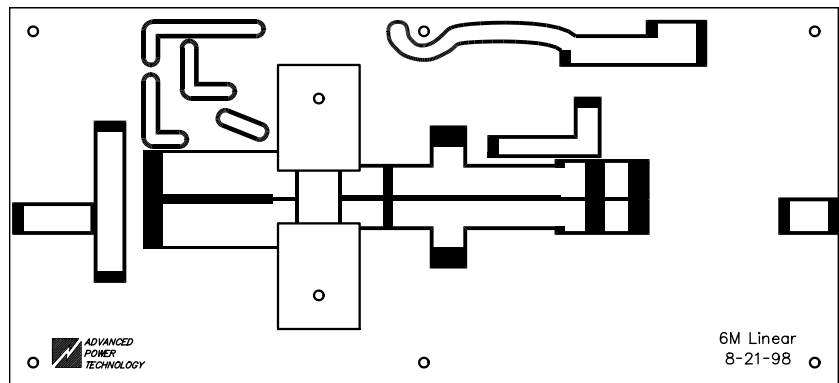


Fig 5—PCB artwork (not to scale, original size 3.35(7.00 inches)

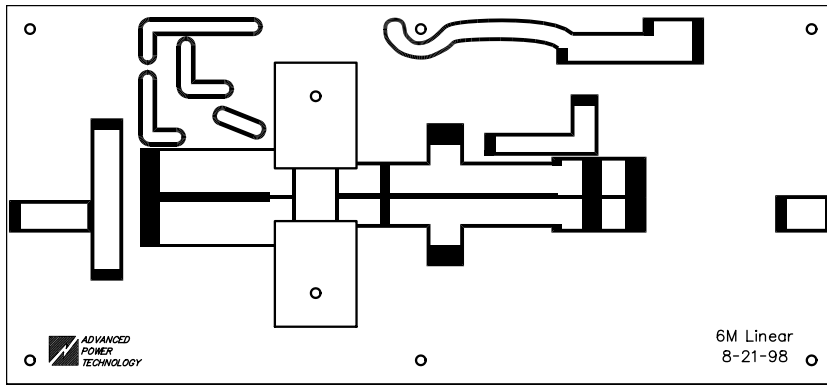


Fig 6—SSB IMD performance.

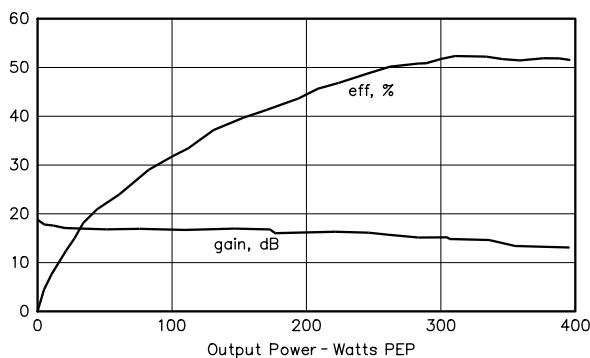


Fig 7—Amplifier efficiency and gain.

Table 1—Amplifier Parts List

C10—1 μ F, 35 V electrolytic capacitor
C1—215-790 pF Arco ⁸ #469 mica compression trimmer
C2, C6, C7—1000 pF, 500 V NP0 chip cap, KD ⁹ #2020N102J501P
C3—20-180 pF Arco #463 mica compression trimmer
C4-C5, C8-C9—0.01 μ F, 500 V chip capacitor
D1—6.8 V, 1 W Zener diode
L1-L2— \approx 70 nH, 3t #18 AWG enameled wire 0.31-inch diameter 0.25-inch long
L3—2t #20 AWG on Fair-Rite #2843010402 bead $\mu_i = 850$
Q1—ARF448A
Q2—ARF448B
R3—10 k Ω NTC Fenwal ¹⁰ #140-103LAG-RB1
R6—1 k Ω , 0.5 W 10-turn trimmer
T1—Primary 2t #20 PTFE, Secondary $3/16$ -inch brass tube on Fair-Rite #2843010402 balun core
T2—6t bifilar #20 PTFE on Amidon #T-94-2 toroid $\mu_i = 10$
T3—3t RG-316 coax, 3t #20 PTFE on three Fair-Rite #5961001801 toroids $\mu_i = 125$
TL1, TL2—30- Ω printed line, 0.6 inches long

Performance

This is the first-known, class-AB application of the ARF448 parts. Until now, the only other linear application is in a pulsed-mode linear amplifier for

magnetic-resonance imaging. The SSB performance was encouraging because these devices were developed to serve the ISM plasma-generation market and no attention to linear performance

was given in their design. The IMD performance with 200 mA of quiescent bias was better than expected. (See Fig 6.) The amplifier was tested with up to 0.5 A of I_{dq} . While the IMD performance improves somewhat at this level, the efficiency degrades significantly.

The gain and efficiency objectives have been met, as shown in Fig 7. The gain is 14.3 dB at 300 W PEP. The efficiency peaks at 51% at the same power. Under single-tone conditions, the drain efficiency is 61% at 250 W. The bandwidth of the amplifier is determined by the input network. The Smith-Chart plot of the input impedance shows the tracks for 50, 50.5 and 51 MHz. With the network adjusted for best match at 50.5 MHz, the SWR at the ± 0.5 MHz bandwidth points is 1.3:1. It would be difficult to increase this SWR bandwidth enough to cover the full 4 MHz of the amateur 6-m band without resorting to resistive loading, which would then reduce the available gain.

Conclusion

This paper has presented a 50 MHz, 300-W PEP linear amplifier using plastic-packaged, high-voltage MOSFET transistors. This is the first-known implementation of a full-duty-cycle-class-AB amplifier using these transistors. The design challenges, approaches to their solution and the resulting amplifier performance are shown. The parts, construction and mechanical layout all have been described in sufficient detail to permit duplication. The new line of plastic-packaged RF power transistors from APT offers designers a new cost-effective solution for efficient layout and performance.

Notes

- ¹R. Frey, "A 50 MHz, 250 W Amplifier Using Push-Pull ARF448A/B," APT9702, Advanced Power Technology Inc.
- ²R. Frey, "A Push-Pull 300 Watt Amplifier for 81.36 MHz," *Applied Microwaves and Wireless*, April 1998.
- ³Smith Chart is a trademark and property of Analog Instruments Co, New Providence, New Jersey.
- ⁴WinSMITH, copyright Eagleware Corp, 1995, available through Noble Publishing, Inc.
- ⁵Fair-Rite Products Corp, PO Box J, One Commercial Row, Walkkill, NY 12589.
- ⁶H. Granberg, "Wideband RF Power Amplifier," *RF Design*, February 1988.
- ⁷AAVID Thermal Technologies Inc, Box 400, Laconia, NH 03247.
- ⁸Arco Electronics, 5310 Derry Ave, Agoura Hills, CA 91301.
- ⁹KD Components Inc, 2151 Challenger Way, Carson City, NV 89706.
- ¹⁰Fenwal Electronics, Inc, 450 Fortune Blvd, Milford, MA 01757.



Measuring Distortion in Linear Amplifiers

*How linear is your “linear”?
Here’s how to measure its distortion.*

By Walter Schreuer, K1YZW/G3DCU

Like most things in life, linear amplifiers are not perfect. While there may be other methods, the two-tone test is hard to beat for assessing nonlinearity. The principle is well known: Two separate signals of equal amplitude—and in close frequency proximity—are applied to the input of the device under test. If the two frequencies are f_1 and f_2 , the distortion products will be seen at frequencies $2f_1 - f_2$ and $2f_2 - f_1$ (third-order), $3f_1 - 2f_2$ and $3f_2 - 2f_1$ (fifth-order), and so on. Fig 1 shows the two-tone spectral picture of my ICOM 761 transceiver at a 50-W output level. For this measurement, I used two well-decoupled audio oscillators at the microphone input and a sophisticated spectrum analyzer on loan from my place of employment. The resolution bandwidth was 100 Hz, requiring a slow sweep speed, making a digital-storage display mandatory. Another requirement is phase-locked tuning. Such an instrument is costly and be-

yond the realm and patience of most home constructors.

Two-tone test reports are frequently published in *QST*. The ratio of the power in any pair of distortion sidebands to the power in the two fundamental signals (in decibels) is a measure of the linearity of the device being tested. Arguably, -20 dB is acceptable, and -40 dB is very good. For measuring amplifiers, the distortion in the driving source must be appreciably less—by at least 10 dB—than the expected distortion of the unit under test. I needed to assess the performance of an unconventional 1-kW amplifier that I had developed and was looking for -30 dB for the third-order products. Obviously, my main station transceiver (see Fig 1) was inadequate for the task. My stand-by unit (Yaesu 840) is somewhat worse and more noisy.

Testing with Two RF Signals

The limitation of a single driving source can be avoided by using two separate RF signals to drive the amplifier under test. If you do not have a second transceiver or exciter, any CW signal sources of sufficient power may

be used. Consider an inexpensive Heathkit of early post-war or even pre-war vintage; they may be found in flea markets. With a frequency separation of, say, 100 kHz, a spectrum-analyzer resolution of 10 kHz will suffice, making for a fast sweep speed and a much-reduced stability requirement. Such a device is relatively inexpensive, and well within the capability of home constructors¹.

While we have avoided the problem of the driving transceiver’s limitations, we have simply traded this for other complications. Solving these is not costly, but requires a fair amount of work. Obviously, we cannot simply place two 50-W or so CW signals in parallel; this would cause tremendous intermodulation, and probably damage to both sources.

The Hybrid Combiner

Hybrid networks are as old as the ancient two-wire telephone, possibly older. In these, the network eliminates or reduces the transmission from the microphone to its associated earpiece.

¹Notes appear on page 57.

In solid-state circuits, they are often used to double the power output while isolating the two sources from each other. Many examples are given by Motorola.² Fig 2 shows two forms of hybrid combiners using ferrite-loaded transmission lines. Fig 2B has been described in an old Philips application note,³ they achieved an isolation of 40 dB from 1 to 30 MHz at a power level of 3 W. I prefer the network of Fig 2A, despite the extra transmission line; the layout is simpler, and the impedance levels are more convenient.

Much emphasis has been given to the importance of the impedance of transmission-line transformers, ever since the publication of the classic paper by Ruthroff.⁴ With modern ferrites, this is not a major concern, especially when the required bandwidth is limited. The length of the winding must be short compared to $\lambda/4$, the common-mode reactance high compared to 50 Ω . In my setup, each transmission line (at 7 MHz) has a physical length of 0.008λ and a winding reactance of over 1000 Ω .

The hybrid resistor, R_H in Fig 2, dissipates one half of the total input power, or 50 W in my application. It is a “floating” component, and this is most inconvenient at this power level. The problem is solved by inserting a transmission-line choke in front of a grounded resistor. The 25- Ω termination may be implemented by two 50- Ω units in parallel; I used 12 parallel-connected 300- Ω , 5-W metal-oxide resistors.⁵

The required 25- Ω output termination must be transformed to 50 Ω . Initially, I used a simple one-conductor autotransformer on a ferrite toroid, 10 turns tapped at seven. The output is slightly reactive because of imperfect coupling. A large series capacitor compensates for this. Fig 3 shows the 25:50- Ω matching transformer.

Good isolation requires accurate terminations at the hybrid and output ports. If the input to the amplifier has an SWR close to unity, all that may be needed is a small adjustment of the capacitor in Fig 3. In most cases, this will not be sufficient, and a tuning unit will be needed. I used a three-pole network from the tables in Motorola AN 267 (see Note 2), with a loaded $Q = 5$. This choice is of no particular significance; I happened to have suitable parts on hand. Fig 4 shows the network. This should initially be tuned for unity SWR at the milliwatt level using a resistive termination. This also applies to the transformer of Fig 4.

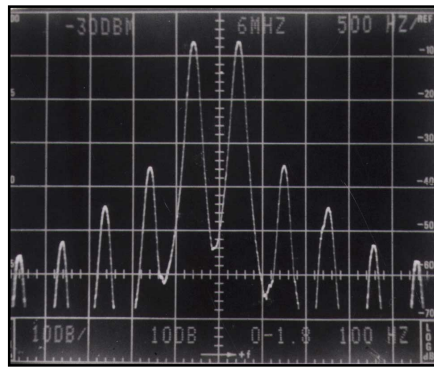


Fig 1—Two-tone spectrum of ICOM 761 at 50-W PEP output.

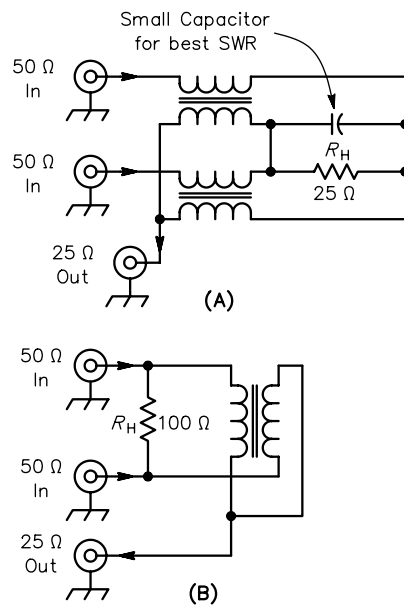


Fig 2—Schematics for two RF hybrid combiners.

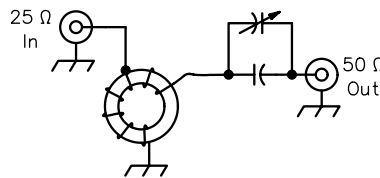


Fig 3—Schematic diagram of a 25:50- Ω transformer. The core is an Amidon FT125-K. The winding is 10 turns of #22 AWG enameled wire with a tap at seven turns. For use above 18 MHz, use seven turns with a tap at five turns. The total capacitance is 930 pF for 7.1 MHz.

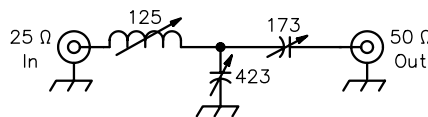


Fig 4—Schematic of a matching network for the amplifier input. The numbers are reactance values, in ohms.

Obtaining and Measuring Isolation

Isolation is measured easily with a spectrum analyzer (SA). For low-level measurements and adjustments, I used an SWR analyzer as the input source; the other input is terminated by the 50- Ω input impedance of the SA. The network of Fig 2A produced an isolation of 45 dB over a wide bandwidth—3.5 to 22 MHz. With the 25:50 transformer of Fig 3, the isolation was tweaked to 55 dB at 7 MHz. The corresponding number at 14 MHz was 48 dB, with a smaller series capacitor. Bringing the hybrid resistor R_H to ground with a transmission line choke required slight retuning. When using the tuned matching unit of Fig 4, this should be initially adjusted for unity SWR, then tweaked for maximum isolation in the hybrid circuit.

The final adjustment is made at a normal working power level. The amount of isolation needed is dependent on the particular exciters. I found 20-dB insufficient, 30 dB more than adequate. Fig 5 shows the two-tone input spectrum at 50 W PEP into a 50- Ω termination, with the isolation adjusted to 35 dB.

It is not permissible to adjust for a good input spectrum when driving the amplifier under test. Valid results require that the isolation be measured (and tweaked) when driving the amplifier to normal power output. Fig 6 shows the setup. The SA coupler is housed in a small box. I used an old-fashioned IF can with three connectors. Fig 7 shows the circuit. The toroid is not critical. Its response is flat from 1 to over 100 MHz! While two SA couplers are shown in Fig 6, one unit may be shifted from port to port. The matching unit is re-adjusted for maximum isolation. I achieved 48 dB at 7 MHz. With the ferrite transformer of Fig 3 replacing the adjustable matching unit, the isolation degraded to 22 dB. (The input SWR of my amplifier is 1.2:1.)

Final Results

The details of the coupling network are shown in Fig 8. The transmission lines work well from 3.5 to 18 MHz; my measurements were made at 7 MHz. It is advisable to use a tuned matching unit at the amplifier input unless the driving-impedance SWR is very close to unity. In my case, using the ferrite transformer (Fig 3) resulted in a 2-dB error (see Fig 9).

My amplifier achieved a respectable -28 dB third-order distortion level. ARRL Lab people would call this -34 dB

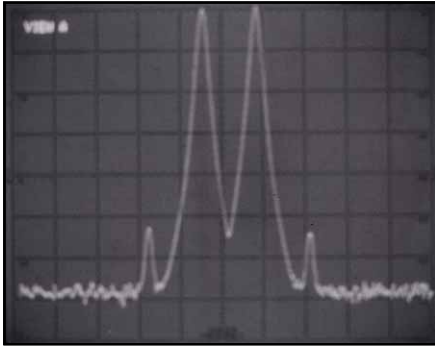


Fig 5—The 50-W amplifier input signal (50-Ω load).

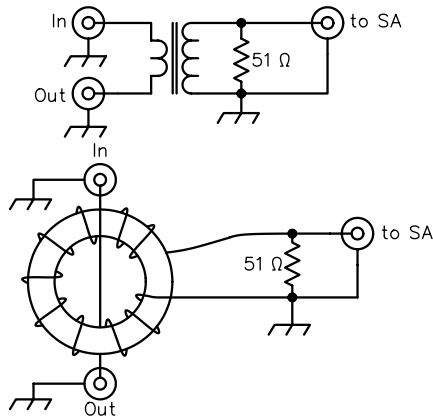


Fig 7—Schematic of the spectrum-analyzer coupler (SAC). The winding is 20 turns of #28 insulated wire on an Amidon FT-50-43.

(because they reference it to the two-tone PEP, rather than a single tone—*Ed.*). One final word of caution: Do not re-adjust the input-matching unit for a better-looking output spectrum. This will produce input distortion to partially cancel and alter the output spectrum, leading to erroneous results.

Notes

- ¹W. Hayward, W7ZOI, and T. White, K7TUA, "A Spectrum Analyzer for the Radio Amateur," *QST*, Part 1: Aug pp 35-43, and Part 2 Sep pp 37-40 1998.
- ²*RF Device Data Book*, Vol 2, Rev 3, Motorola Inc.
- ³*Application Note 530*, Philips, June 1970.
- ⁴*Proceedings of the IRE*, Aug 1959.
- ⁵Stock #286-300, Mouser Electronics. You can contact Mouser at 958 N Main St, Mansfield, TX 76063; tel 817-483-4422; fax 817-483-0931; e-mail sales@mouser.com; Web <http://www.mouser.com>. □□

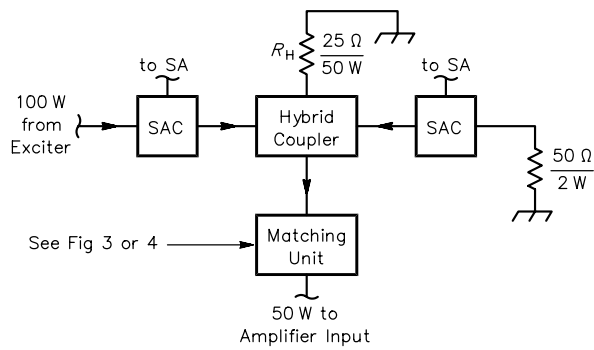


Fig 6—The setup for a high-level isolation test. SAC indicates the spectrum-analyzer coupler.

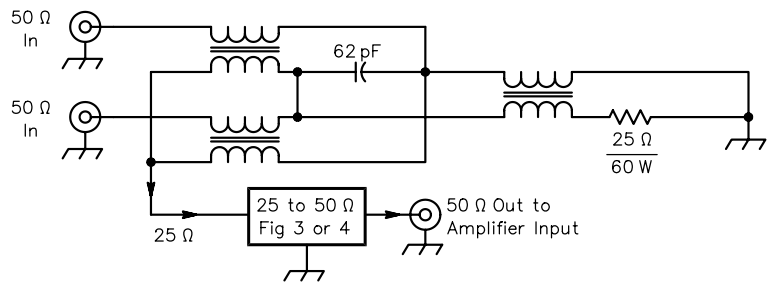
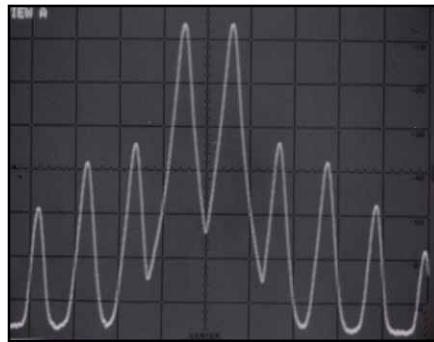
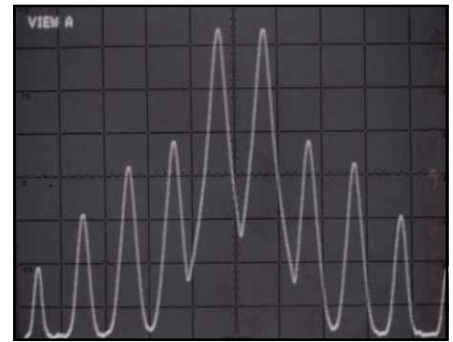


Fig 8—Details of the coupling network. All transmission lines are #22 AWG enameled wire tightly twisted. The windings are eight turns on an Amidon FT125-K toroid core. For operation at 21 MHz and higher, use five turns.



(A)



(B)

Fig 9—1.2 kW PEP amplifier output spectra. (A) was made using a matching unit and with more than 40 dB of isolation between the tones. (B) Shows a 2-dB error from ferrite transformer and 22 dB isolation (input SWR 1.2:1).

HF BANDPASS FILTERS

DCI is in the prototype stage of developing high power bandpass filters for each HF band. The design criteria is for 100 dB of isolation on adjacent bands, 2 KW power handling capability and 0.5 dB of loss in band. We have some filters working now, but are unsure how much interest will be shown by multi-multi operators. They are somewhat costly with a proposed selling price of \$500 US each but the quality and specifications are first class. Our goal is to never have any station interfere with another during multi-multi operation.

Please call Ralph at DCI if you have any interest in these products.

DCI DIGITAL COMMUNICATIONS INC.

Box 293, 29 Hummingbird Bay,
White City, SK, Canada SOG 5B0

Direct (306) 781-4451 • Fax (306) 781-2008
Toll-Free 1-800-563-5351

<http://www.dci.ca> email: dci@dci.ca

RF

By Zack Lau, W1VT

Transmission Lines and Amateur Radio Designer

The most common question about Amateur Radio designer is “Does it do microstrip?” Precisely because of its commercial importance, all the nifty microstrip and stripline models were left out of the amateur version of this popular product. Thus, it intentionally does not. A professional version of this program can be purchased from Ansoft, which acquired Compact Software. Ansoft’s WWW site is at <http://www.ansoft.com/>.

There are also questions about modeling coax with the CAB model, particularly with modeling specific varieties of coax. The most accurate way to do this is to measure the insertion loss of a large length of coax, and optimize the model to match the measured data. I did this with a 100 foot piece of Times Microwave LMR-400. The model and results are shown in Fig 1. I also ran the optimization using the specifications available from the Times Microwave web site: <http://www.timesmicrowave.com/home.cgi>.

The results are quite similar. The model based on measured data shows a little more conductor loss, while the

specification-based model shows more dielectric loss. Since the goal is to separate out the two effects, it helps to include many data points over a wide range of frequencies. The low-frequency points help determine the conductor loss, while the high-frequency points help determine the dielectric loss. Since we are modeling a curved line, more than two points are required.

When running the optimization, it is important that the optimization frequencies correspond to the exact frequencies used in the analysis. The frequencies used in the optimization block also must be used in the frequency block. 903 MHz isn’t “close enough” to 900 MHz for this program.

Of course, the cable should be measured below its cutoff frequency. If it starts acting like waveguide, losses can be quite high. Based on Eq 15.1 of *Radar Engineer’s Sourcebook*¹

$$f < \frac{2v}{1.873\pi(a+b)}$$

f = operating frequency

a = OD of the inner conductor

b = ID of the inner conductor

v = speed of propagation along coaxial line [v is also (velocity factor)*(speed of light)]

When $a = 0.109$ inches, $b = 0.285$ inches and $v = 0.85 \times c$, the operating

frequency must be below 8.65 GHz. Thus, I wouldn’t expect 10-GHz measurements to be useful with this cable, although 3.4 and 5.7 GHz data would improve the accuracy of the dielectric loss factor. These calculations can be quite tricky if you aren’t careful with units. A bit of conversion is needed if you measure coax dimensions in inches but use a metric version of the speed of light.

I’ve not been able to locate the equations for C1 and C2 that are mentioned in the ARD documentation. I suspect they aren’t terribly accurate with popular cables that use braided shields, corrugations or dissimilar metals. Especially considering the ease of using ARD’s optimizer to model cables. However, if you are interested in deriving these equations, I’d recommend Theodore Moreno’s *Microwave Transmission Design Data*, published by McGraw Hill in 1948. It is published on demand by Artech house.² I discovered its availability using Amazon.com’s search engine. Again, be careful with your units and take the time to understand the assumptions made in deriving the equations.

Bill Olson, K1DY, published a useful chart of coax-cable specifications in his September 1987 “>50” *QEX* column. Figure 2 shows a model of UT-141A. UT-141 is 49- Ω coax while UT-141A has a slightly larger dielectric to bring the impedance up to 50 Ω .

225 Main St
Newington, CT 06111-1494
zlau@arrl.org

¹Notes appear on [page 59](#).

```

* Times Microwave LMR-400
* http://www.timesmicrowave.com/home.cgi
*C1 and C2 already optimized to measured data
BLK
CAB 1 2 Z=50 P=30.48M V=0.85 C1=.120833 C2=.014496
MLINE:2POR 1 2
END
*This model is used to find values for C1 and C2 using
*cable loss specifications
BLK
CAB 1 2 Z=50 P=30.48M V=0.85 C1=? .124448 1? C2=? .010426 1?
sline:2por 1 2
end
Freq
50mhz 144mhz 222mhz 432mhz 903mhz 1296mhz 2304mhz
220mhz 450mhz 900mhz 1500mhz 2000mhz 2500mhz
2.7ghz
end
opt
*Measured line loss for 100 ft.
mline f=50mhz ms21=-1.0dB
mline f=144mhz ms21=-1.45dB
mline f=222mhz ms21=-1.8dB
mline f=432mhz ms21=-2.6dB
mline f=903mhz ms21=-3.9dB
mline f=1296mhz ms21=-4.7dB
mline f=2304mhz ms21=-6.7dB
mline f=2.7ghz ms21=-7.2dB
*Times Microwave specifications
sline f=50mhz ms21=-0.9dB
sline f=144mhz ms21=-1.5dB
sline f=220mhz ms21=-1.8dB
sline f=450mhz ms21=-2.7dB
sline f=900mhz ms21=-3.9dB
sline f=1500mhz ms21=-5.1dB
sline f=2000mhz ms21=-6.0dB
sline f=2500mhz ms21=-6.8dB
end
Freq      MS21      MS21
GHz       dB         dB
          MLINE    SLINE
0.050    -0.85     -0.86
0.144    -1.46     -1.49
0.220    -1.82     -1.85
0.222    -1.83     -1.86
0.432    -2.61     -2.63
0.450    -2.67     -2.69
0.900    -3.89     -3.88
0.903    -3.90     -3.89
1.296    -4.77     -4.73
1.500    -5.17     -5.12
2.000    -6.09     -6.00
2.304    -6.61     -6.49
2.500    -6.93     -6.79
2.700    -7.24     -7.09

```

Fig 1—ARD Model of Times Microwave LMR-400. You can download this package from the ARRL Web <http://www.arrl.org/files/>. Look for 99RF05.ZIP, which contains both figures.

Notes

¹W. C. Morchin, *Radar Engineer's Sourcebook* (Norwood, Massachusetts: Artech House, 1993), ISBN: 0-89006-559-4; page 203. <http://www.artech-house.com/index.html>

²T. Moreno, *Microwave Transmission Design Data* (Artech House, 1989), ISBN: 0-89006-346-X. □□

```

*Model UT-141A 50 ohm coax
*Attenuation from Bill Olson's ">50", QEX, September 1987, p.14.
BLK
CAB 1 2 Z=50 P=30.48M V=0.70 C1=? .35545 .7? C2=? .021408 .9?
line:2por 1 2
end
Freq
50mhz 144mhz 5760mhz
432mhz 220mhz
3456mhz 1296mhz
1mhz 10mhz 30mhz 100mhz
300mhz 1ghz 3ghz 10ghz
end
opt
line f=50mhz ms21=-2.4db
line f=144mhz ms21=-4.1dB
line f=220mhz ms21=-5.1
line f=432mhz ms21=-7.4
line f=1296mhz ms21=-13db
line f=5760mhz ms21=-30dB
line f=3456mhz ms21=-22dB
end
Freq      MS21
GHz       dB
          LINE
0.001     -0.34
0.010     -1.09
0.030     -1.90
0.050     -2.46
0.100     -3.49
0.144     -4.21
0.220     -5.23
0.300     -6.13
0.432     -7.40
1.000    -11.49
1.296    -13.18
3.000    -20.72
3.456    -22.40
5.760    -29.76
10.000   -40.79

```

Fig 2—ARD Model of UT-141A. You can download this package from the ARRL Web <http://www.arrl.org/files/>. Look for 99RF05.ZIP, which contains both figures.

Surface Mount Chip Component Prototyping Kits—
Only \$49⁹⁵



CC-1 Capacitor Kit contains 365 pieces, 5 ea. of every 10% value from 1pf to 33µf. CR-1 Resistor Kit contains 1540 pieces, 10 ea. of every 5% value from 10Ω to 10 megΩ. Sizes are 0805 and 1206. Each kit is ONLY \$49.95 and available for immediate One Day Delivery!

Order by toll-free phone, FAX, or mail. We accept VISA, MC, COD, or Pre-paid orders. Company PO's accepted with approved credit. Call for free detailed brochure.

COMMUNICATIONS SPECIALISTS, INC.
426 West Taft Ave. • Orange, CA 92665-4296
Local (714) 998-3021 • FAX (714) 974-3420

Entire USA 1-800-854-0547

Upcoming Technical Conferences

AMSAT-NA Call for Papers

This is the first call to authors who wish to present papers at the 17th AMSAT-NA Annual Meeting and Space Symposium to be held October 8-11, 1999 at the Hanalei Hotel in San Diego, California. Symposium presentations will also be printed in the official *Proceedings* document.

The subject matter should be topics of interest to the Amateur Radio satellite service. Key dates for submitting papers are as follows:

- May 1, 1999—one-page abstracts due
- June 1, 1999—authors will be advised if accepted
- August 1, 1999—camera ready copy of accepted papers due

Send abstracts to Symposium chair Duane Naugle, KO6BT, 4111 Nemaha Dr, San Diego, CA 92117-4522, USA; ko6bt@amsat.org.

Proceedings of the Symposium will be printed by the ARRL and made available at—and immediately after—the meeting. If authors do not wish to present a paper but have a topic of interest, please submit the topic and arrangements may be made for a stand-in presenter. Receipt of submissions will be confirmed.

Thanks to Amsat ANS for this information. For more information, contact Duane Naugle at the address shown above.

The 1999 IEEE MTT-S International Microwave Symposium

June 12–19, 1999; Anaheim, California, USA

The Steering Committee of the 1999 IEEE MTT-S International Microwave Symposium welcomes you to the IMS and to Southern California. Whatever your interest in RF and microwave technology, you are certain to find the fresh ideas and technological inspir-

ation you're seeking at the 1999 IMS.

This year's location offers a variety of opportunities for recreation and cultural enrichment. Anaheim is the home of Disneyland, the best known theme park in the world.

The Los Angeles area boasts many wonderful scientific and cultural attractions, including a new science museum, the new Aquarium of the Pacific, the new Getty Center for Visual Arts, and, of course, the Hollywood Bowl. Los Angeles has perhaps the most pleasant, balmy, subtropical weather in the world. Bring your family, send the kids to Disneyland, install your spouse at the beach, and join us for an exciting, rewarding symposium!

The Technical Program, is, of course, the most important part of the symposium. It consists of four days of paper presentations, three interactive-forum sessions and an uncounted number of workshops. This is your opportunity to learn from the industry's technological wizards, or, if you are one of the industry's technological wizards, to show off your achievements. Here are some program highlights:

- Technical Program
- Technical Workshops
- Radio Frequency Integrated Circuits (RFIC) Symposium
- The ARFTG Conference
- Exhibition
- MAPS '99 Vendor Forum
- Historical Exhibit

Symposium Schedule

To reverse the trend towards more short papers and interactive-forum papers, the IMS is extended this year from 3 to 4 days. We'll have more full-length papers at the 99 IMS! All full-day workshops will be held on Sunday, June 13 and Friday, June 18, but some half-day workshops will be held on Monday, June 14. IMS technical sessions will begin on Monday, June

14, and will end, as in previous years, on Thursday.

For more information go to <http://www.nonlintec.com/ims1999/>.

33rd Annual Central States VHF Conference Announcement

The 33rd Annual CSVHF Society Conference will be held July 23-25, 1999 at the Sheraton Four Points Hotel in Cedar Rapids, Iowa. Early arrivals Thursday evening will be treated to a picnic under the stars with a program and telescope viewing by the Cedar Astronomy Club. The formal conference activities will kick-off Friday morning with antenna-gain measuring. A full slate of technical programs covering topics on DSP, receiver design, VHF power amplifiers, Aurora detection, EME dish construction and much more will be offered for the next 1½ days. The usual Noise Figure Measurement contest/clinic will be held for converters and preamplifiers operating above 50 MHz.

The CSVHF Society has a long tradition of entertaining the family members, and this conference will be no exception. Bus tours to local attractions are capped with dinner and live theater on Friday evening. Meanwhile, the hams will enjoy a lively VHF/UHF flea market at the hotel on Friday evening.

The conference will culminate with a gala banquet on Saturday evening, complete with extensive door prizes, awards and an outstanding program: "The Galileo Mission to Jupiter" by Dr. Donald Gurnett, Professor of Astronomy and Physics at the University of Iowa.

Registration information will be mailed to members in early June. Additional information (and registration for nonmembers) may be obtained by contacting the CSVHF Society President, Rod Blocksom, K0DAS, 690 Eastview Dr, Robins, IA 52328; k0das@amsat.org. □

Letters to the Editor

A Concise Calculation Method for Pi-L Networks

◇ In early January of this year, I finally got around to reading the article by Dr. Karl Lickfeld, DL3FM, regarding new equations for designing Pi-L networks (*QEX*, Sep/Oct 1998). The circuit values in his example seemed strange. I had never seen values for the series and shunt arms in front-to-front L network designs to be equal. My first check on his values was to use *Amateur Radio Designer*. Not too surprisingly, the insertion loss was around 1.5 dB, and the resonant point was low by about 80 kHz from the stated value. I viewed the former as indicating a mismatch.

My next check was with *Micro-Smith*. Sure enough, the impedance value presented to the final amplifier (assuming a 50-Ω, nonreactive load) was 1184.75 -j711.23, not the desired 3125 +j0. Looking the other way, the impedance presented to the antenna (assuming a 3125-Ω nonreactive load at the input) was 19.0652 -j11.94. Looks like a mismatch to me.

Lickfeld says, "Putting together the three separate parts, each of which has the same resonant frequency, forms the complete network." Unfortunately, in a Pi or Pi-L network, the component values that provide a conjugate match between the input and output ports at some frequency do not result in a resonant condition at that same frequency. Therefore, if one desires a conjugate match at some frequency, resonance at that same frequency is not possible at normal values of Q. However, with Q values of 1000 or greater, these frequencies finally begin to approach each other very closely.

Many folks think that designing Pi or Pi-L networks using the front-to-front (or back-to-back if you prefer) method is a recently discovery. It is not. George Grammer, W1DF, authored a three-part article—which appeared in *QST* in 1957 (March, April, May)—that made use of the "classic" L-network equations and the front-to-front method. I had seen the very same equations in Terman a decade earlier.

There are many short-cut equation sets for calculating Pi and Pi-L networks that avoid the step-by-step

method required in the use of front-to-front L networks. All of these are either derivatives of that method or they are probably wrong! Dr. Lickfeld's equations are a case in point.—Vince Bartell, WOMFK, 4424 Jansa Dr, St Paul, MN 55126-2102; vbartell@isd.net

I think the author's goal of concisely calculating component values for Pi-L impedance-matching networks is achievable. His method of designing three resonant (nonreactive input and output) L networks, then combining them into a Pi-L, is formulated simply if the matching progresses along the same constant-resistance and constant-conductance Smith Chart circles. If it doesn't, then the simplification is much more elusive.

We must acknowledge that the author's example on page 48 doesn't seem to produce the desired results. I find that I can avoid error and achieve further simplification by starting at the high-impedance end with:

$$X_{C1\pi} = \frac{R_1}{Q} \quad (\text{Eq 1})$$

To get back to the "R" line at the output of Section 1, I set:

$$X_{L1\pi} = -X_{C1\pi} \quad (\text{Eq 2})$$

After I insert L2 and C2, I want to arrive back at R₁, and so I let:

$$X_{L1\pi} = -X_{C1\pi} \quad (\text{Eq 3})$$

and

$$X_{C2\pi} = X_{C1\pi} \quad (\text{Eq 4})$$

Now I use Dr. Lickfeld's premise about the geometric mean of the impedances with:

$$X_{IM} = \sqrt{R_1 Z_L} \quad (\text{Eq 5})$$

and state:

$$X_{C\Gamma} = -X_{L\Gamma} = -X_{IM} \quad (\text{Eq 6})$$

This works regardless of the value of Q, because all transformations occur along constant-resistance and constant-conductance circles. Note that a tradeoff exists between Q, the current in the components and the harmonic attenuation offered by this circuit. In the example, and with the revised equations: Q = 12, f = 3.65 MHz, R₁ = 3125 Ω, Z_L = 50 Ω, C1 = 167 pF, L1 + L2 = 22.6 μH, C2 + CΓ = 274 pF and LΓ = 17.1 μH.—Ed.

Practical Application of Wind-Load Standards to Yagi Antennas: Part 2

◇ I just received printed copies of the *Mar/Apr '99 QEX* and noted that Eq 7 in Part 2 of my article series is in error. I thought the purpose of filing in electronic form and in your prescribed word-processing format was to avoid just such problems.

The correct equation is:

$$SM = \frac{0.098(OD^4 - ID^4)}{OD} \quad (\text{Eq 7})$$

73, Stu Bonney, K5PB

Signals, Samples and Stuff

◇ I've been rereading your articles in last year's *QEX* (Mar through Sep 1998). One comment caught my attention and left me puzzled.

In Part 2, you write about the SSB modulator, and under "Distortion and Noise Sources" you mention (page 34, column 1):

"...amplitude and phase inaccuracies degrade the opposite-sideband suppression in a phasing-method modulator. ... The DAC performance is generally the limiting factor. The best 16-bit DACs produce amplitude and phase accuracy quite adequate for our needs, resulting in. ..."

I would understand why DAC performance enters this particular question if you did phasing digitally, but combined the two components in the analog domain. However, if you do the whole modulator digitally, the story is different. The modulator runs the real baseband signal through a filter pair with 90° phase shift in one leg. That produces a complex "analytic" (single-sided spectrum) audio signal. Multiply it by a complex carrier, shift the audio signal upward and that's the SSB signal.

Inaccuracies in the phase shift give you imperfect opposite sideband suppression, and a dc offset throws in the carrier. However, that all happens in the digital domain, so the DAC performance doesn't enter the picture.

Suppose we had a perfect phase shifter and a perfect complex-carrier source, and we did the complex multiply without loss of accuracy. The result would be a completely clean SSB signal. An imperfect DAC after that would certainly produce harmonics and intermod. The odd-order ones will live near the desired signal, so some of them will end up where the suppressed sideband was. Nevertheless, they wouldn't sound like sup-

pressed sideband, just like intermod products.—Paul Koning, NI1D, Gage Rd RR2 BOX 116, Wilton, NH 03086

You are correct, Paul, and I certainly could have been clearer about my meaning. As you surmised, I was referring to the DAC's IMD noise and alias products that arrive in the suppressed sideband's spectrum, hence the sub-heading of that section. While these products wouldn't necessarily be intelligible, they would be included in any measurement of the transmitter's opposite-sideband suppression.

The DAC distortion can have strange ways of manifesting itself in sampled systems. I'm reminded of a description of DDS spurious products that takes into account harmonics and aliasing phenomena. As the frequency of some product exceeds half the sampling rate, it "folds back" in frequency, and may reappear in unexpected places. In my design, the sampling rate of four times the IF means that odd-order harmonics of the IF potentially generate aliases in both the desired and undesired sidebands. My experience has been that when everything else is optimized, the transition to analog is the final bar to absolute precision.—Ed.

A High-Performance Homebrew Transceiver: Part 1

◇ That's more like it!! I am eagerly

awaiting subsequent issues on the 160 to 2-meter homebrew station of K5AM (*QEX* Mar/Apr 1999). The fact that I may never build a duplicate is immaterial. I still must "plow through" the power-supply article. Thanks!—Ron Pierce, NI0L, 307 11th Ave NE, Independence, IA 50644

◇ Thank you, thank you, thank you for the front cover! I picked up my copy at the post office and darned near had three wrecks on the way home, from trying to drive and look at that cover at the same time. I might have known it would be a Mandelkern!

Mark has been a beacon for many years, doing absolutely gorgeous, inspiring work. I wish I could duplicate his productivity. I've been twice as long on mine and haven't got it finished yet. Long live homebrew!

I do appreciate what you all have done to turn *QEX* around. I've bought it since it first started, even had a contribution or two in the old original black-and-whites of the early '80s. When it died a couple years back, I figured the technical side of the hobby [died with it]. Here it is reincarnated and better than ever.

I think it's still a shame that it's not part of *QST*. The way it is, there's very little in the way of a vehicle to inculcate the new amateur with the bug of homebrew and experimenta-

tion. That's wrong!—Harold Johnson, W4ZCB, 115 Kindy Forest Dr, Hendersonville, NC 28739

◇ I sent a note to Mark, K5AM, already, then realized I should also tell you that his rig was inspiring. I've appreciated slightly more esoteric things like Jim Tonne's filters, some of the phasing-network theory, the phased AD mixers, but that cover is a "grabber" for sure. Keep it up. I would love to see some practical DSP stuff—like where and how to find coefficients.—Bill Carver, W7AAZ, 690 Mahard Dr, Twin Falls, ID 83301

I like Oktay Alkin's, PC-DSP, Prentice-Hall, Englewood Cliffs, NJ, 1990. I found this title at www.amazon.com, but they may not have it in stock, and it's possibly out of print. Try contacting the publisher directly. The \$20 I paid for it in 1994 was well worth it. Many DSP evaluation boards come with some kind of filter-synthesis software. You may want to try Momentum Data Systems, Fountain Valley, California, www.mds.com.

I'm working up some more-practical DSP material for presentation at the Dayton UHF/Microwave Conference this year. I'll try to include a list of software and hardware vendors. I hope this will appear in *QEX* shortly thereafter.—Ed. □□

Next Issue in QEX

Peter Martinez, G3PLX, has generated another round of excitement with "PSK31: A New Radio-Teletype Mode." Some stations are already on the air with it! Learn about the philosophy behind this mode along with the details. We republish this article—in its entirety—from our sister society RSGB's journal, *RadCom*.

Raymond Mack, WD5IFS, has responded to the call for a switching power supply for beginners. If you've seen some of the quite complicated designs out there now, you'll appreciate the straightforwardness of Ray's design. It's a good way to get started with a technology that's been around for a while, but is now seeing increasing popularity among radio amateurs.

Robert Zavrel, Jr, W7SX, contributes an update on his popular article "Multiple-Octave Bidirectional Wire Antennas" from last year's Jul/Aug issue. This time, the emphasis is on

the extended double-Zepp and its derivatives. Break through the pileups and take names with these high-performance designs.

Follow Editor Doug Smith, KF6DX, through the process of writing a program to plot antenna radiation pat-

terns in 3-D from MININEC-generated data files. Download his BASIC program and do it yourself, too. It's sometimes surprising what you can discern from a single plot of an antenna's entire hemispherical pattern. □□

	
American Radio Relay League 225 Main Street Newington, CT 06111-1494 USA For one year (6 bi-monthly issues) of QEX:	
In the US	
<input type="checkbox"/> ARRL Member \$22.00	<input type="checkbox"/> Renewal <input type="checkbox"/> New Subscription
<input type="checkbox"/> Non-Member \$34.00	Name _____ Call _____
In Canada, Mexico and US by First Class mail	Address _____
<input type="checkbox"/> ARRL Member \$35.00	City _____ State or Province _____ Postal Code _____
<input type="checkbox"/> Non-Member \$47.00	Payment Enclosed <input type="checkbox"/>
Elsewhere by Surface Mail (4-8 week delivery)	Charge:
<input type="checkbox"/> ARRL Member \$27.00	<input type="checkbox"/>  <input type="checkbox"/>  <input type="checkbox"/>  <input type="checkbox"/> 
<input type="checkbox"/> Non-Member \$39.00	Account # _____ Good thru _____
Elsewhere by Airmail	Signature _____ Date _____
<input type="checkbox"/> ARRL Member \$55.00	
<input type="checkbox"/> Non-Member \$67.00	
Remittance must be in US funds and checks must be drawn on a bank in the US. Prices subject to change without notice.	
11/98	



Join the effort in developing Spread Spectrum Communications for the amateur radio service. Join TAPR and become part of the largest packet radio group in the world. TAPR is a non-profit amateur radio organization that develops new communications technology, provides useful/affordable kits, and promotes the advancement of the amateur art through publications, meetings, and standards. Membership includes a subscription to the *TAPR Packet Status Register* quarterly newsletter, which provides up-to-date news and user/technical information. Annual membership US/Canada/Mexico \$20, and outside North America \$25.



TAPR CD-ROM

Over 600 Megs of Data in ISO 9660 format. TAPR Software Library: 40 megs of software on BBSs, Satellites, Switches, TNCs, Terminals, TCP/IP, and more! 150Megs of APRS Software and Maps. RealAudio Files. Quicktime Movies. Mail Archives from TAPR's SIGs, and much, much more!

Wireless Digital Communications: Design and Theory

Finally a book covering a broad spectrum of wireless digital subjects in one place, written by Tom McDermott, N5EG. Topics include: DSP-based modem filters, forward-error-correcting codes, carrier transmission types, data codes, data slicers, clock recovery, matched filters, carrier recovery, propagation channel models, and much more! Includes a disk!



Tucson Amateur Packet Radio

8987-309 E. Tanque Verde Rd #337 • Tucson, Arizona • 85749-9399
Office: (940) 383-0000 • Fax: (940) 566-2544 • Internet: tapr@tapr.org www.tapr.org
Non-Profit Research and Development Corporation

MICROWAVE PARTS FOR BUILDERS

M/A-Com 10 and 24 ghz Gunn Sources Both units produce 5-10 mw of RF and contain a schottky mixer diode for reception, and a varactor diode for modulation and frequency control. Priced from \$US58 to \$US90 each. Both units accept standard horn or flanges for RF connection.

Dielectric-Resonant Oscillator Mechanically tuned from 10.4 to 10.6 ghz, electrically tuned at least 4 Mhz, with Schottky mixer diode for reception. 5 mw of RF into built-in Patch antennas for Rx and Tx. Operates from +5 vdc. \$US28 each.

Microwave Printed-Circuit Board We offer three varieties of laminate useful for microwave experimenters. Our economy pc board is good to 15 ghz, available in .030" or .020" dielectric thickness and costs \$US4 for a piece roughly 4.5" x 6". We also offer Rogers 5880 Teflon pc board good to 90 ghz in the .010" thickness. \$US25 for a piece 4" x 4".

Gaas and PHEMT Transistors, Schottky/PIN/Gunn Diodes, mixers, IC's NE32984D's, SPF-1576's, MC13055P's, ATF21186's, HP5082-2835's and others.

Our complete catalog is found on our website, <http://www.shfmicro.com>. If you can't view our web pages, please send an SASE and we will snailmail you a flyer. Shipping is \$US2 in the USA, \$US5 to Canada or Mexico, and \$US10 anywhere else in the world by Postal mail. UPS shipping available.

No Credit Cards. Cheques in US Dollars to:
SHF MICROWAVE PARTS COMPANY
7102 W. 500 S.
La Porte, Indiana, 46350, USA

web pages at: <http://www.shfmicro.com>
fax anytime to: 1-219-785-4552
e-mail to: prutz@shfmicro.com
If you are not happy, you get your money back!

HERE'S THE BOOK YOU NEED!

Hams Must Comply with the New RF Exposure Rules...

...and this is the one book that explains everything you need to know about them—in plain English. Simple worksheets and tables allow you to determine if your station is in compliance. If it's not, you'll learn how to modify your station or antenna. In most cases, it's not at all difficult to comply with the new Rules. To ensure you're in compliance, you need the information in this book.

\$15

RF EXPOSURE and YOU

by Ed Hare, W1RFI

- What are the FCC RF exposure regulations?
- How do they apply to *my* station?
- Is it hard to meet them?
- Do I have to prepare paperwork for the FCC?
- Do I have to lower my tower? Or raise it?
- Are there any restrictions on using my H-T?



Order your copy today!

RF Exposure and You

ARRL Order Number 6621—Retail \$15 plus \$4 for shipping and handling (UPS).

What do I need to do?

The answers to these questions, and many more, are inside, with the FCC Rules relating to Amateur Radio translated into plain English.



PUBLISHED BY:
THE AMERICAN RADIO RELAY LEAGUE



Includes the worksheets and tables needed for almost any station!

ARRL

tel: 860-594-0355 fax: 860-594-0303
e-mail: pubsales@arrl.org World Wide Web: <http://www.arrl.org/>

We'll be happy to take your order or provide you with the location of an ARRL Publications Dealer in your area.

Call our toll-free number **1-888-277-5289** today. 8 AM-8 PM Eastern time Mon.-Fri.

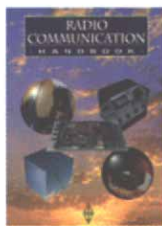
Radio Society of Great Britain Products Imported by ARRL!



Communication Reference

Packed with technical information!

Radio Communication Handbook



Covers semiconductors, HF and VHF/UHF receivers, transmitters and transceivers, microwaves, propagation, HF and VHF/UHF antennas, amateur satellites and space communications, image techniques, power supplies, and much more. PCB layouts included. 760 pages. ARRL Order No. 5234—\$38

Calling All LowFERs!

The LF Experimenter's Source Book

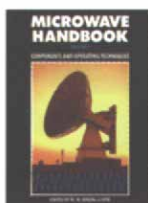


Food for the dedicated Low Frequency experimenter! In the US, unlicensed "Lowfers" may operate 1-watt between 160 and 190 kHz. Are you up for the challenge? Antennas, propagation, receivers, transmitters, special modes and test equipment. Plenty of detail for the LF beginner! 146 pages (comb bound). ARRL Order No. 7148—\$15

Good radio housekeeping!



The RSGB Guide to EMC
Diagnose and cure unwanted RF interference and achieve electromagnetic compatibility (EMC). Also covers filters and braid-breakers. 204 pages. ARRL Order No. 7350—\$30



Microwave Handbook, Volume 1
Operating techniques, system analysis and propagation, microwave antennas, transmission line and components, microwave semiconductors and tubes. 200 pages. ARRL Order No. 2901—\$35

Microwave Handbook, Volume 2
Construction techniques, common equipment, microwave beacons and repeaters, test equipment, safety, filters and additional circuit data. 244 pages. ARRL Order No. 3606—\$35

Microwave Handbook, Volume 3
Microwave theory and practice, reference information, practical designs, hints and tips. Covers 1.3-24 GHz. 284 pages. ARRL Order No. 3975—\$35



RadCom 1997 on CD-ROM

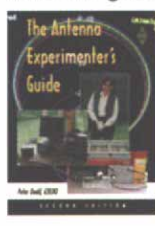
All of the words, diagrams and photographs of the technical articles, news and reviews published in RadCom magazine during 1997. Includes a fully searchable keyword index covering all 12 issues; all 1200 pages including all advertisements; and Adobe® Acrobat® Reader for Windows. ARRL Order No. 7156—\$30

VHF/UHF Handbook

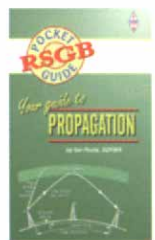
A guide to the theory and practice of VHF/UHF operating and transmission lines. Includes essential background on antennas, EMC, propagation, receivers and transmitters, together with construction details for many projects. Plus, information on specialized modes such as data and TV. 317 pages. ARRL Order No. 6559—\$35.95

Antennas

Take the guesswork out of experimenting!



The Antenna Experimenter's Guide
Build and use simple RF equipment to measure antenna impedance, resonance and performance. General antenna construction methods, how to test theories, and using a computer to model antennas. 158 pages. Order No. 6087—\$25



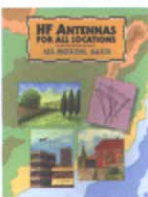
NEW! Pocket Guide! Your Guide to Propagation

This handy, easy-to-read guide takes the mystery out of radio wave propagation. It will benefit anyone who wants to understand how to get better results from their station. ARRL Order No. 7296—\$10



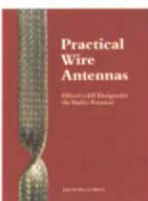
**Outstanding Antennas!
HF Antenna Collection**
Articles from RSGB's RadCom magazine. Single- and multi-element horizontal and vertical antennas, very small transmitting and receiving antennas, feeders, tuners and more. 240 pages. ARRL Order No. 3770—\$18

Antennas for every situation!

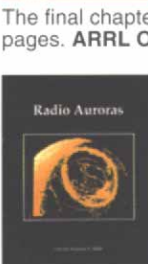


HF Antennas for All Locations
Design and construction details for hundreds of antennas, including some unusual designs. Don't let a lack of real estate keep you off the air! 322 pages. ARRL Order No. 4300—\$35

Build the antenna that's right for you!

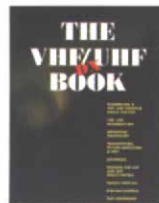


Practical Wire Antennas
Dive into the practical aspects of HF wire antennas: how the various types work, and how to buy or build one that's right for you. Marconis, Windoms, loops, dipoles and even underground antennas—they're all covered! The final chapter covers matching systems. 100 pages. ARRL Order No. R878—\$14



Radio Auroras
Explore the world of Amateur Radio communications via auroral propagation. What causes auroras, how they are forecast and how to best use them to work DX. You'll find an abundance of tables and charts. 96 pages. Order No. 3568—\$18

Operating

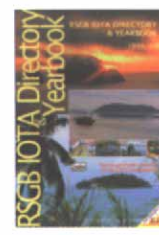


The VHF/UHF DX Book

Assemble a VHF/UHF station, and learn about VHF/UHF propagation, operating techniques, transmitters, power amplifiers and EMC. Includes designs for VHF and UHF transverters, power supplies, test equipment and much more. 448 pages. Order No. 5668—\$28



**Complete guide to country identification!
RSGB Prefix Guide**
DXCC listings by prefix, useful data such as CQ/ITU Zones, hours +/- on UTC and latitude/longitude. Ed 4, October 1998. Order No. 7237—\$12.95

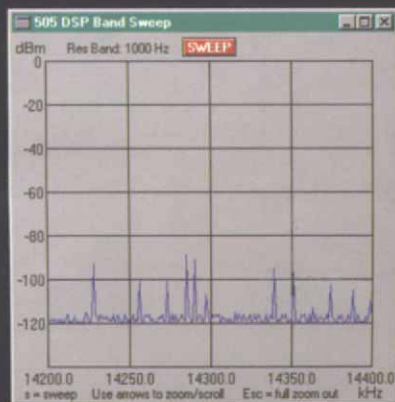


**The official IOTA award sourcebook!
RSGB IOTA Directory and Yearbook - 1998/99**
Try your hand at island expeditioning! The entire IOTA (Islands on the Air) award material, much statistical information and features many national island programs. ARRL Order No. 6079—\$15

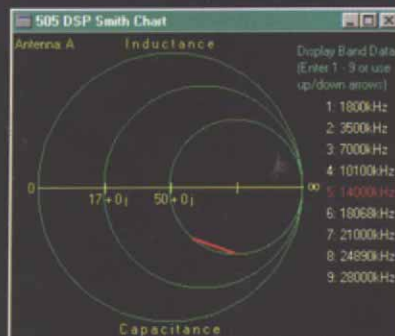
ARRL

225 Main St, Newington, CT 06111-1494 tel: 860-594-0355 Order Toll Free 1-888-277-5289

fax: 860-594-0303 e-mail: pubsales@arrl.org World Wide Web: <http://www.arrl.org/>



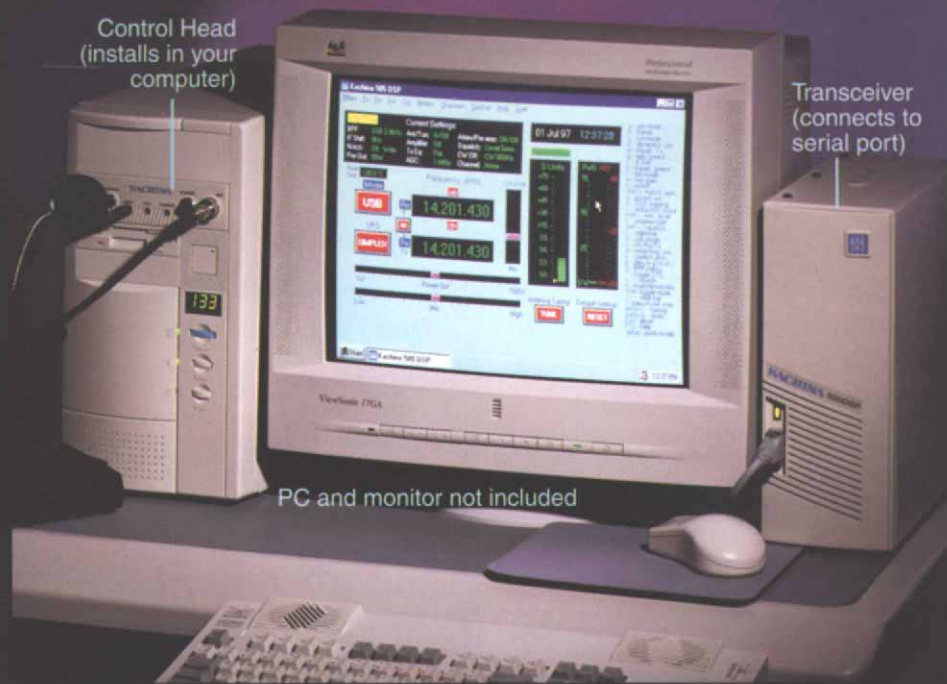
"Band Sweep" window allows you to look for the pile-ups. "Point and click" the mouse to instantly change frequency and join in.



"Smith" chart window instantly displays your antenna Z for the entire band.

Control Head
(installs in your
computer)

Transceiver
(connects to
serial port)



PC and monitor not included

Logbooks	Entries	Print	Help	Quit!
001	01 Apr 97	17:51	28,350.000kHz	USB 100w 57 56 KA9NE Greylake, IL Weather snowing
002	01 Apr 97	17:53	14,187.000kHz	USB 100w 59+15 59+5 JA7 Sendai, Japan Ham for 30 yrs
003	01 Apr 97	17:54	3,993.500kHz	LSB 100w 59+20 58 K0 Denver, Co Name is Joe
004	01 Apr 97	17:55	1,877.000kHz	LSB 100w 44 54 W4FTE Rimrock, Az New antenna
005	01 Apr 97	17:56	7,040.500kHz	CW 100w 569 589 N4Y San Diego, Ca Mobile rig
006	01 Apr 97	17:58	14,012.000kHz	CW 100w 599 599 Y03TR Switzerland Strong signal

Built-in logging software lets you keep track of your QSOs.

The New Approach to HF Radio!

The Kachina 505DSP Computer Controlled Transceiver

Features:

- Operates with any Computer Running Windows 3.1, 95 or NT. (Computer need not be dedicated to 505DSP control)
- 100 Watts PEP Output
- Covers all Amateur HF Bands on TX, plus 30 kHz-30 MHz Receive
- IF Stage 16/24 Bit DSP
- 11 DSP Bandpass Filters
- CW Keyboard Transmission and 9 CW Buffers
- 2 Antenna Ports and 3 Accessory Ports to Interface with External Amplifiers, Antenna Tuners and TNCs

- Automatic Frequency Calibration from WWV or other External Standard
- "Snapshot" Keys for Instant Recall of Frequencies and Settings
- Optional Internal or External Antenna Tuners

You will have heard about the revolutionary new Kachina 505DSP Computer Controlled Transceiver by now. Perhaps you're in the market for a new rig, and wondering if computer control is really the way to go.

If the other 100 watt radios on the market could draw you a graph of band activity, antenna impedance, calibrate meters to show S-units, volts, dBm, ALC, VSWR, forward power or reflected power, let you type your CW messages from a keyboard, or calibrate themselves from WWV, you wouldn't need a 505DSP. But

the simple fact is, most other rigs don't have any of these features.

Even without the extras afforded by computer control, the 505DSP is a heck of a rig, above all, built in the USA to commercial standards. With sophisticated IF stage, 16/24 bit DSP technology, 11 "brick-wall" bandpass voice/CW/data filters down to 100 Hz wide (no ringing), excellent receiver sensitivity, carrier and opposite-sideband suppression and a low distortion P.A.; you'll soon wonder why all radios aren't designed this way.

To ensure that your 505DSP stays current for years to come, Kachina has a policy of providing free software upgrades from our internet website, so you won't be stuck with "last years model" as revisions are made.

And our customer service is among the best in the business. You'll speak to a real person, not a machine. Guaranteed!

Like more information? Visit our website listed below for detailed specifications, to download a demo version of our control software or for a list of the dealers nearest you.

KACHINA COMMUNICATIONS, INC.

P.O. Box 1949, Cottonwood, Arizona 86326, U.S.A.
Fax: (520) 634-8053, Tel: (520) 634-7828
E-Mail: sales@kachina-az.com □ Website: www.kachina-az.com

Now With
Keyboard CW
& QRZ® Callsign
Data Base!